International Erasmus Mundus Master in
QUATERNARY AND PREHISTORY

Buccal and Occlusal Dental Microwear Analysis of the Neanderthal Specimens from Ciota Ciara cave (Piedmont, Italy): Detecting Diet and Non-alimentary Traces through a Holistic Methodological Approach

Candidate
Mirabello Mattera

Supervisor: ***Marina Lozano***

Co-supervisor: ***Julie Arnaud***

Academic year 2022/2023

To Sarah

Contents

CHAPTER 1: Introduction

Dental microwear represents one of the most applied techniques, among the paleoanthropologists, to reconstruct the human tooth-use of past periods. But why is dental microwear considered so important? Diet, particularly food preference, may, but does not necessarily, follow dental form. While teeth can limit food choice, availability of preferred resources can play an even more important role. Dental morphology, alone, may not be enough to detect the dietary habits of extinct species; therefore, it is necessary to consider lines of evidence that reflect actual activities of the fossils rather than adaptations suggesting what an individual was capable of eating (Ungar, 2019). Moreover, unlike the other animal taxa, human dental remains are an invaluable source of information not only related to dietary behaviors; In fact, there is a well-established field of study that provides a way to identify and interpret dental micro-features related to the so-called extra- or para-masticatory activities. These analyses provide valuable information on several tasks of cultural origin and, consequently, yield even more perspective on the multiple uses of dentition by extinct human species. To achieve this, the accurate analysis of microscopic observations, in all the microwear studies, plays a key role in providing a correct identification and interpretation of a series of traces (striations and pits) that are located on the teeth surfaces. In general, dental microwear is performed on either the buccal or occlusal areas, both surfaces are rarely examined in the same study; in addition, each type of surface follows a standardized and well-established protocol of analysis. However, recent studies involved the use of new microscopy instrumentation to test the advantages that can be gained from the methodological comparison of different equipment. Given these premises, dental microwear studies have largely focused on the analysis of several hominin teeth since its earliest applications. In this context, excluding our own species, *Homo neanderthalensis* is undoubtedly the most studied and best-known taxon in the human fossil record. Thus, many publications have detected both dietary habits and cultural activities related to various Neanderthal populations, spread in different eco-geographical contexts, by applying a dental microwear methodology.

The purpose of this research is to perform, for the first time, a dental microwear analysis on the newly discovered Neanderthal specimens from the Middle Pleistocene site of Ciota Ciara cave. Thus, the current study has three main aims for contextualize, from a paleoanthropological point of view, the Ciota Ciara's dental sample in the current academic scenario. First, the accurate analysis and recognition of dental micro-features will provide insight into various type of antemortem and postmortem alteration that affected the fossil remains. Having done so, it will be possible to identify more clearly the possible traces of para-masticatory activities for the reconstruction of cultural tasks. A second aim will involve the application of a standard buccal microwear protocol to obtain data on both dietary behaviors and foodstuff variability from the preserved molars of this hominin group. Therefore, the case study of Ciota Ciara will be used to better understand and illustrate the complexity of reconstructing both dietary and cultural behaviors, from dental microwear, in a well-contextualized Neanderthal population. Finally, the application of a holistic comparative methodology, that will include the use of multiple microscopy instrumentations, will allow to explore the potential and limitations of this approach related to the quantitative observation of the dental features. An ongoing interest for dental microwear scholars, in fact, is to introduce more standardization in some aspects of the methodology to increase reproducibility, repeatability and above all, comparability. The current analysis stands on the line of research of previous comparative studies (i.e. Hernando et al., 2020) and is configured as a methodological contribution to provide further quantitative data to be used for future investigations.

CHAPTER 2: State of the Art

2.1 What is Dental Microwear?

Dental microwear, as defined by P. S. Ungar (2018), is the study of microscopic scratches and pits that form on a tooth's surface as the result of its use. These traces can be preserved on the tooth enamel even for millions of years, in fact several research (both in paleontological and bioarchaeological field) applied dental microwear methodologies as a direct tool to reconstruct primarily the dietary behaviors of the past (Ungar, 2018). Different types of dental microwear analysis have been applied on a wide range of extinct and extant animals, such as: Mesozoic dinosaurs (e.g. Schubert et al., 2005; Williams et al., 2009), fishes (e.g. Purnell et al., 2006), or non-primate mammals[1] (e.g. Palombo et al., 2005; Rivals & Deniaux, 2003). However, most of microwear studies were conducted by dental anthropologists on fossil primates and hominins, to evaluate the role of dietary changes during the temporal phases of human evolution; specifically the main anthropological fields of microwear application are related to: the diet of prehistoric human populations (e.g. Mahoney, 2006; Pérez-Pérez et al., 2017), the diet of *Australopithecus* and early *Homo* genus (e.g. Estebaranz et al., 2012; Grine et al., 2006; Walker, 1981); the diet and ecology of living and extinct primates (e.g. Teaford, 1988; Galbany et al., 2009; Teaford & Runestad, 1992). For a comprehensive (but not updated) list of human and non-human taxa examined using dental microwear methods, see Ungar et al. (2009: 394-395). Moreover, other innovative applications on human microwear have been recently developed to indagate further complex aspects, such as: food processing (e.g. Teaford & Lytle, 1996) mastication biomechanics (e.g. Gordon, 1984), and non-alimentary activities (e.g. Lozano et al., 2008, 2017; Minozzi et al., 2003)

2.2 Reconstructing Human Tooth-use through Microwear Analysis

Paleodiet and Microwear: Reconstructing human paleodiet is a fundamental step to obtain information about different types of past behaviors, in particular: how people survived, how was the stability of the populations, what kind of environmental adaptations existed, which type of exploiting strategies were applied, etc. Applications of dietary reconstruction cover all the chronological phases of the human history (from the early prehistory to recent times) and involves several specialistic fields of research, such as: early hominine diet, the implications of food for human evolution, the transition from hunting and gathering to agriculture, the development of specialized food systems, impact of cultural contacts on diet, etc. Paleodiet reconstruction entails different types of techniques that could be classified, depending on the source of information, into two main divisions: direct and indirect methods. Direct methods are those that assess alimentary behaviors from the signatures on the skeletal and dental remains. For example: isotopes analysis on bones, certain skeletal diseases related to food intake and/or insufficient intake, gut or coprolites contents, are all direct indicators that yield diet clues related to the single individual level (Pearsall, 2016). On the contrary, indirect methods involve mainly the archaeological remains of food (or their residues) found associated to anthropic activities.

[1] Tooth microwear also revealed how feeding, in fossil ungulates, tracked important paleoenvironmental changes related to the vegetation (e.g. Semprebon et al., 2010)

For example: processing of food through cooking, food residues trapped on tools, botanical macro and micro-remains associated to archaeological layers, butchery activities on faunal remains, are all indirect indicators of alimentary practices that yield information related to the community or extra-community levels (Pearsall, 2016).

The fossil dental remains provide the most reliable data for dietary reconstruction since teeth are directly involved in the masticatory processes[2] and represent the better-preserved human specimens[3] found in the archaeological assemblages. However, many dental features such as: rate of attrition, alveolar resorption, and dental calculus may provide only a general and limited view related to past human diet and/or subsistence economy (e.g. Eshed et al., 2006; Fyfe et al., 1993; Hillson, 2007). In this context dental wear studies have produced exceptional results since tooth wear is directly reflected by tooth use at both macroscopic (Macrowear) and microscopic (Microwear) levels. Actually, the generalized dentition of most hominoids evolved to consume a wide spectrum of aliments resulting in the capability to adapt, through environmental pressure, to an omnivorous diet (Walker, 1981). By engaging in their primary functions, teeth experience wear that is defined as the continuous loss of their mineralized tissues from tooth-to-tooth and tooth-food-tooth contact. Watson & Schmidt (2019) argue that tooth wear is a multifactorial process that involves three main interacting phenomena: attrition[4], abrasion[5], and erosion[6]; each of these mechanisms is continuous, unidirectional, and age-progressive (Watson & Schmidt, 2019). As mentioned above, human tooth wear can be evaluated at two main different levels: macrowear and microwear. By summing on a long time scale these repetitive interactions, mainly between the enamel and food materials, the continuous activity of the chewing system ends with dentine exposure (Eshed et al., 2006). In fact, macrowear is defined as the examination of gross dental wear patterns with a particular focus on wear facets linked to exposed dentine (Fiorenza et al., 2011), it is visible to the naked eye or at low magnification. On the contrary, microwear observations only reflects traces that has occurred relatively recently (a short-term signal): the so-called “last supper effect” (true only for occlusal surfaces) defined by Grine (1986), it can provide clues about an individual’s diet in the last weeks (or even days) before its death (Wood et al., 2012), but is only visible under the microscope at higher magnifications.

Focusing on microwear analysis, is well-know that the constant contact between the enamel surface and abrasive particles, usually harder than enamel, is directly involved in the formation of dental

[2] As biostructures that facilitate interaction between bodily and external environments, teeth provide the first step in the digestion of food through mechanical breakdown. Teeth function to prepare (anterior teeth) and reduce (posterior teeth) food for chemical and mechanical digestion in the gut (Watson & Schmidt, 2019).

[3] Tooth enamel, the protective outer layer of the dental crown, is the hardest and most mineralized tissue in the human body (Welborn, 2020: 21847). Specifically, enamel consists of over 95% of carbonate apatite: a calcium phosphate mineral that can be found in all mineralized tissues in vertebrates (Beniash et al., 2019).

[4] Attrition is caused by wear of the tooth surface through friction resulting from tooth-on-tooth contact. A critical element contributing to this process is occlusion and masticatory loading (Watson & Schmidt, 2019: 2).

[5] Abrasion is the loss of surface detail from friction with exogenous material such as the presence of foreign abrasives. Most abrasives come from the foods consumed (Watson & Schmidt, 2019: 2).

[6] Erosion is the reduction of dental surfaces due to non-bacterial exogenous or endogenous chemical substances. Endogenous sources include bodily contributors such as vomiting or acid reflux or decreased salivary flow and dehydration (Watson & Schmidt, 2019: 2)

microwear pattern. Hardness of the food particles is measured using Mohs scale[7] on a range from 1-10 and dental enamel is scored on a range between 4.5-5 approximately (Staines et al., 1981). For this reason, any particle that exceeds this parameter tends to create microwear features on the enamel surface. These abrasive particles can be classified as either intrinsic or extrinsic: the intrinsic ones are localized within the food especially plants, such as: silica elements that compose the structure of phytoliths (Piperno, 2014). While the extrinsic particles, usually introduced into diet accidentally, are represented by those microscopic mineral grains (sand, dust, grits, ash, etc.) which enter into contact randomly with food items (Romero et al., 2012a). Therefore, a basic assumption is that the presence of abrasive particles, during the chewing process, tends to leave identifiable traces on the enamel surfaces called "pits" and "striations"[8] (or "scratches"); in simple terms is possible to affirm that the dental microwear pattern formation is directly reflected by the biomechanical properties of food and by the associated jaw movements to process it. In fact, several experimental studies analyzed in detail the mechanical causes of these associations: hard and/or brittle food items require greater compressive forces and the consequent crushing motions produce pits on the dental surface, whereas the consumption of more tough and abrasive food items requires shearing motions that are related to dental striations (Lucas, 2004) (Fig. 2.1). Considering specifically primate and human specimens, the microwear studies were focused on the analysis of the molars (when possible) in the occlusal or buccal surfaces since their relationship to diet seems especially direct (Ungar, 2018).

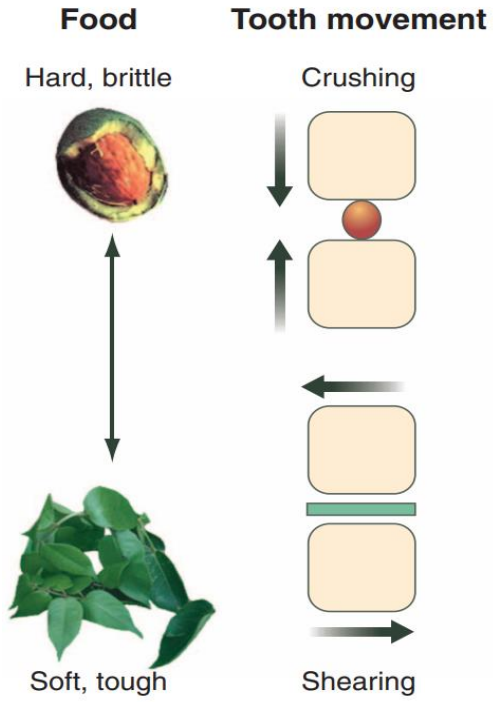

Figure 2.1 Schematic representation of the crushing and shearing processes. When processing hard foods (like a seed), the two opposing surfaces (pink blocks) move perpendicularly to each other (black arrows) and induce fractures into the hard object through crushing. On the contrary, the cracks need to be propagated through tough foods (like a tree leaf). This is achieved through movements of the opposing surfaces parallel to each other (black arrows), a process known as shearing. Figure taken from (Ungar & Sponheimer, 2011)

Occlusal surface: Occlusal dental microwear refers to the microscopic features of wear on the working area of molar teeth that is affected by dietary activities. Dahlberg & Kinzey (1962) published the first occlusal microwear analysis working on human dental specimens with optical light microscopy. After almost a decade, Walker (1976) conducted the same observations on an extant primate sample (cercopithecoid monkeys). Then a growing number of studies started to apply qualitative methodologies by counting occlusal microwear features (e.g. Grine, 1986; Puech, 1979; A. Walker et al., 1978). And, shortly after, the development of analytical quantitative techniques allowed the researchers to acquire more reliable interpretations of occlusal dental microwear by detecting other parameters, such as: teeth position, facet identification, and the orientation of wear facets that may affect the micro-dental pattern (e.g. Gordon, 1984; Grine, 1986; Teaford & Walker,

[7] Mohs hardness of a mineral, expressed in terms of a scale and devised (1812) by the German mineralogist Friedrich Mohs, is determined by observing whether its surface is scratched by a substance of known or defined hardness (Broz et al., 2006)

[8] A dental striation is defined as a linear mark that equals or exceeds in length 10 micrometer (Romero et al., 2012b)

1984). Therefore, detailed studies on occlusal wear patterns were linked to specific steps in the process of mastication. In particular, Kay & Hiiemae (1974) argued that nutrients are first processed during the so-called "puncture-crushing stage" where there is not a real tooth-to-tooth occlusal contact between the opposite molars, but the food is just mechanically reduced. The true chewing activity starts from the time when the food fragments become small enough for the molar cusps to collide with each other. This point of intercuspation is defined as the "power stroke" of the masticatory cycle and it is divided into two main phases (Kay & Hiiemae, 1974). Each step of this process is well-synthetized in the work published by Fiorenza et al. (2019): 1) "Phase I" is described as a guiding step where the opposing molar crests slide past each other, and the trapped food is exposed to a shearing action. Then, at the end of Phase I, food is compressed (crushing) between fossas and cusps of molars which are moving to result in centric occlusion (Fiorenza et al., 2019: 49) . 2) While "Phase II" is described as an anterior-medial movement where the lower molars move out of occlusion. During Phase II food is processed by grinding through the contact between the lingual slopes of the mandibular molar cusps and the buccal surfaces of the maxillary molar cusps, which act as a "pestle and mortar" (Fiorenza et al., 2019: 49) (Fig. 2.2). To analyze the occlusal wear facets, Maier & Schneck (1981) developed a numerating system that allow to identify 13 pairs of homologous facets in hominoid molars (Fig. 2.3). The importance of these studies, for microwear research, is to develop standardized protocols that allow scholars to sample and compare the micro-dental features following established criteria.

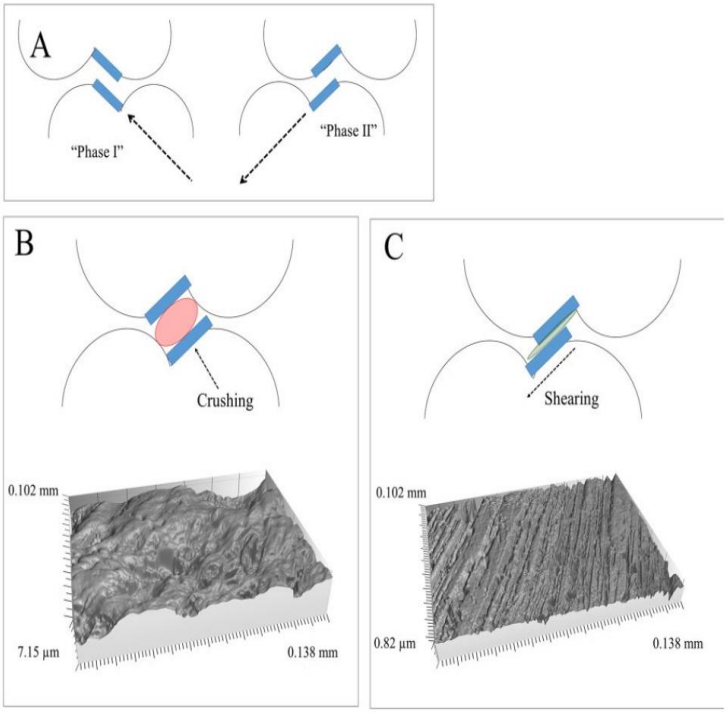

Figure 2.2 Microwear facets **(A)** "Phase I" and "Phase II" occlusal 9 facets identified relative to tooth movements. **(B)** Crushing leads to high complexity with heavy pitting on a hard object feeding *Sapajus apella* molar, whereas **(C)** shearing action leads to an anisotropic surface texture with long parallel striations on a folivorous *Alouatta palliata* molar. Illustrations represent the right molars as viewed from the distal side so that buccal is to the right and lingual is to the left. Figure and citation taken from (Ungar, 2019: 4)

Buccal surface: Buccal dental microwear refers to the microscopic features of wear on the vestibular area of premolar and molar teeth that is affected by dietary activities (Pérez-Pérez et al., 2017). The earliest investigations of the buccal surfaces on humans were conducted by P. F. Puech, (1976), who argued that the number, the length and the orientation of the microwear striations are directly correlated to the movements of the masticatory apparatus. By the 1980s, a growing number of publications analyzed the vestibular surface of molars as a new field of investigation for dietary reconstruction; moreover, further studies suggested that the number of horizontal striations increase proportionally in relation to plant-based diets, while the number of vertical striations increases proportionally in relation to a higher meat consumption (Lalueza-Fox et al., 1996). Therefore, many indices were developed to characterize the diet using the number of horizontal and vertical striations (Lalueza et al., 1996). The standard

buccal microwear protocols require to detect 2 main aspects related to the striations: orientation (vertical, horizontal, meso-distal, disto-mesial) and total sum (Fig. 2.4); each type of striation is also characterized by three further variables: number, length, and standard deviation of length (Romero et al., 2013). Based on the proportion and correlation between the previous variables is possible to obtain clues for differentiate harder from softer diets.

Non-Alimentary Activities and Microwear: Analysis of human dental microwear is not only associated to diet, but it can also reveal interesting aspects about pathologies or cultural behaviors. Therefore, some tooth wear facets not related to food consumption, may also result from para-masticatory activities such as: bruxism, repetitive grinding or clenching, or also by the use of anterior arcade of the jaws as a "third hand" to perform tasks (Silvester et al., 2021). These type of para-masticatory or cultural traces[9] tend to show different characteristics when compared to diet-related ones by observing size (width, length), location (more frequent in anterior teeth), orientation, disposition, and regularity of the features (Lalueza Fox, 1992; Lozano et al., 2008). Moreover, based on the previous criteria, Lozano et al. (2008) proposed to divide these micro-features into specific categories: vestibular striations[10], vestibular-lingual striations[11], dental chipping[12] (or enamel flakes), and polished enamel[13] (Lozano et al., 2008). The first approach, in this field, was made by de Lumley-

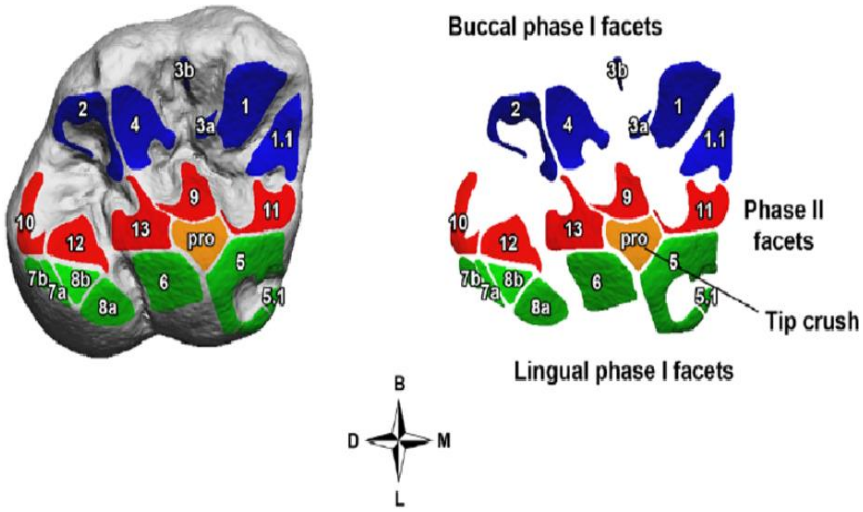

Figure 2.3 Wear facet of molars are labeled following the numbering system developed by (Maier & Schneck, 1981) and are grouped according to the chewing cycle phases of (Kay & Hiiemae, 1974): Buccal Phase I (facets 1, 1.1, 2, 2.1, 3 and 4), Lingual Phase I (facets 5, 5.1, 6, 6.1, 7 and 8), and Phase II (facets 9, 10, 11, 12 and 13). B, buccal; D, distal; L, lingual; M, mesial. Figure taken from Fiorenza, Benazzi, Tausch, et al. (2011)

[9] Cultural scratches are created when an individual holds something between his/her anterior teeth with one hand, while with the other hand cuts that item with a tool. This behavior is known as 'stuff-and-cut' (Molnar et al., 1972)

[10] The vestibular striations are usually located on the labial surface of the anterior teeth and include the following characteristics: linear, well-defined, parallel to each other along most of their length, and frequently are orientated in a right oblique (RO) and vertical (V) way (Lozano et al., 2008: 718).The lower part of the striations usually display a "V"shaped transverse section combined with small triangular fractures in the borders called Hertzian cones (these cones are the result of the interaction between the pressure exerted by the action of cutting and the resistance offered by the surface to be cut). The morphological traits of vestibular striations are the same as those displayed by cutmarks on bone (Lozano et al., 2008: 718)

[11] The vestibular-lingual striations are only identified on the occlusal surface enamel and on the exposed dentine. They are wear-features of linear morphology that run along the occlusal surface in the vestibular-lingual direction. These striations suggest movement towards the front (vestibular) and back (lingual) of the mouth. Striations are generally perpendicular to the longitudinal axis of this surface (Lozano et al., 2008: 720)

[12] Dental chipping is characterized by the splintering (or cracking) of small enamel fragments from the tooth crown (Fiorenza, Benazzi, & Kullmer, 2011)

[13] Polished enamel can be defined as enamel areas that present a softened and smoothed appearance (Lozano et al., 2008: 720)

Woodyear (1973) that discovered several scratches visible to naked eye on a sample of incisors from the site of Hortus (France). These traces were only observed on the labial surface of the anterior teeth, for this reason she attributed the cause to a cultural task similar to an ethnographic habit documented in some Inuit populations. This practice involves the action of cut, using a knife, pieces of meat by holding them into the mouth; frequently this activity can leave visible scratches, by the contact knife-to-tooth, on the labial surfaces of the anterior teeth (both incisors and canines) (de Lumley-Woodyear, 1973). Is possible that parallel events happened in the past, hominins could accidentally stroke their dental enamel with sharped stone flakes generating dental damages similar to cutmarks found on faunal remains (Lozano et al., 2008). These cultural micro-features on the labial surfaces can also yield interesting clues by detecting their orientation, in fact this characteristic seems to be related to the hand laterality[14] (Lozano et al., 2017); an interesting example of study was published by Lozano et al. (2004) concerning the analysis of para-masticatory traces on the pre-neanderthal sample from Sima de los Huesos, the results were furtherly compared through modern in vivo experimentations (Lozano et al., 2004). Other publications analyzed similar labial dental features on fossil hominins (e.g. Bermúdez de Castro et al., 1988; Lalueza Fox, 1992; Lozano et al., 2008; Lozano et al., 2004; Trinkaus, 1983), ancient anatomically modern humans (e.g. Lukacs & Pastor, 1988) and living populations (e.g. Bax & Ungar, 1999). In addition, the study of dental chipping, associated with non-masticatory activities, gets complicated because the blows that produce enamel flakes can have an antemortem[15] or postmortem[16] origin. The enamel cracking of the tooth crown has been found in different agricultural and hunter-gatherer populations and even in several hominin specimens (Fiorenza, Benazzi, & Kullmer, 2011). As argued by the previous scholars: the mechanism of dental chipping is still poorly understood, therefore it is important to remember that Constantino et al., (2010) have demonstrated that chipping can also occur during the masticatory process of especially hard food items, in this way also information about the bite force and diet can be obtained (Constantino et al., 2010).

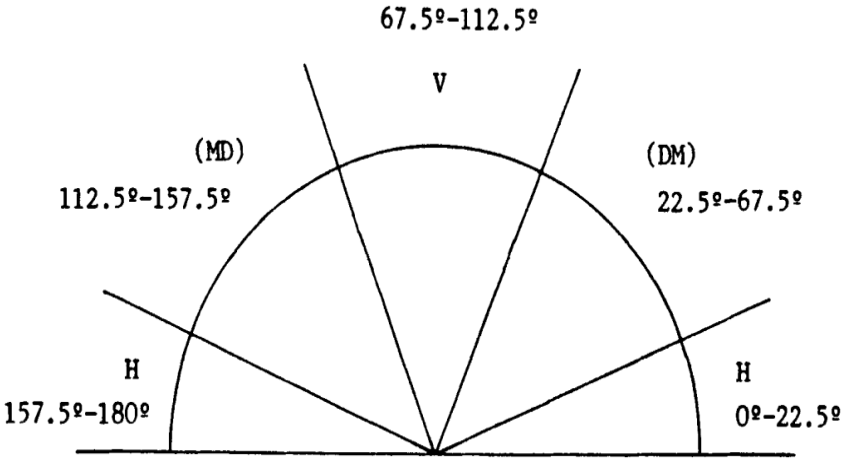

Figure 2.4 Range of orientations of tooth striations MD (mesio-occlusal to disto-cervical): 112.5-157.5" (left lower and right upper molars), 22.5-67.5" (left upper and right lower molars), DM (mesio-cervical to disto-occlusal): 22.5437.5" (left lower and right upper molars), 112.5-157.5" (left upper and right lower molars), H (horizontal): 0-22.5" and 157.5-180.0" (all teeth), V (vertical): 67.5-112.5" (all teeth). Image and citation taken from Pérez-Pérez et al. (1994)

[14] Hand laterality refers to the preference in the use of one hand over the other (left-handed or right-handed) (Lozano-Ruiz et al., 2004)

[15] Enamel antemortem microfractures can be recognized due to a smoothed contour of the break made by the active action of saliva, tongue movements, and functional use of teeth during the individual's life. Moreover, this type of chipping is often located on the incisal part of the labial surface in the contact zone between the labial and the occlusal surfaces (Lozano et al., 2008: 720)

[16] Well-defined enamel cracking is more likely caused by post-depositional events (Lozano et al., 2008)

2.3 Dental Microwear Methodologies:

2.3.1 Early Studies: The first dental microwear rudimental descriptions were conducted by early comparative anatomists and paleontologists more than a century ago, basically the main purpose of these works was to understand the complexities of mastication. John Ryder (1878) published a monograph about the function of different mammalian dental systems and their jaw movements through the simple observation of the traces on teeth (Ryder, 1878). Then, almost fifty years later, Simpson (1933) published an important study where he demonstrated that dental structures must be considered as dietary guides since teeth are directly involved in specific types of jaw movements. Based on Simpson's assumption, Baker et al. (1959), Butler (1952), and Mills (1955) firstly detected that the scratches orientation, on the occlusal wear facets, could be used to interpret the directions of jaw motions, and, presumably, to reconstruct diets. As already mentioned in the previous paragraph, dental microwear methodologies started to be applied in the anthropological field only when Dahlberg & Kinzey (1962) examined modern and fossil AMH's samples using a binocular optical light microscope. Then Walker (1976) used the same optical methodology to analyze dental specimens of living primates. These early studies classified the dental surfaces just qualitatively, defining them as scratched or pitted or polished (Ungar, 2018).

***2.3.2 Scanning Electron Microscopy and Quantitative Analysis*:** The use of microscopic observations has a primary role for dental microwear studies, and the most common methodology applied, in the anthropological literature, refers to the Scanning Electron Microscopy (SEM). Scholars noticed gradually that the optical light microscopy had significant limitations for this field of research, in fact measuring individual features at higher magnifications can be difficult because teeth tend to be curved and a great area of the field of view results out of focus. For this reason, through technological innovations, these optical lenses were automatically replaced by more accurate high or low vacuum scanning electron microscope (SEM), which offers: an increase of the depth of field at higher magnifications, removing of out of focus areas, clear features for measurement directly from photomicrographs (taken using a digital ruler), a digitizing tablet, and a mouse-driven pointer on a computer screen (Ungar, 2018)**.** Therefore, by the late 1970s, several researchers (i.e. Grine, 1977; Rensberger, 1978; Ryan, 1979; A. Walker et al., 1978) had adopted the scanning electron microscopy (SEM) as the preferential tool for the microwear methodology. An important point was stressed in the papers published by Gordon (1984, 1988), where he argued that using the SEM microwear approach, to evaluating past diets, can be useful only if other distortion factors (such as: magnification, tooth position, facet type, and SEM instrumentation settings) are under predetermined control, a standardized methodology may offer a greater transparency and repeatability of results (Gordon, 1988). Scanning variability of magnification can varies from 35x (e.g. A. Walker, 1981) up to 6000x (e.g. Ungar & Grine, 1991) but are more typically standardized between 100x and 500x (e.g. Grine & Kay, 1988), in particular Teaford & Walker (1984) developed a standard protocol for the use of SEM applied to primates by using the second molar and a predetermined magnification of 500x (Teaford & Walker, 1984). Therefore, the adoption of SEM related to a standard procedure quickly led researchers to detect a number of discrete microwear features that could be used to describe dental surfaces in a quantitative way (Ungar et al., 2009). However, it soon became obvious that working with larger samples of increasing variety required an extra methodological step, in fact quantitative characterization of dental surfaces would be necessary to provide statistical analyses to

infer feeding behavior of fossil hominins; therefore, several approaches focused on characterizing average numbers, sizes, shapes, and orientations of the microwear features (Ungar et al., 2009). This set of approaches ranged from counting and measuring scratches and pits on paper photomicrographs using calipers and protractors (e.g. Gordon, 1982; Grine, 1986b; Ungar & Grine, 1991) or a digitizing tablet (e.g. Pastor, 1993; Teaford & Walker, 1984), and more recently through a range of automated and semi-automated software (e.g. Lalueza-Foxet al., 1996; Pérez-Pérez et al., 2003; Ungar, 1995). The SEM microwear literature includes a wide spectrum of key measures for distinguishing diets based on the previous quantitative variables analyzed, in fact Ungar et al. (2006) indicated that the four most used measures for occlusal surfaces in SEM analyses are: pit percentage, pit width, scratch width, and mean-orientation vector length (feature orientation and length) (Ungar et al., 2006). Some of the most productive research using SEM has involved the study of dental microwear and diet in wild primates[17], therefore quantitative data related to lengths, widths, and orientations of microwear traces proved particularly useful data for distinguishing primates by broad diet category (Ungar et al., 2009).

Limitations: However, SEM-based microwear approaches have some inherent limitations. Ungar et al. (2009) made a complete list of all the possible troubles related to SEM observations: 1) the real three-dimensional (3D) dental-wear surfaces are displayed in two dimensions (2D) images[18]. 2) The shadowing effects give the illusion of depth, but there is always information lost in the process. 3) The information lost depends on the positions of the light or electron source relative to the tooth surface and the eye-piece tube or detector. 4) Scratches appear and fade as a specimen is moved on its stage, which makes it difficult to get a complete picture of the surface and even slightly different orientations can lead to quite different observations. 5) Microwear surfaces can show hundreds of striations and pits, their boundaries are irregular and commonly overlap; so, it can be difficult to determine the endpoints of scratches and especially pits. 6) The average number of features recognizable and their measurements vary between observers. 7) Characteristics of the microscopes themselves such as the voltage and type of electrons used (backscattered versus secondary), or thickness and properties of coating materials on specimens, may influence the results. Taken together, all these elements can lower the signal-to-noise ratio and limit the potential of microwear to reveal diet.

2.3.3 Optical Light Microscopy (OM), New Developments: The SEM-based analyses, however, are time-consuming and expensive. Preparation of specimens, imaging of surfaces, and identification of features on photomicrographs for just one individual can take hours, moreover SEM's maintenance and supplies can be very expensive (Ungar et al., 2009). For this reason, Solounias & Semprebon (2002) proposed a return to low-magnification through the binocular light microscopes, the advantage is that these optical instruments certainly offer a rapid and inexpensive approach, and it has gained an increasing popularity in recent years. Therefore, new exploring studies, using OM instruments, allowed to obtain excellent results even on human specimens thanks to new analytical protocols from

[17] Much of the primate microwear research that followed focused on documenting differences between samples, and on trying to understand the mechanics of feature formation (Ungar et al., 2009: 393)

[18] When measuring features in 2D space, SEM methods also assume surfaces to be planar and parallel to the recorder, which is hard to maintain in complex surfaces such as teeth, particularly as surfaces horizontal to the electron beam show poor contrast. This effect was, however, partially overcome through the use of a digitizing program that corrected for foreshortening of features (King et al., 1999).

the traceology field (Hernando et al., 2020). Specifically, beyond the clear advantages of money and timesaving, Hernando et al. (2020) argued that in term of comparisons between OM and SEM, the biggest difference concerns the greater number of horizontal striations counted with OM that appeared to be more recognizable than using SEM (Hernando et al., 2020).

2.3.4 Confocal Light Microscopy and Dental Microwear Texture Analysis (DMTA): A more recent technological and methodological advance is the so-called Dental Microwear Texture Analysis (DMTA) and is mostly applied on dental occlusal surfaces, even if in recent times the technique was also applied to buccal surfaces (i.e. Hernando et al., 2022). DMTA basically combines the use of white-light confocal microscopy with scale-sensitive fractal analysis (SSFA) and is defined as "Texture analysis" because the main purpose is to scan and detect the dental surface characteristics rather than feature counts (typical of OM and SEM approaches) (Ungar et al., 2003). The topographic DMTA analysis is applied by using a computerized software (Toothfrax® software) that was developed by Peter Ungar's team in collaboration with Worcester Polytechnic Institute, the process of analysis works synthetically in this way: the data are leveled, defects are removed, and the surfaces are measured using volumes, areas, and vectors, resulting in a quantitative description of the surfaces at different scales (Schmidt et al., 2019). Toothfrax® software is used to calculate many complexity[19] and anisotropy[20] parameters, such as: area-scale fractal complexity (*Asfc*), heterogeneity of complexity (*HAsfc*), scale of maximum complexity (*Smc*), exact proportion Length-scale anisotropy of relief *(epLsar*) and texture fill volume (*Tfv*). Teeth with heavily pitted microwear surfaces tend to have high texture complexity[21] (that means a higher level of surface roughness and relief), whereas those with aligned striations (that means uniformity in the wear patterns on the tooth) tend to have high anisotropy values[22] (Schmidt et al., 2015). Ungar's team applied this innovative methodology to early human ancestors and fossil primates (e.g. Grine et al., 2013; Scott et al., 2005; Ungar & Sponheimer, 2011); their results made it clear that the DMTA approach held great promise for dietary reconstruction (Schmidt et al., 2019). Another important study was conducted by El-Zaatari (2010) that analyzed the microwear patterns of several modern hunter-gatherer groups using DMTA for detecting their dietary habits (El-Zaatari, 2010). DMTA has several advantages when compared to previous approaches: it provided three-dimensional data, a more realistic representation of the dental surface, is non-destructive, more automated, less subjective, and resulted in lower inter-observer errors (Ungar, 2015).

[19] Complexity parameters refer to the variation of surface features as roughness (Ungar et al., 2003)

[20] Anisotropy parameters refers to the direction and orientation concentration of the surface features (Ungar et al., 2003)

[21] High complexity surfaces could result from the intake of a highly abrasive diet, which can be caused by the ingestion of hard vegetable (El-Zaatari, 2010)

[22] High anisotropy surfaces could result from a diet that is predominantly based on animal proteins since the mastication of meat (which is a tough but not hard) would have required repetitive directional jaw motions (El-Zaatari, 2010)

2.4 Microwear Studies Applied to Human Taxa, a Focus on Neanderthal's Specimens

2.4.1 Introduction: As seen in previous sections, dozens of studies have applied dental microwear methodologies to reconstruct dietary behaviors and non-alimentary practices of a wide range of extinct hominin species. In this context, excluding our own species, *Homo neanderthalensis* is undoubtedly the most studied and best-known taxon in the human fossil record (Fiorenza et al., 2015). Based on the current state of scientific knowledge, Neanderthal groups occupied a wide range of geographic areas: West from the Iberian Peninsula East to Siberia and North from Germany South to the Levant. The natural attitude of the Neanderthals to settle in diverse eco-geographical niches, from the Mediterranean margin to steppic and arctic tundra areas, implies that this hominin species was successfully adapted to varied environments (Power et al., 2018). Using the previous assumption is possible to argue that the Neanderthal' diets and cultural behavior must have been flexible enough to survive into several Euroasiatic latitudes. Although, unfortunately, research on Neanderthal ecology, cultural practices, subsistence strategies, and diet, have received remarkably little attention until new archaeological disciplines, from the 1960s, started to shed more light on this topic (Ready, 2010). These analytical methods such as faunal analysis, lithic technology, and taphonomy processes led the scholars to interpret the Neanderthals as narrow spectrum foragers related to a rigid animal protein-based diet (e.g. Kuhn & Stiner, 2006; Lalueza Fox & Pérez-Pérez, 1993), and this hypothesis was furtherly reinforced by the study of stable isotopes[23] and Neanderthal body anatomy[24]. Only in recent times, these studies have been largely questioned since new high-accuracy protocols (improvements in stable isotopes, dental wear, zooarchaeological field, etc.) and emergent disciplines (dental calculus analysis, paleopathology, paleogenetic, etc.) finally show that the dietary profiles, subsistence strategies and cultural practices of the Neanderthal groups were much more variable and richer (even based on the different geo-chronological context) than previously thought.

2.4.2 Review of Microwear literature about Neanderthals:

It's obvious that dental microwear studies, if taken alone, cannot yield complete information about the Neanderthal diet behaviors, and it is necessary to combine other evidence to reach more reliable hypotheses. Reading all the most comprehensive studies about dietary variability, it is possible to argue, very generally, that microwear evidence have revealed that Neanderthals predominantly consumed meat with a possible increased use of plants in the southern wooded area of Eurasia (e.g. El Zaatari et al., 2011; Fiorenza, Benazzi, Tausch, et al., 2011). Specifically, Fiorenza et al. (2011) argued that the microwear of Neanderthals who occupied cold-steppe environments emulates the "carnivorous" pattern of living Fuegians groups and Inuit islanders who inhabited cold wet scrublands (Fiorenza, Benazzi, Tausch, et al., 2011). But, in any case, dental wear is silent on the low-ranked food and type of plants consumed, meaning these analyses offer only an incomplete overview of the Neanderthals diet in different eco-geographical locations (Power et al., 2018). However, the purpose

[23] Stable isotopes analysis suggested that Neanderthals obtained nearly all of their dietary proteins from animal sources and occupied the higher level of the food trophic web, similar to the top-level carnivores of that time (Richards & Trinkaus, 2009)

[24] The iconic robusticity of Neanderthal skeletons, with relatively short limbs and heavy trunks, was interpreted by several scholar as a reflection of extremely high levels of physical activity and adaptation to cold climate conditions. This situation may have imposed significant metabolic requirements that would have forced Neanderthals to acquire a energy-rich diet mostly related to meat consumption (Weinstein, 2008)

of this section is just to summarize the main results obtained in previous microwear studies (divided into 2 sections: dietary and para masticatory activities) referable to Neanderthal specimens, in this way it will be possible to contextualize and compare the dental sample from the Ciota Ciara cave in the current academic scenario.

Neanderthal's diet reconstruction: One of the first microwear study was conducted by Puech (1981) on the dental specimens from La Ferrassie site (France). Observing density-orientation of enamel grooves and the worn localized on the anterior teeth, he proposed that this Neanderthal group relied on a highly abrasive diet composed of animal proteins and, especially by the continuous consumption of desiccated meat which could have incorporate exogenous particles, this phenomenon could have caused an increase of abrasiveness (Puech, 1981). However Brace et al. (1981), in a publication of the same year, strongly questioned the hypothesis of Puech (1981) by comparing the same specimens to a modern Australian aborigines sample; therefore, Brace et al (1981) offered a more plausible explanation for which the anterior dental worn, observed on the La Ferrassie individuals, was probably caused by the use of incisors as "third hand" for non-alimentary tasks (Brace et al., 1981). This episode affected the next historical development in the microwear field, in fact most of anthropologists subsequently avoided the anterior dentition to reconstruct human paleodiet, and from that moment the focus was oriented on microwear patterns found on posterior teeth (specifically, on buccal and occlusal surfaces of molars) (Fiorenza et al., 2015). Then, Lalueza Fox & Pérez-Pérez (1993) started to analyze the hominin's buccal surfaces looking at the microwear pattern on the deciduous molars of the Neanderthal child (Gibraltar 2) from Devil's Tower site. The buccal traces of this individual revealed a clear pattern of vertical striations, suggesting a carnivorous diet also linked to a huge quantity of abrasive particles contribution (Lalueza Fox & Pérez-Pérez, 1993). But another study, published by the same authors, analyzed a larger Middle Paleolithic sample composed of 21 Neanderthal teeth from different European and middle-eastern localities (Amud, El Salt, Gibraltar, Hortus, La Quina, Macassarques, Malarnaud, Marillac, Saint Césaire, and Tabun); the result was in contrast with the previous data, in fact the heterogeneity of buccal microwear striations indicates the plausible exploitation of a wide range of food items, and the authors interpret this high intragroup variation as inconsistent with the previous hypothesis of a strictly animal meat diet (Pérez-Pérez et al., 2003). Moreover, this study tried to correlate buccal microwear density with the climatic conditions of Europe during different Late Pleistocene phases: data shows a significant increase of microwear scratches found on specimens dated to glacial periods, while interglacial MIS corresponded to a sensible reduction of this striation's density (Pérez-Pérez et al., 2003). The previous phenomenon seems to be related to a shift in Neanderthal subsistence strategies during cold MIS (Pérez-Pérez et al., 2003). Recently the application of occlusal dental microwear texture analysis (DMTA) yield interesting results linked to Neanderthals. Specifically, Toussaint et al. (2010) described the first Neanderthal specimen analyzed with this technique: a sub-adult from Trou de l'Abîme at Couvin (Belgium). The microwear traces on the deciduous molar examined here, suggests a diet mostly consisting of tough nutrients, typical of meat-based diet. Therefore, an important analysis was conducted by El Zaatari et al. (2011) considering a very large sample (N=25), the authors confirmed that the Neanderthal microwear patterns follow specific paleoecological contexts. All the examined Neanderthal specimens, in this work, are well-dated and localized in a wide geographical range. Subsequently this advantage allowed the authors to divide the Neanderthal sample into three different paleocological groups correlating the past vegetal cover expansion with the occlusal dental surfaces (complexity vs anisotropy) (El Zaatari et al., 2011). A map with the dietary variability shows that the Neanderthals individuals from wooded environments (Amud 1, El Sidron 1, Grotta Breuil 2,

Saccopastore, Tabun 1, Zaffaraya 1) had easily access to a wide spectrum of vegetal food sources probably consumed in their daily alimentation. On the other hand, the Neanderthals specimens from cold-steppe and open habitats (Arcy-sur-Cure IVb6 B9, Guttari 3, La Quina 5 & 20, Ochoz 1, Spy 1, Subalyuk) were compared with a modern sample (including several hunter-gatherers with known diets), the result display close similarities to living Fuegians populations, suggesting a diet mostly consisting of terrestrial animals (El Zaatari et al., 2011). Finally, the third group is composed by Neanderthals who lived in ecological contexts with mixed vegetation that indicate a diet with affinities to the modern Chumash population, including approximately the same proportion between vegetal and meat sources (El Zaatari et al., 2011). Is interesting that the only outlier is the microwear pattern of Monsempron 3 that differs from all other Neanderthals previously analyzed, this individual shows similarities to the Khoe-San population from the Kalahari Desert suggesting a predominant vegetarian diet (El Zaatari et al., 2011). After this important study, many other authors used DMTA technique to distinguish the diet of other Neanderthal individuals. For example, Hlusko et al. (2013) observed the microwear patterns of Neanderthal teeth from Moula-Guercy (France), the result displayed a close similarity with the wooded habitats group suggesting a diet mostly composed by animal proteins (Hlusko et al., 2013). Then Harvati et al. (2013) conducted a microwear analysis on a Neanderthal sample from Kalamakia (Greece), the results show a mixed diet for these individuals (Harvati et al., 2013). Another study, using DMTA, was published by Karriger et al. (2016) and the Neanderthal sample consist of 19 molars from Krapina site (Croatia) and 4 molars from Vindija cave (Croatia). The authors argue that the Croatian individuals, compared to other Holocene modern human DMTA data, show dental texture related to low *Asfc* values (low surfaces relief) which indicates a higher quantity of meat into their diet (Karriger et al., 2016). Another interesting study was conducted by Estalrrich et al. (2017) both on dietary and para-masticatory behaviors of Neanderthals from El-Sìdron site (Spain), the sample consist of eight individuals which biological sex has been established. The intra-group observations of the microwear signatures shows that the females had a more abrasive diets or have used their teeth in more para-masticatory activities than did the males (Estalrrich et al., 2017). Another DMTA work is a re-study of the Neanderthals specimens from Hortus site (France), including several permanent and deciduous molars belonging to different individuals and divided in 3 chronological sub-phases: IVb – Va – Vb (Williams et al., 2018). The results show that the clear differences between individuals from Hortus correspond to both sub-phase variation in climate and intrinsic lifeways, in particular Neanderthals specimens related to sub-phase Vb exhibit reduced dietary hardness (*Asfc*) suggesting a greater consumption of soft foods like meat (F. L. Williams et al., 2018). The last DMTA work analyzed the molars of a Neanderthal individual (La Quina 5) from the French site of la Quina. The study was conducted by comparing this individual to other well-known specimens (both Neanderthals and modern pastoralist populations), the result shows a low anisotropy value implying the use of heterogeneous masticatory regimes like those characterizing foragers of the Americas (Williams et al., 2022).

N*eanderthal's para-masticatory activities reconstruction*: In contrast, regarding studies on the para-masticatory activities of Neanderthals, the number of analyses drops dramatically when compared to diet-related ones. However, several studies noticed that non-masticatory wear of Neandertals is accented when compared to modern hunter-gatherer populations, in fact incisors and canines typically appear much more worn than the premolars and molars (Lozano et al., 2017). The first study on this field was conducted by de Lumley (1973) on the Hortus sample and it's been already described in the previous section (See paragraph n. 2.2.2), from that moment a growing number of scholars started to focus their attention on this issue. A comprehensive paper is certainly the one published by Krueger

et al. (2017), where the authors analyzed a total of 45 permanent Neandertal anterior teeth. The sample ranges in chronology from MIS 7 to MIS 3 and includes specimens from 24 sites in eight countries across Western Eurasia: Croatia (2), Czech Republic (2), France (13), Great Britain (1), Hungary (1), Spain (1), Iraq (1), and Israel. The para-masticatory traces were processed with several statistical analyses and compared to historic modern human populations, in fact the Neandertal sample varied significantly by habitat, suggesting this factor was a principal driving force for differences in anterior tooth-use behaviors (Krueger et al., 2017). The authors affirm that: "The Neandertals from open habitats showed significantly lower anisotropy and higher textural fill volume than those inhabiting more closed, forested environments. The texture signature from the open-habitat Neandertals was most similar to that of the Ipiutak and Nunavut, who used their anterior teeth for intense clamping and grasping behaviors related to hide preparation. Those in more closed habitats were most similar to the Arikara, who did not participate in non-dietary behaviors. These Neandertal individuals had a broad range of texture values consistent with non-dietary and dietary behaviors, suggesting they varied more in anterior tooth-use behaviors and exploited a wider variety of plant and animal resources than did those from open habitats" (Krueger et al., 2017: 13). Another interesting study was published by Estalrrich & Rosas (2015) , this analysis detected para-masticatory features on 19 Neandertal individuals from l'Hortus (France), Spy (Belgium), and El Sidrón (Spain) sites, and the result shows that the differences detected on the overall activity-related dental wear pattern denote a division of labor by age and sex in these Neandertals groups (Estalrrich & Rosas, 2015). Another study was conducted by Lozano et al. (2017), the main aim of this work was focused on the reconstruction of the human handedness, using the orientation of the para-masticatory features on the anterior teeth, in a large sample of extinct hominins (from the early specimens of genus *Homo* to archaic *Homo sapiens*) (Lozano et al., 2017). The study also analyzed a pre-Neanderthal sample (previously considered as *Homo heidelbergensis*) from Sima de los Huesos (Spain), and a Neanderthal sample from eight European sites; in conclusion the authors argue that the Neanderthal individuals displayed a right-to-left hand ratio identical to that among modern human populations (Lozano et al., 2017).

CHAPTER 3: Site description and Materials

3.1 *Ciota Ciara* – Archaeological Site Description:

3.1.1 General introduction: The Ciota Ciara site is part of Monte Fenera's karstic system, and it is located at the entrance of the Sesia valley in Piedmont (north-western Italy), in particular the cave is positioned on the west part of the mountain at 670 m a.s.l. and it can be accessed from 2 main entrances (Fig 3.1). The archaeological importance of the Ciota Ciara cave is well-known since the beginning of the last century, however real and systematic excavations started just in the 60s when some test pits were realized (Daffara et al., 2021). The excavations were carried on during the 2009, after a period of fifteen years, in a systematic and multidisciplinary way by a research team from the University of Ferrara (Directed by professor M. Arzarello) in collaboration with *Soprintendenza Archeologia del Piemonte* (Fig. 3.1). In this context, four main stratigraphic units, with human activities, have been identified (103, 13, 14, 15) and each one corresponds to different modalities of frequentation of the site (Angelucci et al., 2019) (Fig. 3.2). Moreover, preliminary dating analyses of these units indicate that the human frequentation of the atrial part may date, in general, to the second half of the Middle Pleistocene period (Vietti, 2016).

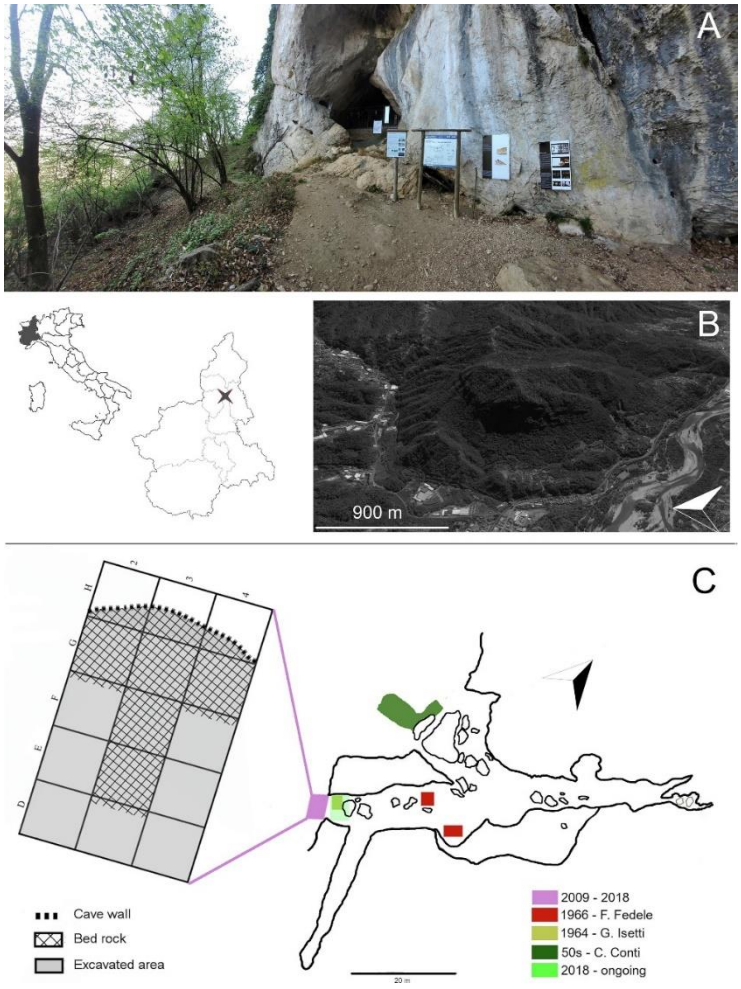

Figure 3.1 (A) South-western entrance of the Ciota Ciara cave; (B) Location of Monte Fenera and, on the right, view of the west side of the mount; (C) Planimetry of the Ciota Ciara cave showing the areas investigated during the 50s and the 60s and detail of the excavated area in the atrial sector of the cave. Pictures and citation taken from Berruti et al. (2023)

In 2018, the archaeological investigation was conducted also in the inner part of the cave, close to the protective gate (Arnaud et al., 2022) where units 13 and 14 were identified. Specifically, S.U. 14 corresponds to an intense human occupation, and S.U. 13 corresponds to a subsequential sporadic human occupation (Angelucci et al., 2019). The lithic assemblage of the stratigraphic units (13, 14, 103) is classified as Mousterian and is mainly composed by flakes, retouched tools, cores, hammers, and debris (Arzarello et al., 2012). Raw materials were exploited only through direct percussion technique (hard hammer), while different knapping methods have been recognized: S.S.D.A. (Système par Surface de Débitage Alterné, Forestier, 1993), Discoid, and Levallois (Arzarello et al., 2012). Moreover, lithic artefacts are made of various raw materials: quartz is predominant, followed by spongolite, sandstone, mylonite, opal and allochthonous flint (Daffara et al., 2019).

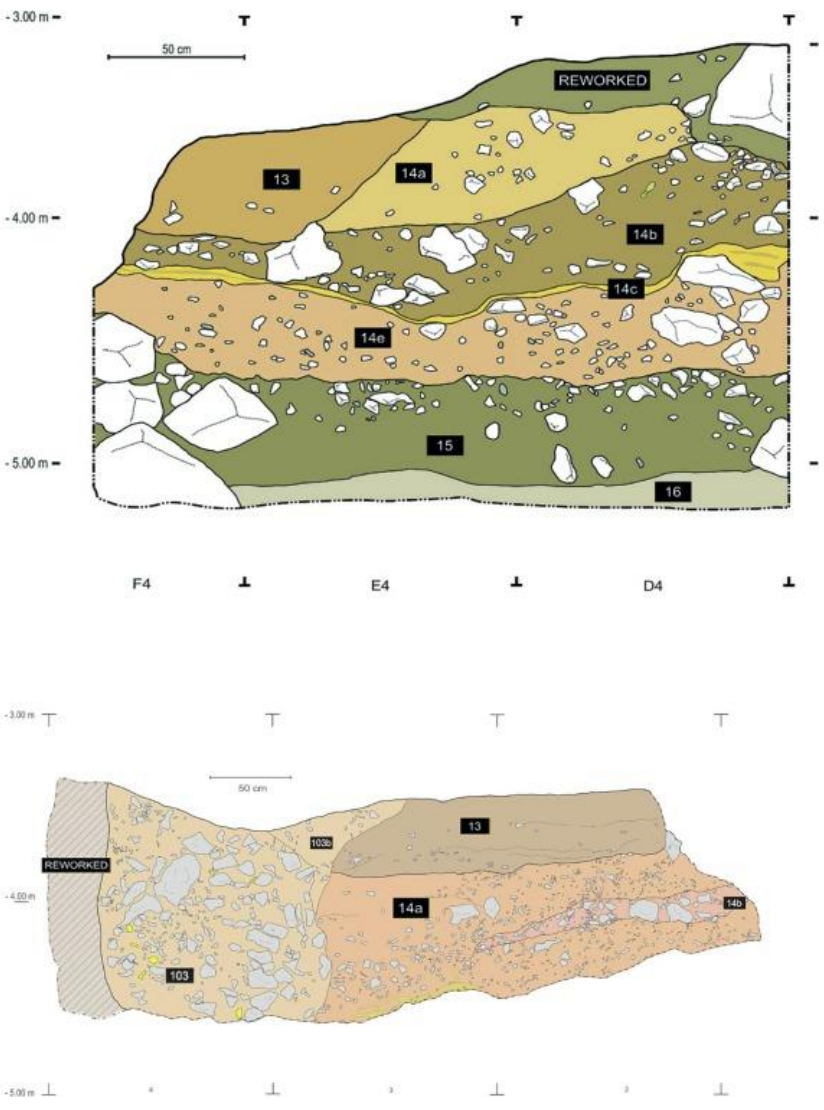

Figure 3.2 Ciota Ciara: Stratigraphic cross-sections across squares F4–D4 (top) and D4–D2 (bottom), at the end of 2016 excavation campaign. Pictures and citation taken from Angelucci et al. (2019)

3.1.2 Palaeoecological, Archaeozoological and Lithic use-wear Studies: Since one of the current work aims is to identify possible dietary micro-features on teeth, it was decided to further investigate previously completed research on other Ciota Ciara's materials (lithic industries and macro/micro faunal assemblages). Specifically, archeozoological, palaeoecological and lithic use-wear analyses will allow a comprehensive understanding of the environmental background and subsistence practices of the Neanderthal groups in this geo-chronological context, these recorded data will be cross-referenced and compared with the results of the current analysis to support (or not) the interpretation of the diet-related dental microwear features found on the analyzed human specimens.

Palaeoecological analysis: a first palaeoecological study, on Ciota Ciara's S.U. 13, 14 and 103, was published by Berto et al. (2016). The accurate analysis of both large and small mammals' assemblages allowed the reconstruction of a high biodiversity paleoecological context. For a complete list of all taxa analyzed in this study see Berto et al. (2016: 672-674). To obtain the paleoenvironmental reconstruction at Ciota Ciara cave, "Habitat Weighting" method was applied; while in order to infer the palaeoclimatic, "Mutual Climatic Range" method was applied. The authors argued that the paleontological data shows a paleoenvironmental condition mostly dominated by a woodland zone and just a slight climatic change is observable between stratigraphic units 13 and 14 (specifically, the climate was similar to the present one in S.U. 13 and colder in S.U. 14.) (Berto et al., 2016). As already mentioned previously, new radiometric dating indicates a frequentation of the atrial part of the cave, in general, to the second half of the Middle Pleistocene period (Vietti, 2016). In any case, paleoclimatic and paleoenvironmental data offer the possibility to speculate what types of faunal and plant resources might have been exploited and consumed by Neanderthal groups in the Piedmont area.

Archaeozoological analysis: an interesting archeozoological study was performed on Ciota Ciara's macro-faunal materials by Buccheri et al. (2016). Specifically, the analysis of several skeletal remains from the Stratigraphic Unit 14 (S.U. 14) allowed the identification of clear cut-marks on different type of animal taxa and bones. The position of the cut-marks can be related mainly to skinning and butchery activities made with unretouched flakes of different raw materials (Buccheri et al., 2016). The authors also noticed that, besides numerous herbivores remains, also some *Ursus spelaeus* and *Canis Lupus* bones displayed clear butchery traces related to disarticulation and flesh consumption. Is interesting to notice that the carcass processing activities of *U. spelaeus*, by Neanderthal populations, is just attested in other few European Middle Paleolithic localities: Biache-saint-Vaast (France), Taubach (Germany), and Scladina cave (Belgium), Nietoperzowa Cave (Poland). This further information is crucial because it allows to understand what kind of relationship existed between human populations and other carnivores in the occupation of the Ciota Ciara cave (i.e. Buccheri et al., 2016; Daffara et al., 2014), but more importantly, it allows to make indirect assumptions about part of the dietary behavior (related to meat consumption) of the Neanderthal groups in this geo-chronological context.

Lithic use-wear analysis: in addition, there is a study on the lithic use-wear analysis, conducted by Berruti & Arzarello (2012), on the Mousterian lithic assemblage from U.S. 13 of Atrio sector of the Ciota Ciara cave. The authors, in the conclusion, argue that: analyzing the set of lithic artifacts that shows use-wear traces, it seems evident a preponderance of worked materials with a hardness ranging from medium-hard to medium-soft which, according to Odell (Odell, 1981), range from fresh wood to leather and from dry wood to fresh antlers (Berruti & Arzarello, 2012). This study provides additional clues about part of the food resources that may have been exploited by the Ciota Ciara Neanderthals.

3.2 Materials

3.2.1 The Neanderthal specimens: The Ciota Ciara site has yielded human remains attributed to *Homo neanderthalensis* (Fig. 3.3). Specifically, the first findings include a fragment of temporal bone (Mottura, 1980) and two isolated teeth (Fenera 2 and 3), these latter two were collected in May 1989 without a clear archeological context and described in a publication by Villa and Giacobini few years later (Villa et al., 1996). Although, in more recent time, several new teeth specimens (N = 8) and an occipital fragment of cranium were discovered in the cave between 2019-2022 excavation campaigns. The occipital bone is particularly significant because it shows clear morphological features that suggest its appurtenance to an archaic form of *Homo neanderthalensis*. All the human remains have been found in the same layer: at the base of the S.U. 13. Regionally, these specimens are the only Middle Paleolithic human remains found in a certain stratigraphic context and for which it is possible to acquire data that goes beyond the morphological evaluation (Arnaud et al., 2022). As already mentioned, the radiometric dating analysis of the context yielded a preliminary chronology attested around the second half of the Middle Pleistocene period; if this dating is confirmed by the future analysis, it would represent one of the oldest recognized Neanderthal occupations in Europe.

3.2.2 Identification and state of preservation of the dental sample: The sample analyzed in the current analysis consists of seven *Homo neanderthalensis*' teeth (N = 7) divided in different typologies: three incisors, one canine and three molars. Each dental specimen has an identification code indicating: year of discovery, level and cut, square number, and sequence number. The eighth specimen ("CC22_13/9_G8") was discarded following the microwear selection criteria listed in paragraph *n.* 4.4.1. The teeth have been taxonomically attributed to *Homo neanderthalensis* based on morphological features (Arnaud et al. 2022, 2023), moreover the accurate analysis of the dental typology and rank was previously recognized by Julie Arnaud (University of Ferrara) following the basic rules of dental identification in paleoanthropology. Specifically, the sizes of the teeth crowns found in the Ciota Ciara cave were compared to a large comparison collection of more than 500 dental specimens including several human populations chronologically placed between the Paleolithic and recent periods (Arnaud et al., 2023). The three molars show reduced dimensions when compared to other teeth included in the comparison collection; specifically in terms of mesio-distal diameter, the tooth is positioned outside the variability range of Neanderthals (Arnaud et al., 2023). On the other side, the anterior dentition shows a crown size that is included in the variability range of the Neanderthal species (Arnaud et al., 2023). As already mentioned previously, all the human remains were found in a clear stratigraphic context of which the orientation, position and slope in the square was recorded; the only exception is related to the specimen "CC21_13/7_G8" (incisor) of which just the correspondent stratigraphic unit is known because it was found during the sieving process of the soil. A brief description of the dental specimens and their state of preservation will follow in according to the chronology of discovery.

- *CC19_13/3_E8_74*: is a second lower right incisor. The root is complete and the state of preservation of the enamel is optimal. It doesn't show erosion by use-wear or by post-depositional processes.

- *CC20_13/4_F8_52*: is a first upper left molar. Part of the root is missing and the state of preservation of the enamel is almost good. It shows an important occlusal erosion by use-wear and spots of black coloration probably due to chemical precipitation (manganese).

- *CC20_13/7_G7_238*: is an upper canine. The root is complete and the state of preservation of the enamel is optimal. Even in this case there is not erosion by use-wear and there is just a small crack on the labial surface, probably due to taphonomic processes.

- *CC21_13/7_G8*: is a superior incisor. The preservation is not good because the entire lingual and occlusal areas are destroyed by post depositional processes, but the labial face is preserved, and the enamel is in a useful state for the analysis.

- *CC21_13/7_G8_433*: is a second upper right molar. The roots are complete, and the preservation of the enamel is optimal. It doesn't show erosion by use-wear or by post depositional processes. It displays several residues of sediment in the occlusal part, specially between the cusps.

- *CC21_13/8_H7_36*: is a lower left incisor (first or second). The occlusal area is totally eroded probably due to post-depositional events, but the enamel on both the labial and lingual faces is in a good state of preservation.

- *CC22_13/5_F9_134*: is a first lower right molar. A small part of the roots is missing but the preservation of the enamel is optimal around all the surfaces. It shows a clear occlusal erosion by use-wear.

It is interesting to note that the anatomical determination of these teeth permits to assume a minimum number of individuals equal to one. However, the fossils specimens show different degrees of tooth wear: the two incisors, canine and upper second molar show a lower level of wear when compared to the other two molars (CC22_13/5_F9_134 and CC20_13/4_F8_52). For this reason, the current data suggest the presence, at least, of two distinct individuals (Arnaud et al., 2023).

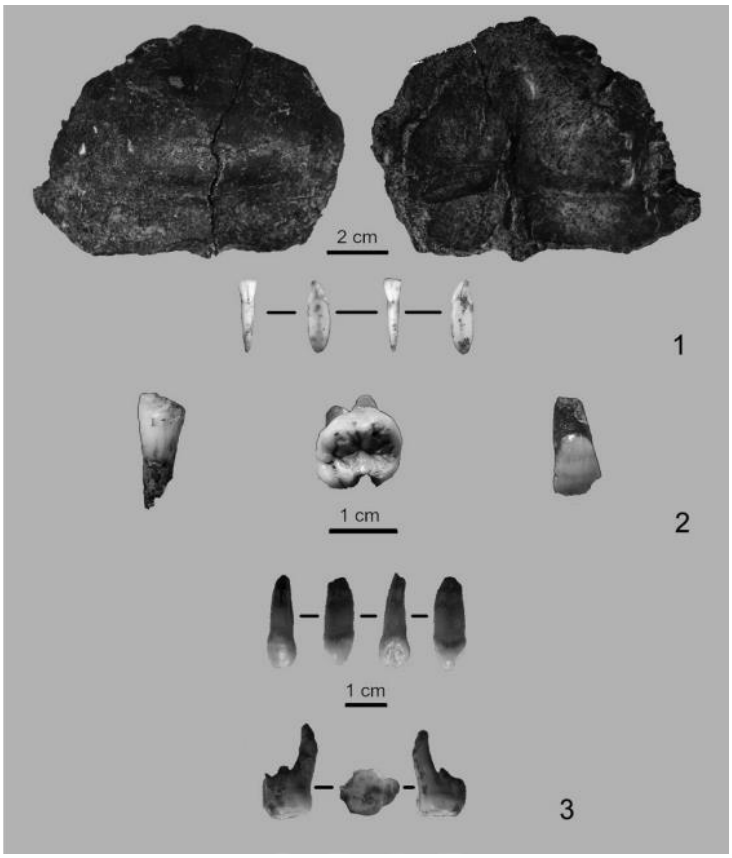

Figure 3.3 Human remains found during the 2019-2021 excavation campaigns in the internal part Ciota Ciara's cave: Occipital bone and incisor (1) (2019); two incisors and a molar (2) (2020); Canine and molar (3) (2021). Citation and picture taken from Arnaud et al. (2022)

CHAPTER 4: Methodology

4.1 Sample Selection and Teeth Cleaning phases

All Neanderthal dental specimens, from the archaeological context of Ciota Ciara Cave, have been accurately described in the previous chapter, but not each tooth can be used in a standard microwear study because of various constraints that limit the data acquisition. Therefore, this paragraph will show the main selection criteria of the dental material related to the current analysis and the consequent first cleaning process of the chosen specimens.

4.1.1 Sample selection: the complete assemblage is composed of eight dental remains found inside the Ciota Ciara cave between 2019-2022 excavation campaigns, plus two isolated permanent teeth (Fenera 2 and 3) collected in 1989 and described in a publication by Villa and Giacobini (Villa et al., 1996). These two teeth were found out of the stratigraphic context, and both were excluded from our study since the original specimens are currently inaccessible; however, it is important to mention that a previous analysis of dental microwear was already carried out and published by the same authors few years after the discovery of these first Neanderthal dental remains from the Fenera alpine caves (Villa et al., 1996). The remaining specimens, on the other hand, were sampled according with two main selection criteria:
1) The first step was to identify rank and type of each specimen because, in dental microwear studies, different teeth may give different information (Ungar, 2018). Since the current study aim is to analyze both paleodiet and para-masticatory activity's traces, all tooth types were considered here. As already specified in the earlier chapter, both dental typology and rank were previously recognized by Julie Arnaud (University of Ferrara) following the basic rules of dental identification in paleoanthropology[25] (see paragraph 3.2.2).
2) The second step was to select, at macroscopic level, only those intact teeth that shared an optimal state of enamel preservation without visible surface erosions and scattered cracks. This checking phase is crucial since a compromised tooth surface could suffer further damage and enamel removals in subsequent protocol process, whereas a well-preserved enamel surface may allow both molds (silicon negatives) and casts (epoxy-resin positives) to be replicate with a high level of feature resolution. For this reason, each single tooth was carefully observed by recording and describing every morphological and taphonomic alterations related to their state of preservation (see paragraph 3.2.2). As mentioned earlier, all dental findings were intact with the only exception of the specimen named "CC22_13/9_G8" which, being a small occlusal molar fragment, was excluded from the current protocol. Fortunately, all the other remains (N=7) had a good overall surface condition of the coronal enamel even though clear post-depositional signs were present in some areas (see paragraph 3.2.2), but not so severe that one of them should be totally excluded from the current analysis. After these initial general observations, the attention was focused on the occlusal and buccal surfaces of teeth (especially of molars) which represent the major areas of investigation of dental microwear works. Usually these two different surfaces (occlusal vs buccal) are rarely analyzed in the same study, but recent research have proved that both surfaces can offer complementary information with regards to understanding the turnover of microwear patterns (e.g. García-Gonzalez et al., 2015; Hernando et al., 2020, 2022). However, lingual surfaces were also considered as a comparative model since another aim of this study is to demonstrate that the traces found on the other dental surfaces (buccal and occlusal) have not been totally caused by post-depositional agents. Based on the previous

[25] To acquire a basic overview on the recognition of human teeth, see Hillson (1996)

description of materials (see paragraph 3.2.2), it was decided to exclude the following dental surfaces since the subsequent application of silicone could have penetrated the porous areas of the tooth causing irreversible damages: part of the lingual surface of tooth n. “CC20_13/4_F8_52” (molar), part of the lingual surface of tooth n. “CC21_13/7_G8_433” (molar), the complete lingual and occlusal surfaces of tooth n. “CC21_13/7_G8_//” (incisor), the complete occlusal surface of tooth n. “CC_21_13/8_H7_36”.

4.1.2 Teeth cleaning process: All the original Ciota Ciara’s human specimens are stored, with all the necessary precautions, inside a protective case at “Dipartimento di Studi Umanistici” (University of Ferrara) (Fig. 4.1). The cleaning process of the selected specimens were made at the Paleoanthropological laboratory of the University of Ferrara (Ferrara, Italy) by adhering to strict control standards for protect the Neanderthal remains from any potential damage or contamination: use of mask, latex gloves, clean instrumentations, and controlled room temperature/humidity. The standard tooth cleaning procedure include the use of cotton swabs soaked in pure acetone rinsed in 70-95% ethanol and gently applied on the enamel surface, the process is complete when the tooth is finally airdried (Galbany et al., 2004). Usually, this type of cleaning is a standard practice to remove adhesive residues and dust which may hide possible dental micro-features (Galbany et al., 2006). However, in the current case of study a simple dry cleaning with a soft brush was chosen to avoid possible DNA contamination of the specimens using liquids[26] (Willerslev & Cooper, 2005). All the Ciota Ciara’s teeth were gently and carefully brushed, with the only exception of tooth n. “CC21_13/7_G8_433” (molar) that displayed an occlusal surface enriched in soil particles deeply adhering between the cusps and, for this reason, the mechanical removal action of the dry brush was ineffective.

Figure 4.1 Original Dental specimens from the Ciota Ciara cave that have just been removed from their safety case for the cleaning process at the Paleoanthropological Lab. Ferrara University. Photo taken by M. Mattera with a reflex camera Nikon D3100 (December 2022)

[26] For a comprehensive overview on the treatment of human teeth as a paleogenetic source, see Higgins & Austin (2013)

4.2 Molds (Negatives) and Casts (Positives) Elaboration

The following methodology is based on other published works (e.g. Galbany et al., 2004, 2006; Goodall et al., 2015) and was conducted and applied under the supervision of Julie Arnaud (University of Ferrara) and Marina Lozano (IPHES). The entire protocol was set up in two different laboratories: the Paleoanthropological laboratory at the University of Ferrara (Ferrara, Italy) and the Archaezoology laboratory of IPHES (Tarragona, Spain). As mentioned in the previous teeth cleaning step, even during these phases the same strict control standards (see paragraph 4.1.2) were applied to avoid possible damages to the original specimens.

4.2.1 Molds (Negatives) Elaboration: As argued by Galbany et al. (2004), the main reason for using tooth replication techniques, in paleoanthropology, is related to the rarity and fragility of original hominin specimens that cannot be studied directly by SEM; in addition, the replicas allow in turn to visualize inaccessible areas on the original dental remains (Galbany et al., 2004). Silicon-based replication procedures were originally developed for medical and odontological care, but then become frequently used in dental microwear research (Ungar & Spencer, 1999). The negative casts are usually made by applying hydrophobic polyvinylsiloxane silicones that can duplicate features with resolutions to a fraction of a micron (Galbany et al., 2004). As mentioned earlier, the mold protocol was set up at the Paleoanthropological laboratory of Ferrara University and was divided in several phases. First, the original Neanderthal specimens, already cleaned, were placed on a clean polystyrene slab that had been perforated previously to accommodate each tooth related to an identification label. Then a high-resolution Polyvinylsiloxane President microSystem^{TM} (green color) - Regular body (Coltène®)[27] was applied on the teeth 'surfaces using a gun-dispenser as recommended by various investigators (i.e. Galbany et al., 2004; Goodall et al., 2015) (Fig. 4.2). The silicone paste was applied to the entire dental crown (as a small hat) only when the enamel was intact all around (Fig. 4.3), on the contrary it was applied to each single surfaces (buccal, occlusal, and lingual) in all other cases.

Figure 4.2 Photo of the Molding Process at the Paleoanthropological Lab. of Ferrara University. High resolution silicone is applied individually to each specimen using a gun dispenser, teeth are placed back into the polystyrene slab at the end of the process. Photo taken by J. Arnaud with a reflex camera Nikon D3100 (December 2022)

[27] Coltène® brand developed several silicone pastes related to different characteristics. *Light Body* provides a more faithful cast. *Regular Body* shows enough resolution to analysis by SEM at high magnification. *Heavy Body* shows somewhat less resolution (Galbany et al., 2004: 6)

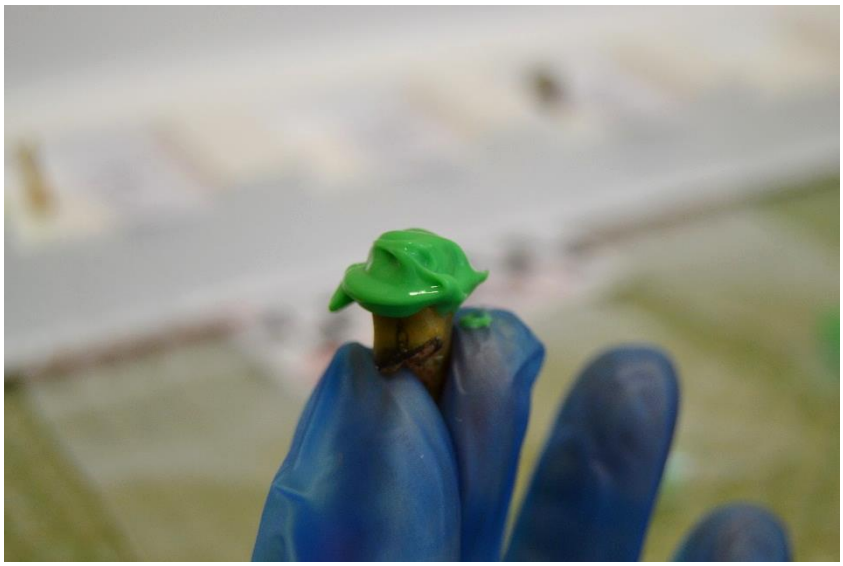

Figure 4.3 Particular image of specimen n. "CC20_13/4_F8_52" during the Molding Process at the Paleoanthropological Lab. of Ferrara University. Original Neanderthal specimens with an intact dental crown can be totally covered by the silicone paste as in this case. Photo taken by M. Mattera with a reflex camera Nikon D3100 (December 2022)

Based on previously described morphological and taphonomic alterations related to the preservation sate of the Ciota Ciara's teeth (see paragraph 3.2.2), it was chosen to apply the silicone to the following single tooth surfaces: labial and lingual surfaces of tooth n. "CC_21_13/8_H7_36" (incisor), the labial surface of tooth n. "CC21_13/7_G8_//" (incisor). As recommended by Galbany et al. (2004), the silicone was pushed on the surfaces by applying a slight pressure with the dispenser tip, this expedient allow to reduce the chance of bubble forming in contact to the enamel surface (Galbany et al., 2004). After being left to dry for a few minutes (3-5 minutes approx.), the negative molds were pulled out from the teeth and stored inside labelled plastic bags to protect them from particles and further alteration (Fig. 4.4). Two equal groups of negatives molds were produced (a double copy for each tooth), a first group of silicone impressions was made just to be stored for future analyses, while the second group of casts were used to made positive epoxy casts.

Figure 4.4 Photo taken at the end of the Molding process at the Paleoanthropological Lab. of Ferrara University. Double copies of negatives were preserved in labelled plastic bags. Photo taken by M. Mattera with a reflex camera Nikon D3100 (December 2022)

4.2.2 Casts (Positives) Elaboration: The second main step included the processing phase of the previous negative molds, using melted epoxy-resin, to obtain high resolution positive casts of the teeth. As argued by Galbany et al., (2004), epoxies are generally the easiest constituents to apply since they offer the best combination of working time, setting time, viscosity, resolution of detail, and dimensional stability, not only for dental anthropology field (Galbany et al., 2004). This step was set up at the Archaezoology laboratory of IPHES (Tarragona, Spain) by using a high-resolution polyurethane resin (Epoxy Eporai 1060 A) from the previous second group of molds. Before pouring the epoxy resin into the negatives, the two components (A+B) were stirred by hand using a wood stick to eliminate air bubbles from the mixture (parts A and B are mixed in a 1:4 weight ratio). Meanwhile, it was necessary to glue the molds on a plastic basement and build a containment wall around them using another mixture of silicone (President microSystem^{TM} Heavy body – blue color) (Fig. 4.5), this procedure was useful for those molds that presented flatness or irregularities and to prevent epoxy-resin from seeping out of the negatives before it sets. Finally, the fixed molds were placed on a plastic tray covered with a sheet of paper, at this point the epoxy-resin was poured carefully into the silicone impressions by using a Pasteur pipette (Fig. 4.6). The casts were left to solidify under a fume hood (to avoid extraneous agents) in a controlled laboratory environment for at least 48 hours. At the end of this process, the solidified molds were stored inside new labelled plastic bags and closed in a protective case.

Figure 4.5 Photo of the cast elaboration at the Archaezoology laboratory of IPHES (Tarragona, Spain). The previous molds were glued on a plastic basement to keep them locked during the casts realization. Photo taken by M. Mattera with an Apple iPhone SE of second generation (January 2023)

Figure 4.6 Photo of the cast elaboration at the at the Archaezoology laboratory of IPHES (Tarragona, Spain). The epoxy resin mixture was poured inside the negative impressions using a pipette. Photo taken by M. Lozano with an Apple iPhone SE of second generation (January 2023)

4.3 Pre-Treatment Procedure, Microscopy Settings, and Images Comparison

This paragraph represents the methodological core of the current work since our proposal is to record multiple microwear observations in homologous dental areas, using different type of microscopes, to detect potentials and limitations of this approach. Therefore, the following sections will explain how the analytical tools were set up in according to the research objectives.

4.3.1 Pre-Treatment Procedure: As already mentioned previously, original specimens are too valuable to be studied directly by Scanning Electron Microscopy because this type of technology only works with metallized surfaces. The sample, in fact, requires an irreversible gold coating layer that permits the conduction of electrons over the surface (Galbany et al., 2004). For this reason, the dental casts used in the current study received a pre-treatment before being observed under the ESEM and the procedure was set up at the Scientific and Technical Resources Department of Universitat Rovira i Virgili (Tarragona, Spain). Specifically, the dental casts have been separated mechanically from their molds and glued to numerated metallic stubs (Fig 4.7). After that, casts were sputter coated with a 30 nm gold layer related to a time of exposition of 90 seconds using a BAL-TEC Sputter Coated SCD 004 (Fig. 4.8). It is important to mention that in order to observe both the buccal and lingual surfaces of the different complete teeth, it was necessary to re-glue the casts on the stubs with opposite orientation and expose them to a second process of gold coating.

Figure 4.7 Pre-Treatment procedure set up at the Universitat Rovira i Virgili - scientific and technical resources Department. Example of positive cast (specimen n. "CC20_13/4_F8_52") that has been separated from his negative mold and glued on a metallic stub. Photo taken by M. Mattera with an Apple iPhone SE of second generation (March 2023)

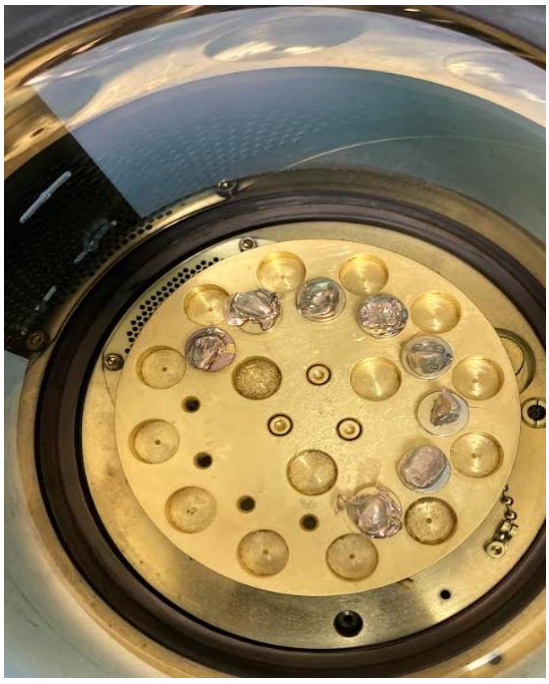

Figure 4.8 The Ciota Ciara's teeth casts after the sputter coating process at the Universitat Rovira i Virgili - scientific and technical resources Department. Photo taken by M. Mattera with an Apple iPhone SE of second generation (March 2023).

4.3.2 Microscopy Settings: The currently study involved the use of 4 different Microscopes. As already mentioned previously, standard buccal dental microwear protocols involved mainly the use of Scanning Electron Microscopy (see paragraph 2.3.2).

Environmental Scanning Electron Microscope (ESEM): One of the microscopy equipment used in this study consisted of a FEI QUANTA 600 Environmental Scanning Electron Microscope (ESEM) located at the Universitat Rovira i Virgili - Scientific and Technical Resources Department (Tarragona, Spain) (Fig. 4.9). As previously mentioned, teeth's casts were mounted on a metallic stub prior to introducing them into the microscope's chamber to ensure their correct positioning on the chamber stage. Inside the microscopy chamber, the gold-coated samples were positioned perpendicularly to the electron beam. It is important to remark that the ESEM, for this study, was always used in low vacuum mode and not in environmental conditions because is not a necessary requirement for teeth casts. The casts were analyzed using the methodology of Pérez-Pérez et al. (1994) with the following parameters: large field detector-LFD, pressure of 0.68 Torr, voltage of 20 kV, 4.5 spot size, working distance was variable between 15 and 20 mm, and magnification detail range between a minimum of 20x (for a general whole image) and a maximum of 510x (for capture the details). The standardize paleodietary protocol concern the acquisition of pictures taken at 100x magnification on the medial area of the molar's buccal surface, avoiding both the occlusal and cervical thirds. In fact, Pérez-Pérez et al. (1994) argued that: this standard procedure is widely used for microwear analysis on the buccal surface of teeth to infer dietary habits because it covers a significantly broad patch of enamel, where striations of various lengths are clearly the main feature that can be observed. On the other side, the predetermined magnification related to molar's occlusal surfaces is established at 500x (Teaford & Walker, 1984). Concerning the lingual surfaces and the labial surfaces of the anterior dentition, all the samples were observed and analyzed in their occlusal third, middle third and cervical third' areas, using a free range of magnification, mainly to detect and discriminate para-masticatory or taphonomical traces to be compared.

Figure 4.9 Observation process of Ciota Ciara's dental casts using ESEM microscope at the Universitat Rovira i Virgili - scientific and technical resources Department. Photo taken by M. Mattera with an Apple iPhone SE of second generation (March 2023).

Zeiss (Metallographic Optical Microscope): the second microscopy equipment is a Zeiss Axioscope A1 optical microscope located in the Lithic laboratory of IPHES (Tarragona, Spain) (Fig. 4.10). The microscope was equipped with a Differential Interference Contrast system (DIC) and three Epiplan lenses were used for this study: a 50x a 100x and a 200x. The camera used with the OM is a 6.3 MP Color Blackfly S USB 3.0 Camera, 1/1.8″, FLIR, and the software used to control image acquisition is Kivy Capture MIC Z. Then, the software Helicon Focus 5.3 (Plisson and Zotkina, 2015) was used by applying a "pyramidal" mounting method C, since it eliminates common image aberrations that form when working with highly reflective materials as gold coated epoxy casts (Hernando et al., 2020).

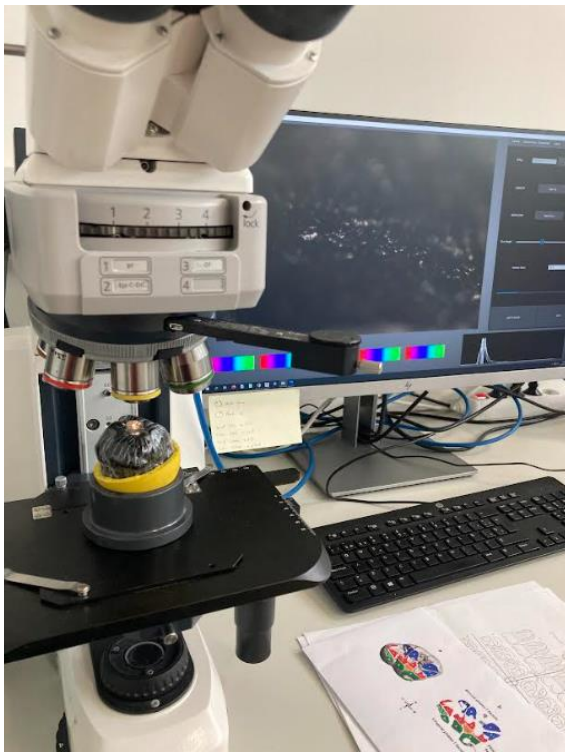

Figure 4.10 Observation process of Ciota Ciara's dental casts using Zeiss microscope at Lithic laboratory of IPHES (Tarragona, Spain). Photo taken by M. Mattera with an Apple iPhone SE of second generation (April 2023).

Hirox (3D Digital Microscope): the third microscopy equipment is a Hirox KH-8700 3D Digital Microscope located in the Lithic laboratory of IPHES (Tarragona, Spain) (Fig. 4.11). This tool was equipped with a dual illumination revolver zoom lens (MXG-5000REZ) which together with the high intensity LED light source allows for the observation of specimens with a color temperature (5700 K) close to that of daylight (5460 K). This lens consists of a triple objective turret with a different zoom range per objective, allowing for magnifications ranging from 35x to 5000x (HFOV 8,6 mm–60 μ) (Martín-Viveros & Ollé, 2020). However, the currently study employed only 4 types of lenses: 35x, 50x, 100x and 140x. Hirox incorporates a dual illumination system that allowed for the observation of sample topography using two typologies of light: ring and coaxial. For this analysis, ring and coaxial lights were used indistinctly according to the observation conditions required by the dental specimens.

Confocal Microscope: the fourth microscopy equipment is a Confocal Microscope - Sensofar® S Neox 3D optical profilometer located in the Lithic laboratory of IPHES (Tarragona, Spain). The dental casts were positioned under the light beam as horizontal as possible, initial observations were done between 5x and x10 magnification to find the area of interest on the buccal middle third of

molars. The buccal surfaces data were finally measured at 100x to obtain comparable images. Is important to remark that the confocal profilometer, for this study, does not follow the standard DMTA procedures (without the use of the Tootfrax® software), but the images were obtained just to have a methodological comparison.

Figure 4.11 Observation process of Ciota Ciara's dental casts using Hirox microscope at Lithic laboratory of IPHES (Tarragona, Spain). Photo taken by M. Mattera with an Apple iPhone SE of second generation (April 2023).

4.3.3 Images processing and comparison: to properly compare each dental micro-features (see paragraph 5.4 in "Results"), images acquired from the microscopes were processed by using the photo editing software Adobe Photoshop®: images were cropped to an area of 0,56 mm^2 following the methodology of Pérez-Pérez et al. (1994). Then an automatic adjustment of grey levels was applied to enhance image contrast (Galbany et al., 2004), this step provides a useful visualization of microwear features for the next quantitative data acquisition on ESEM images (see paragraph 4.4.1). Subsequently, graphic tables were developed to compare the processed images, the tables are divided by specimen and allow a clear and uniform visualization of microwear 'differences in homologous dental areas. For methodological standardization the length and orientation of the striations were recorded within the surveyed area, although some of them surpassed the limits of microscopes' photograph. Each graphic table will be associated to a pair of informative tables divided for different microscope (ESEM, Hirox and Zeiss) with the following data: counted striations and/or pits, average length of the striations, average orientation of the striations; then, for each of those, the following variables will be provided: Mean, Standard deviation, Maximum and Minimum length recorded. The main problem related to this comparative methodological approach was already noticed in previous studies on tool use-wear analysis (i.e. Martín-Viveros & Ollé, 2020), in fact different microscopes do not yield a direct equivalence in the magnification of the pictures. This issue is mostly caused by the differences between the microscope's camera associated, plus the variable field of view that they record. Several comparative works have pointed out many difficulties in the selection of homologous dental areas; this issue happen mainly because, besides reporting the original magnification, the

critical information needed to allow comparison between images obtained with different microscopes is the inclusion of a scale bar and/or a reference to the horizontal field of view (Hernando et al., 2020: 8) However, in the current study it has been possible to select and take pictures of the same dental areas (with the previously listed microscopes) by using a table of equivalence among the magnifications (Mag) and the horizontal field of view (HFOV), the table was taken from the work of Martín-Viveros & Ollé (2020) (Table 4.1).Considering these references, the same screen dental areas in the three microscopes, can be selected to check how effectively the images' microfeatures are comparable.

Post-mortem and ante-mortem features (not related to diet), on the other hand, were detected and compared using images at different magnifications. Specifically, post-depositional alterations (as enamel cracks, post-mortem dental chipping etc.) were not properly recorded and scored in this work (see paragraph 5.2 in "Results"), since the recognition protocols must be carried out by observing the originals teeth following a standard methodology (e.g Bonfiglioli et al., 2004; Scott & Winn, 2011). In fact, other dental surfaces of the Ciota Ciara's sample, discarded by using the previous listed selection criteria (paragraph 4.1.1), shows evident traces of post-depositional effects (e.g. the lingual area of tooth *n*. CC21_13/7_G8_433); for this reason is not possible to give a correct numerical percentage, for the current analysis, related to the post-mortem features. However, ante-mortem/para-masticatory features were studied and described mainly by comparison (see paragraph 5.3 in "Results"), following the methodologies designed by different authors (i.e. Bonfiglioli et al., 2004; Lozano et al., 2008). Bonfiglioli et al (2004) designed a scored table related to ante-mortem chipping, these features are classified on a three-grade scale by evaluation of its size and depth: grade 1 - slight crack or fracture (0.5 mm), or larger but superficial enamel flake loss; grade 2 - square irregular lesion (1 mm) with the enamel more deeply involved; grade 3 - crack bigger than 1 mm involving enamel and dentine or a large, very irregular fracture that could destroy the tooth (Bonfiglioli et al., 2004: 449). On the other side, possible para-masticatory labial striations detected on the Ciota Ciara's sample, were studied following the identification criteria developed by Lozano et al. (2008).

Microscope model	Mag	*HFOV Deltapix/Aco-z	Mag SEM	HFOV SEM
Zeiss Axio Scope A.1	50×	2265/2942 µ	135×	2210 µ
	100×	1130/1467 µ	260×	1150 µ
	200×	564.32/726 µ	510×	585 µ
	500×	225.93/295 µ	1250×	239 µ
Hirox KH-8700	35×	8665 µ	35×	8514 µ
	50×	6065 µ	50×	5960 µ
	100×	3032 µ	100×	2980 µ
	140×	2166 µ	140×	2125 µ
	150×	2021.8 µ	150×	1986 µ
	200×	1516.4 µ	200×	1490 µ
	250×	1213 µ	250×	1192 µ
	400×	758. 2 µ	400×	745 µ
	600×	505.5 µ	600×	497 µ
	700×	433.3 µ	700×	425 µ
	800×	379.1 µ	800×	373 µ
	1000×	303.3 µ	1000×	298 µ
	2000×	151.6 µ	2000×	149 µ
	3000×	101.1 µ	3000×	99 µ
	4000×	75.8 µ	4000×	74.5 µ
	5000×	60.7 µ	5000×	59.7 µ

Table 4.1 Equivalence among the magnifications (Mag) and the horizontal field of view (HFOV) achieved in the three microscopes models (OM, 3D DM, and SEM). *HFOV = value according to DeltaPix and Aco-z Softwares in Zeiss model and monitor size in 3D DM and SEM models. Hirox KH-8700 (21.5″), SEM FEI Quanta 600 (19″). Table and citation taken from Martín-Viveros & Ollé (2020)

4.4 Quantitative data and Statistical analyses

4.4.1 Quantitative data: On each resulting image, dental microfeatures were counted and measured by using an open access software, ImageJ. Specifically, the segmented line tool was applied to measure lengths and widths of the microwear features, and the angle tool for calculate the orientations when necessary. The metric scale is always expressed in micrometers (μm), it was set each time the image was changed by adapting it to the metric scale bar already showed on the captured photograph from the microscopes. To optimize the visualization of the striations on the dental surfaces, the "ROI manager" tool was chosen, it allows a double process of counting each striation and, at the same time, measuring several variables related to them. Then, each counted element was underlined in red color using the function “Fill” to maximize the visibility of dental features pattern. This methodological procedure allows 1) To calculate and obtain quantitative data for each analyzed feature. 2) to graphically detect similarities and differences in the number of microwear traces by comparing images taken from different microscopes. All the quantitative data from ImageJ were exported and processed on EXCEL and PAST v. 4.09 software for the statistical analyses.

4.4.2 Statistical analyses: Statistical analyses will be divided in two main paragraphs. The first section will cover the statistical analysis of the methodological microwear comparison between different microscopes. Specifically, quantitative data related to number of striations recorded and total mean of the striations’ length will be divided and measured for several variables (NT, NDM, NMD, NH, NV) and, then, compared using numerical/percentage tables and boxplot graphs. Therefore, to test the significant differences between the previous variables, some statistical tests will be applied. All statistical tests and plots were created using PAST v. 4.09 software by exporting the numerical data previously organized in EXCEL. On the other hand, statistical analyses for a preliminary paleodiet reconstruction were performed on previously obtained quantitative data (only on molar buccal surfaces) following a standardized methodology derived by other similar microwear studies (e.g. Galbany et al., 2005; Pérez-Pérez et al., 1994; Pérez-Pérez et al., 1999, 2003). As already mentioned, the methodology in question considers the complete analysis of buccal striations: a striation was defined as a linear feature being at least four times longer than its width (4:1 ratio), and with a minimum length of 15 micrometers (μm) (Pérez-Pérez et al., 1994). Since the width of diet related striations on the buccal enamel surfaces range from 1 to 5 μm, striations longer than 15 μm can be easily oriented to define their maximum diameter and to discriminate them from pits. Striation lengths were measured in μm and their orientation classifieds in degrees from 0º to 180º relative to the cement-enamel junction, this landmark was also used to properly orient the dental specimens in the ESEM chamber. For each observed striation, the orientation angle was classified into four, 45º orientation class-groups following the methodology developed by Perez-Perez et al. (1994) (Fig. 2.4). Four discrete orientation categories were derived: horizontal (H), vertical (V), mesio-distal (MD) and disto-mesial (DM). For each category (H,V, MD and DM), as well as for all observed striations (T), the number of striations (N), their average length (X) in μm, and the standard deviation of their length (SD) were calculated. Thus, 15 quantitative variables were derived (NT, XT, STDT, NV, XV, STDV, NH, XH, SH, NMD, XMD, STDMD, NDM, XDM, STDDM), which constitute the buccal microwear pattern analyzed sample. Moreover, to compare the obtained results with other buccal microwear data, indexes of relative frequently of striations by orientation were calculated by dividing the number of horizontal and vertical striations by the total number of observed striations (NH/NT, NV/NT). An index of the number of horizontal to vertical striations (NH/NV) was also calculated. Intra and inter-observer error is a major problem in microwear measurements. But Ciota Ciara’s sample images were processed just by a single observer (M. Mattera), for this reason no comparison for inter-individuals statistical error differences were performed.

CHAPTER 5: Results

This chapter will essentially describe, in the first part, the various problems/alterations that were detected during the standard microwear protocol phases and recognized only later on the images obtained with the microscopes. Specifically, one paragraph will be focused on the methodological errors made during the previous steps of the experimental protocol (paragraph 5.1), while another paragraph will concern the analysis of taphonomic/post-depositional processes recognized on the Ciota Ciara's teeth casts (paragraph 5.2). In the second part of the chapter, on the other hand, the recognized ante-mortem/para-masticatory traces (paragraph 5.3), the results obtained from the methodological comparisons of the dental micro-features (paragraph 5.4), and the statistical analyses related to the previous comparative study and the preliminary dietary reconstruction (paragraph 5.5), will be presented.

5.1 *Detecting Methodological Errors*

As already mentioned, dental microwear is a powerful tool. But sometimes paleodietary interpretations based on microwear data are vulnerable to error from several sources. The most common issues are mainly related to numerous methodological errors, including inconsistencies in the specific tooth and wear facet chosen for analysis (Krueger et al., 2008), variable or inappropriate cleaning/casting/molding methods (Williams & Doyle, 2010), variable instrumentation settings, images aberrations, and inconsistent feature definitions (Gordon, 1988). Moreover, observer variation in the interpretation and measurement of microwear features is considered, by several authors, as potentially one of the more problematic aspects of standard dental microwear analysis (Galbany et al., 2006; Grine et al., 2002). Although the publications related to the methodological obstacles in dental microwear analysis are few (e.g. Galbany et al., 2004), and the information loss associated with tooth replication techniques is rarely considered (Mihlbachler et al., 2019). A list, with photographic examples, of all the methodological errors observed in the study of the Ciota Ciara dental specimens will follow:

5.1.1 Dental Surface Alterations: surface alterations that do not have a post-depositional cause can be numerous and of different origins, in the current study the following alterations were observed: irregular surface deformations and porosity, presence of embossed air bubbles or other contaminants, and dark surface patches.

Irregular surface deformations and porosity: These are very pronounced surface deformations that may depend on the properties of the silicone, in fact, materials that cure slowly and begin to shrink relatively early in the curing process are less accurate and show blurred and unexpected traces (Sawaura et al., 2022). But it may also depend on the carelessness and inexperience of the experimenter because these deformations are mainly caused by an incomplete shrinking process during the molding phase that doesn't allow the silicone to adhere properly on the surface of the dental enamel. The result obtained makes it possible to visualize a kind of tear mark with plastic deformations and accentuated porosity (air bubbles) due to the failure of the silicone adherence, implying that the molds were peeled off from the tooth surface before the required time. Fortunately, this type of methodological error was found, in a wide area, only on the labial surface of sample *n*. "CC21_13/7_G8" (Fig. 5.1, 5.2) This is an uncommon error that is not much mentioned in scientific publications about dental microwear methodologies, in this case, it was mainly due to the experimenter's inexperience in the use of high-definition silicones during the molding process. While, spread microscopic air bubbles porosity are more common (Galbany et al., 2004).

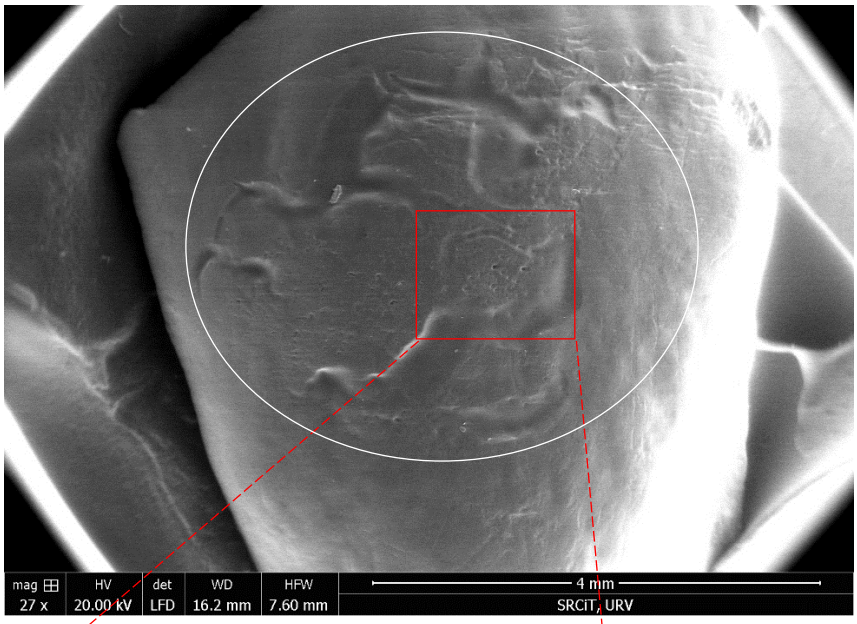

Figure 5.1 ESEM capture image of the cast specimen *n*. CC21_13/7_G8 (Incisor) labial surface at 27x magnification. Notice that the plastic surface deformations (inside the white circle) on most of the occlusal/middle third area were due to a mistake occurred during the molding phase. Photo taken by M. Mattera and M. Lozano using the FEI QUANTA 600 environmental scanning electron microscope (ESEM) at the Universitat Rovira i Virgili - scientific and technical resources Department. (March 2023)

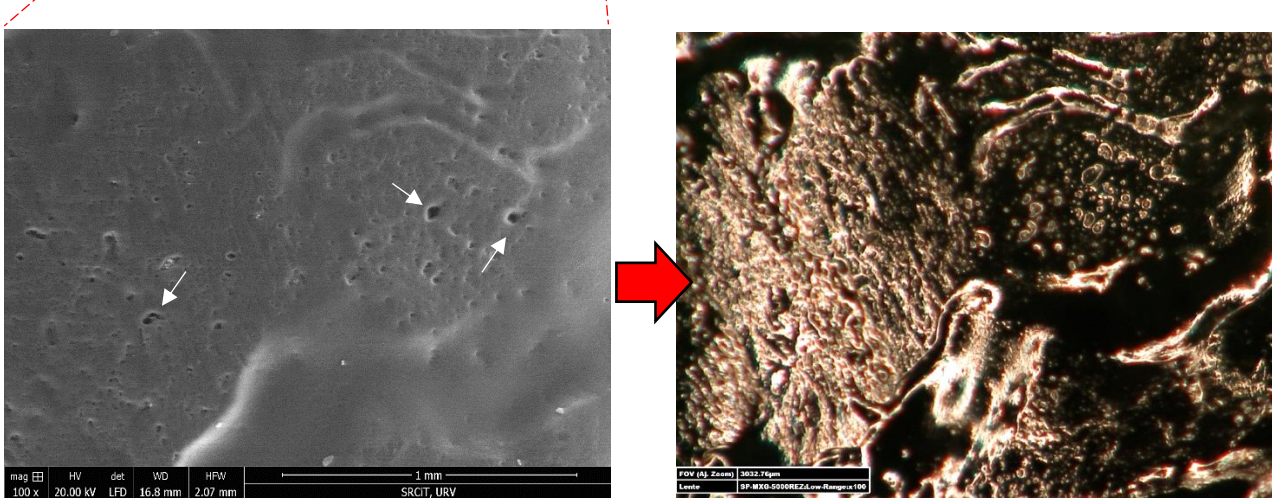

Figures 5.2 On the left photo, detail at 100x magnification of the cast specimen *n*. CC21_13/7_G8' middle third area; is possible to recognize evident plastic deformations and spread porosity (white arrows) caused by a failure of the silicon application. Photo taken by M. Mattera and M. Lozano using the FEI QUANTA 600 environmental scanning electron microscope (ESEM) at the Universitat Rovira i Virgili - scientific and technical resources Department (March 2023). On the right photo, detail at 100x magnification of the same labial area using a Hirox KH-8700 3D Digital Microscope located in the Lithic laboratory of IPHES (Tarragona, Spain) and taken by M. Mattera (April 2023).

Presence of embossed air bubbles and other contaminants: unexpected errors can also occur during the cast formation process; it can often happen that air bubbles (left by the previous molding process) or other contaminants, can create rounded surface masses in relief that causes a loss of information, more or less extensive, in different areas of the replica. These are rather common mistakes since the air bubbles formed in the previous process will be filled by the epoxy-resin solution. The recommended way to prevent this type of problem is to make multiple molds of the same tooth surface, and then choose the one that is most suited for obtaining a good-quality positive. Different surface areas of the dental specimens in this study exhibited this problem by observing them with different types of microscopes and at multiple magnifications/size ranges (Fig. 5.3, 5.4, 5.5).

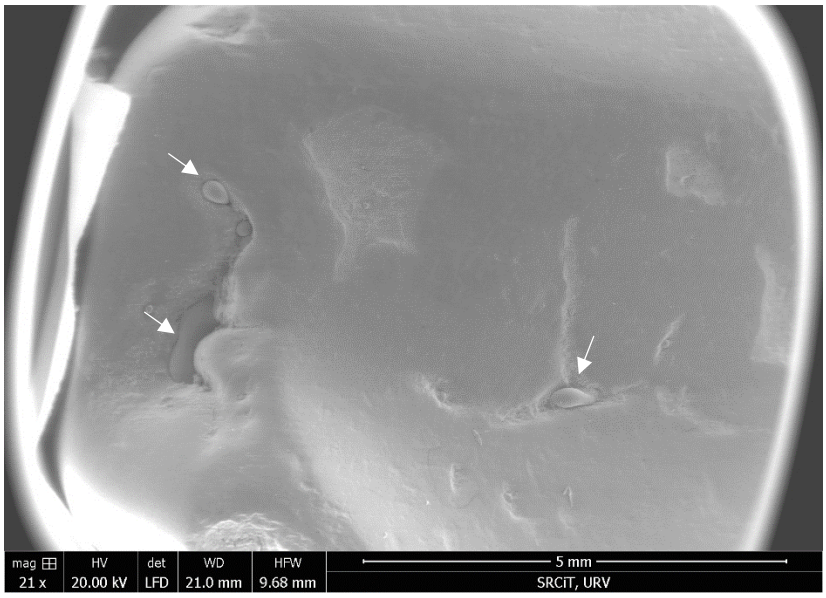

Figure 5.3 ESEM capture image of the cast specimen *n.* CC20_13/4_F8_52 (molar) occlusal surface at 21x magnification. Notice that the air bubbles contaminations (white arrows) are clearly visible in distinct areas of the molar surface even at lower magnification. Photo taken by M. Mattera and M. Lozano using the FEI QUANTA 600 environmental scanning electron microscope (ESEM) at the Universitat Rovira i Virgili - scientific and technical resources Department. (March 2023)

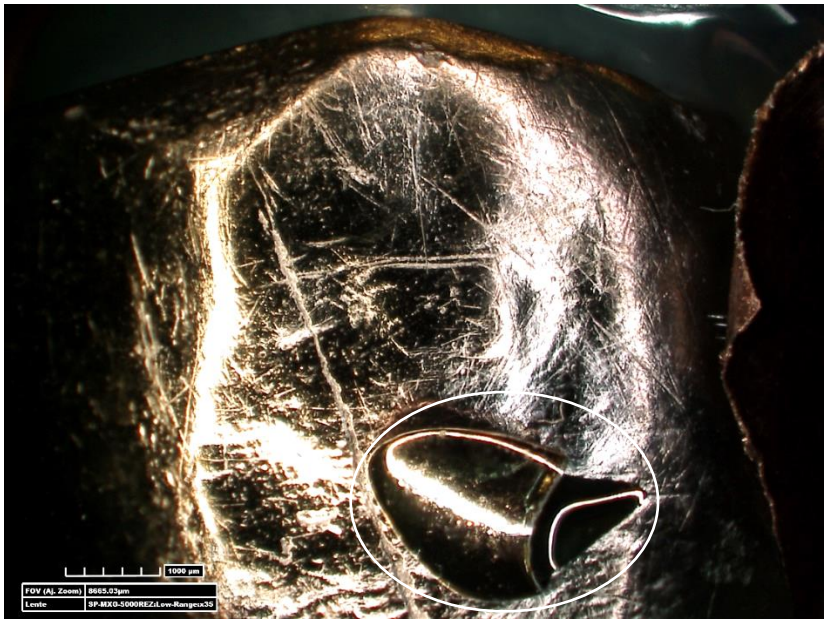

Figure 5.4 Hirox capture image of the cast specimen *n.* CC20_13/7_G7_283 (canine) labial surface at 35x magnification. This cast show a huge air bubble mass in relief (white circle) that caused a loss of data in most part of the middle third area of the upper canine. Photo taken by M. Mattera using a Hirox KH-8700 3D Digital Microscope located in the Lithic laboratory of IPHES (Tarragona, Spain) (April 2023)

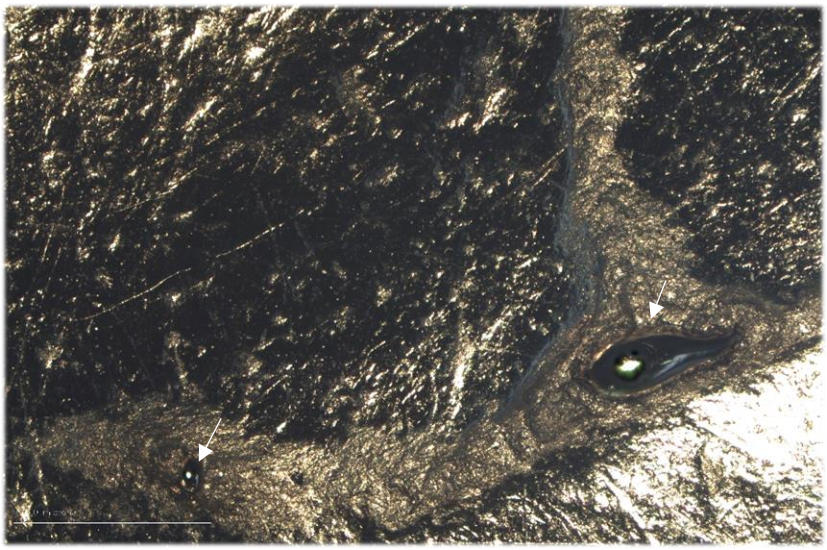

Figure 5.5 Zeiss capture image of the cast specimen *n.* CC20_13/4_F8_52 (molar) occlusal surface at 50x magnification. Air bubble mass in relief of different dimensions (white arrows) are clearly visible on the dental surface. Photo taken by M. Mattera using a Zeiss Axioscope A1 optical microscope located in the Lithic laboratory of IPHES (Tarragona, Spain) (April 2023)

Dark surface patches: Another common issue is related to the presence of dark patches on the enamel surface by using Scanning Electron Microscopy, Galbany et al. (2004) argued that these features are usually formed by the accumulation of dust on the mold that don't allow for the normal electron dispersal inside the SEM chamber (Galbany et al., 2004). The images appear with black and irregular patches spread on the cast surface at high magnification (Fig. 5.6).

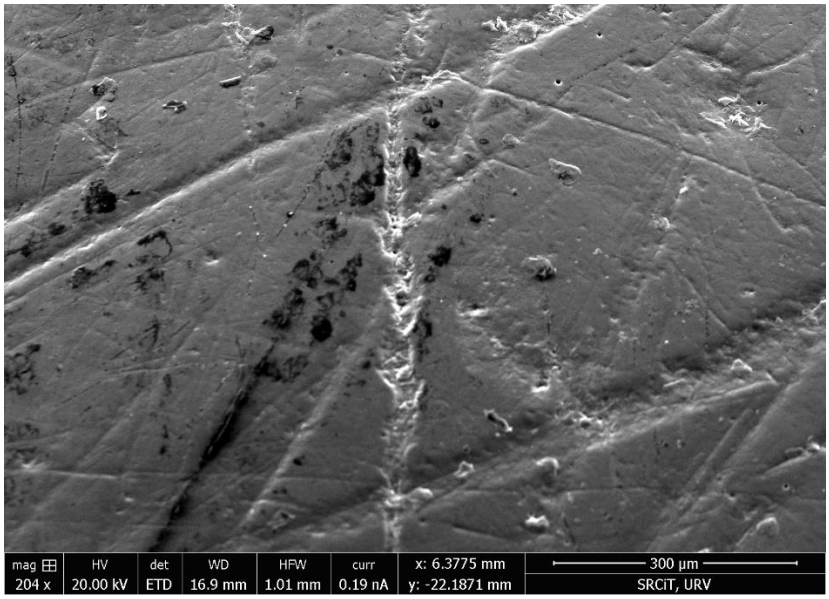

Figure 5.6 ESEM capture image of the cast specimen *n.* CC19_13/3_E8_74 (incisor) labial surface (middle third) at 204 x magnification. Dark surface patches are clearly visible on the dental surface, this phenomenon creates problems in the observation of tooth scratches. Photo taken by M. Mattera and M. Lozano using the FEI QUANTA 600 environmental scanning electron microscope (ESEM) at the Universitat Rovira i Virgili - scientific and technical resources Department. (March 2023)

5.1.2 Microscopy Images Aberrations: There are also problems related to the technical instrumentation of the microscope that affects image quality. Could happen that images obtained with Scanning Electron Microscopy may appear more or less blurred depending on how much worn the tungsten filament (responsible for the emission of electrons) is, and in these cases, it needs a replacement. Other times, as mentioned by Galbany et al. (2004), SEM images can be affected by high electrostatic charge caused by an incorrect colloidal argent belt between the stub and the cast (necessary for electron dispersal) (Galbany et al., 2004)**.** This event shows unclear images alternating with horizontal lines that create distorted vision (Fig. 5.7). To correct this issue, strips of metallic adhesive tape (in this case copper) can be applied laterally (right and left) to the dental casts, allowing for proper surface calibration of the electron beam in the SEM chamber (Fig. 5.8).

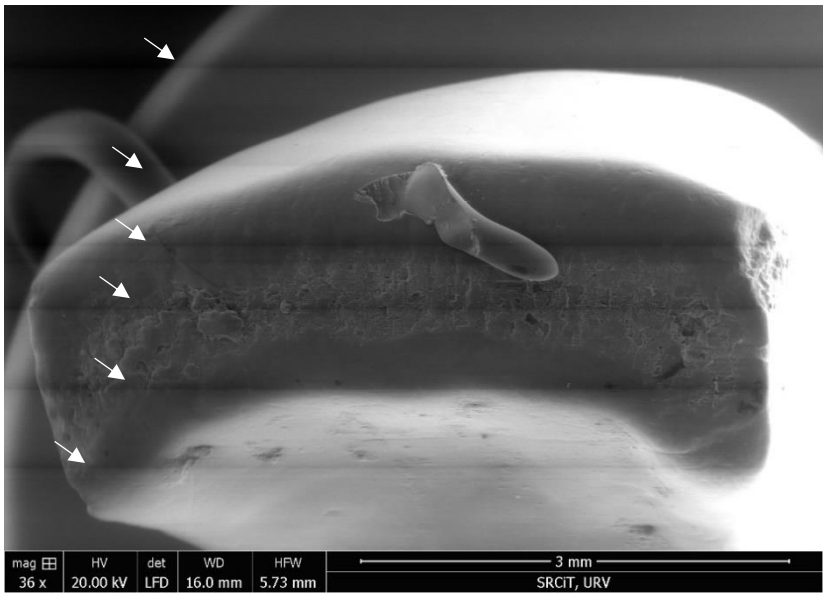

Figure 5.7 ESEM capture image of the cast specimen *n.* CC19_13/3_E8_74 (incisor) occlusal surface at 36x magnification. The horizontal lines (white arrows) on the image are clearly visible, this event doesn't allow for a correct observation of the specimen on the computer screen. Photo taken by M. Mattera and M. Lozano using the FEI QUANTA 600 environmental scanning electron microscope (ESEM) at the Universitat Rovira i Virgili - scientific and technical resources Department. (March 2023)

Figure 5.8 Example of the cast specimen *n.* CC20_13/7_G7_283 (canine) after the application of a metal tape (copper) (white arrows). This process will help for a proper surface spread of the electron beam in the SEM chamber. Photo taken by M. Mattera with an Apple iPhone SE of second generation (March 2023).

5.1.3 Intra and Inter-Observation Errors: Intra and inter-observer errors are considered as one of the major problems in dental microwear measurements. But, as already mentioned previously in the methodological chapter (paragraph 4.4.2), the Ciota Ciara's sample measurements were taken once just by a single observer , for this reason, no comparison for intra and inter-individual statistical error differences were performed.

5.2 *Detecting Taphonomic/Post-mortem alterations*

Additionally, the dental microwear methods may be also limited by taphonomic and post-depositional processes, in fact these phenomena can affect enamel surfaces and modify or obliterate dietary microwear features. In general post-depositional alterations on fossils are common and, considering the huge number of erosive agents which can impact the archaeological record, dental microwear alteration processes are difficult to identify adequately (Micó et al., 2023). These situations often produce a potential bias in dietary interpretations. The current paragraph will explore in detail the possible taphonomic alterations that were detected on the dental sample from Ciota Ciara cave.

***Taphonomic alterations observed on Ciota Ciara's sample*:** Although the dental specimens from Ciota Ciara cave present, in general, an excellent external state of enamel preservation; it was possible to recognize some clear surface alterations not strictly related to food ingestion features, but rather referable to post-depositional damages. Specifically, the present paragraph analyzes all the Neanderthal dental specimens from Ciota Ciara's cave in order to describe the intensity and the type of erosion/abrasion that can be observed on their enamel surfaces. The main purpose of this section is to determine if post-mortem alterations can be recognized. In fact, paleodietary research requires the analysis of tooth surfaces not affected by post-mortem erosion. Therefore, to demonstrate a clear relationship between the abrasiveness of diet and the buccal/occlusal microwear pattern, it is necessary to discern between both taphonomic altered surfaces and well-preserved ones. Several post-mortem effects were readily identifiable in the analyzed sample; but the presence of these alterations was not homogeneous in all the studied teeth. A complete list of detected traces, analyzed with the previous described methodology (see paragraph 4.3.3), will follow:

Post-mortem enamel chipping: It is usually possible to distinguish post-mortem chipping from antemortem one by observing several characteristics. But, unfortunately, the standard protocols of chipping identification are built on the observations of original dental specimens. This is due to the fact that enamel-dentine color and visual appearance are important elements to identify these features. In fact, post-mortem chipping is generally characterized by exposed enamel that is whiter than adjacent surfaces. As enamel is brittle but dentine is not, the enamel frequently fractures at the level of the dentine, which is generally dull yellow in color. As for appearance, post-mortem chipping results in exposed enamel with sharp and well-defined edges (G. R. Scott & Winn, 2011). Unfortunately, original colors are totally lost on the dental casts, and even the use of SEM microscopy only yields black-white images. Despite all this, it was possible to detect noticeable signs of dental chipping on the Ciota Ciara's sample, only one specimen of the sample had features linkable to enamel splintering due to clear post-depositional processes. Post-mortem enamel chipping was identified on the right part of the incisal third labial area of specimen *n*. CC21_13/8_H7_36 (Incisor) (Fig. 5.9 and 5.10). Both the ESEM and Hirox images, on the same area, clearly show that a large area of the labial surface was affected by an important removal of enamel; in fact, is possible to detect very sharp and defined breakage edges, and the difference between the smooth enamel (on the left preserved area) and the underlying composition of dentin (on the damaged portion) is evident. In the image taken at x35 magnification (direct light) with the Hirox microscope, it was possible to select and measure (in red color) the whole area affected by this phenomenon (Fig. 5.10 above). The constant post-mortem dehydration process tends to decrease the strength of the enamel structure; for this reason, successive taphonomic processes usually cause dental alterations with the characteristics previously listed. The surface measurements of the chipping were taken using ImageJ software on the focused Hirox image (x100 magnification): the max length correspond to 3,935 mm, the max width correspond to 3,680 mm, and the total area corresponds to 6,607 mm^2. Based on the methodological reference of Bonfiglioli et al. (2004), the post-mortem micro-chipping of this specimen can be scored as grade 3.

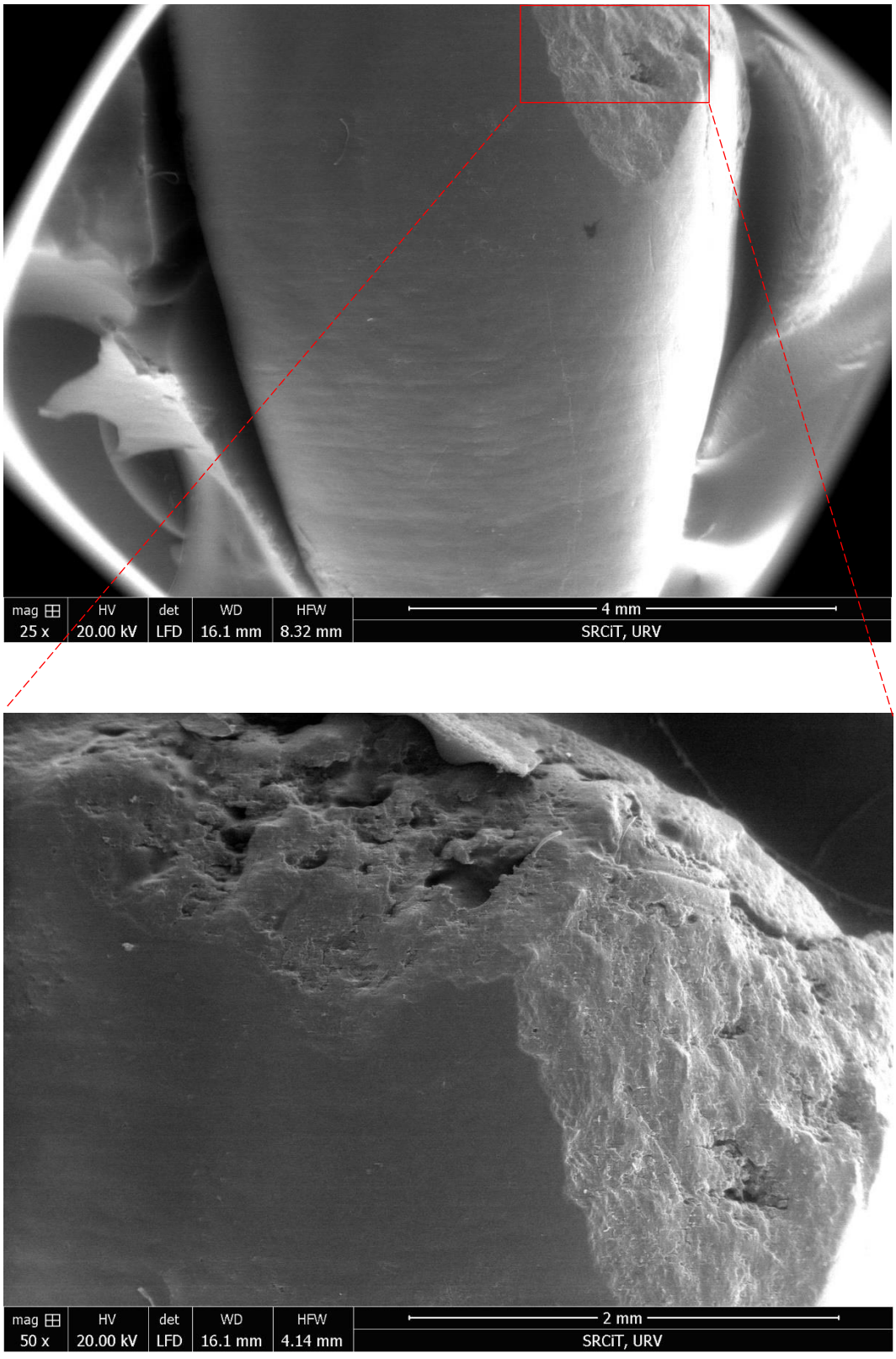

Figures 5.9 Above, ESEM capture image of the cast specimen *n.* CC21_13/8_H7_36 (Incisor) incisal and middle third labial surfaces at 25x magnification. Below, focus on the right part of the incisal third area of the incisor at 50x magnification. Is possible to notice a clear well-defined enamel removal caused by a possible post-depositional event. Photos taken by M. Mattera and M. Lozano using the FEI QUANTA 600 environmental scanning electron microscope (ESEM) at the Universitat Rovira I Virgili - scientific and technical resources Department (March 2023).

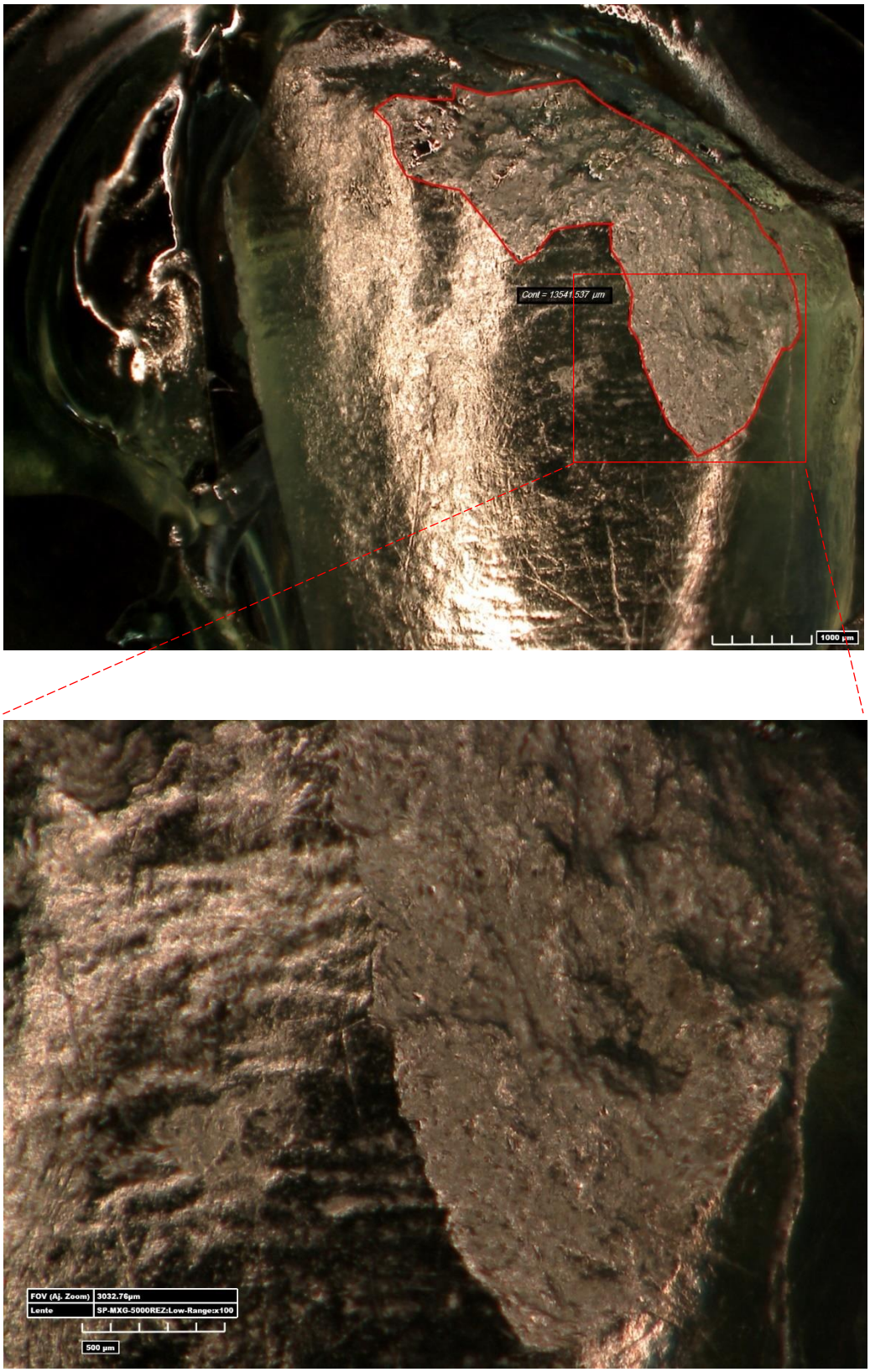

Figures 5.10 Above, Hirox capture image of the cast specimen *n.* CC21_13/8_H7_36 (Incisor) incisal and middle third labial surfaces at 35x magnification (direct light). The chipping area was selected in red. Below, focus on the right part of the incisal third area of the tooth at 100x magnification (direct light), is possible to notice the same characteristics described for the previous ESEM image. Photos taken by M. Mattera using a Hirox KH-8700 3D Digital Microscope located in the Lithic laboratory of IPHES (Tarragona, Spain) (April 2023).

Post-mortem enamel cracks: the Neanderthal dental sample from Ciota Ciara cave also exhibit a high rate of enamel cracking that were observed on several teeth surfaces. Generally, fresh cracks in fossil enamel show very sharp edges and may suggest a diagenetic cause. While rounded edges are evidence of a reshaping action, therefore these cracks may have been acquired during the lifetime (Rensberger, 1987). Considering the fracture features observed on the sample, Ciota Ciara's dental remains were probably affected by post-mortem stresses. Specifically, fractures and cracks of different intensities were observed in this study, especially on molars where these features appear very deep. As mentioned for the dental chipping, no numerical percentage can be given because the observation of the enamel cracks, under the microscopes, was not done in a systematic way. Despite that, several dental surfaces yielded examples of multiple fractures; as specimen *n.* CC20_13/4_F8_52 for which it was recorded a deep and irregular fracture located in the center of the worn occlusal surface and projected in the buccolingual direction, from the focused ESEM image at 100x magnification (Fig. 5.11 below), it can be seen that the jagged edges of the crack are compatible with post-depositional stress, probably due to a compression on the occlusal area. The same tooth shows two other vertical fractures along the buccal area that are very well observed in the 3D images captured by Hirox microscope at 50x and 100x magnification (direct light) (Fig. 5.12). In particular, the large crack on the left has very well-defined edges and its depth emphasizes the underlying dentin structure, whereas the fracture on the right is less pronounced and appears more like a kind of superficial groove (Fig. 5.12 below). Another similar example could be seen on specimen n. CC21_13/7_G8_433 whose buccal surface is crossed by an irregular vertical fracture, the crack shows notched edges compatible with a post-mortem alteration, and its depth can be appreciated by observing the images captured with the Hirox microscope at 35x (direct light) and 100x magnification (transverse light) (Fig. 5.13). Is interesting notice that, illuminating the sample with the transverse light, superficial enamel information related to the paleodiet features (scratches) are lost for a reflection phenomenon; but, on the other hand, post-depositional dental fractures that go deep inside the enamel crystals, are revealed with excellent details (Fig. 5.13 below)

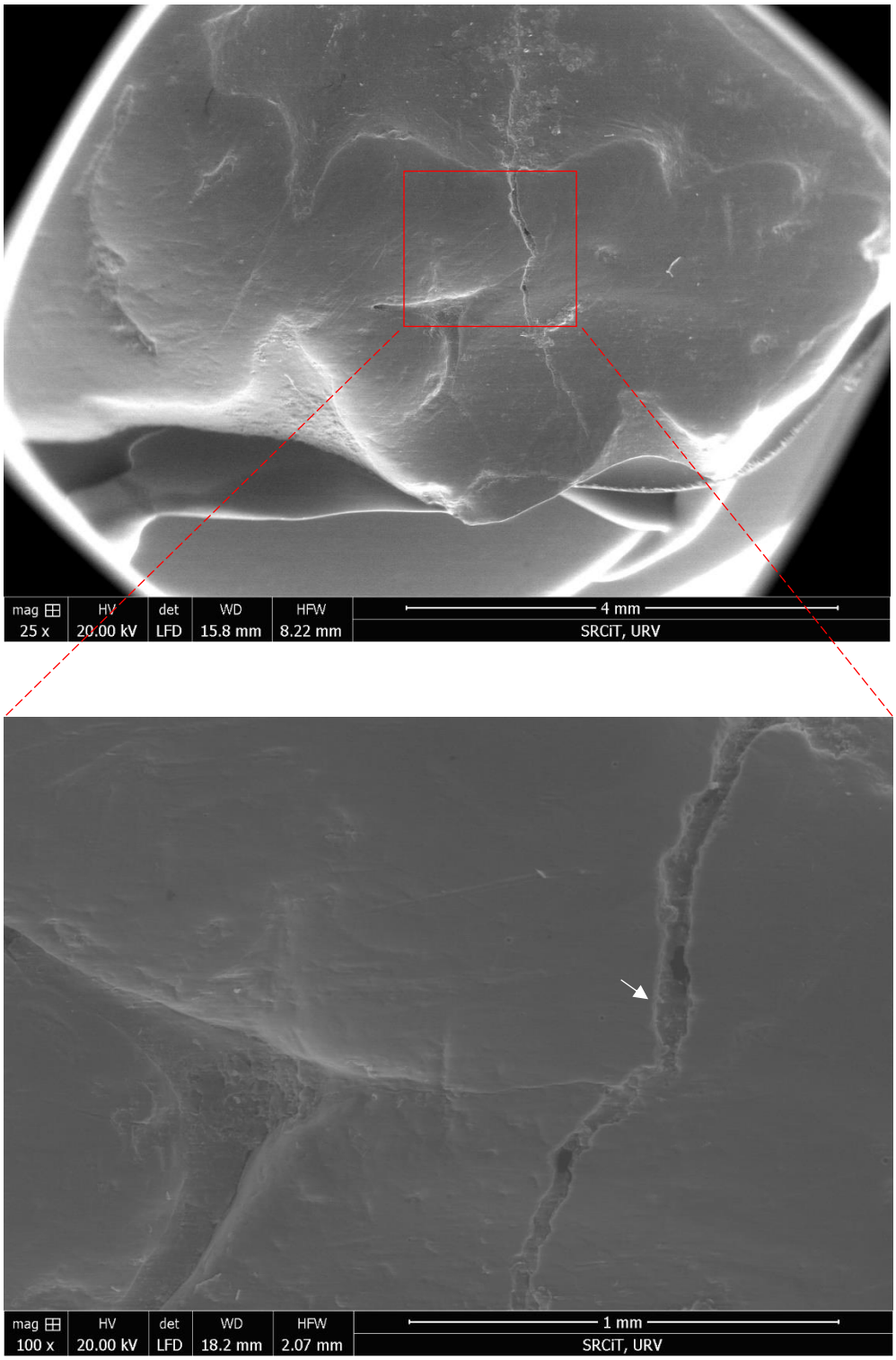

Figures 5.11 Above, ESEM capture image of the cast specimen *n.* CC20_13/4_F8_52 (Molar) occlusal surface at 25x magnification, showing a vertical post depositional fracture. Below, focus on the central part of the area at 100x magnification. Is possible to observe the jagged edges of the crack (white arrow) compatible with a possible post-depositional cause. Photos taken by M. Mattera and M. Lozano using the FEI QUANTA 600 environmental scanning electron microscope (ESEM) at the Universitat Rovira i Virgili - scientific and technical resources Department (March 2023).

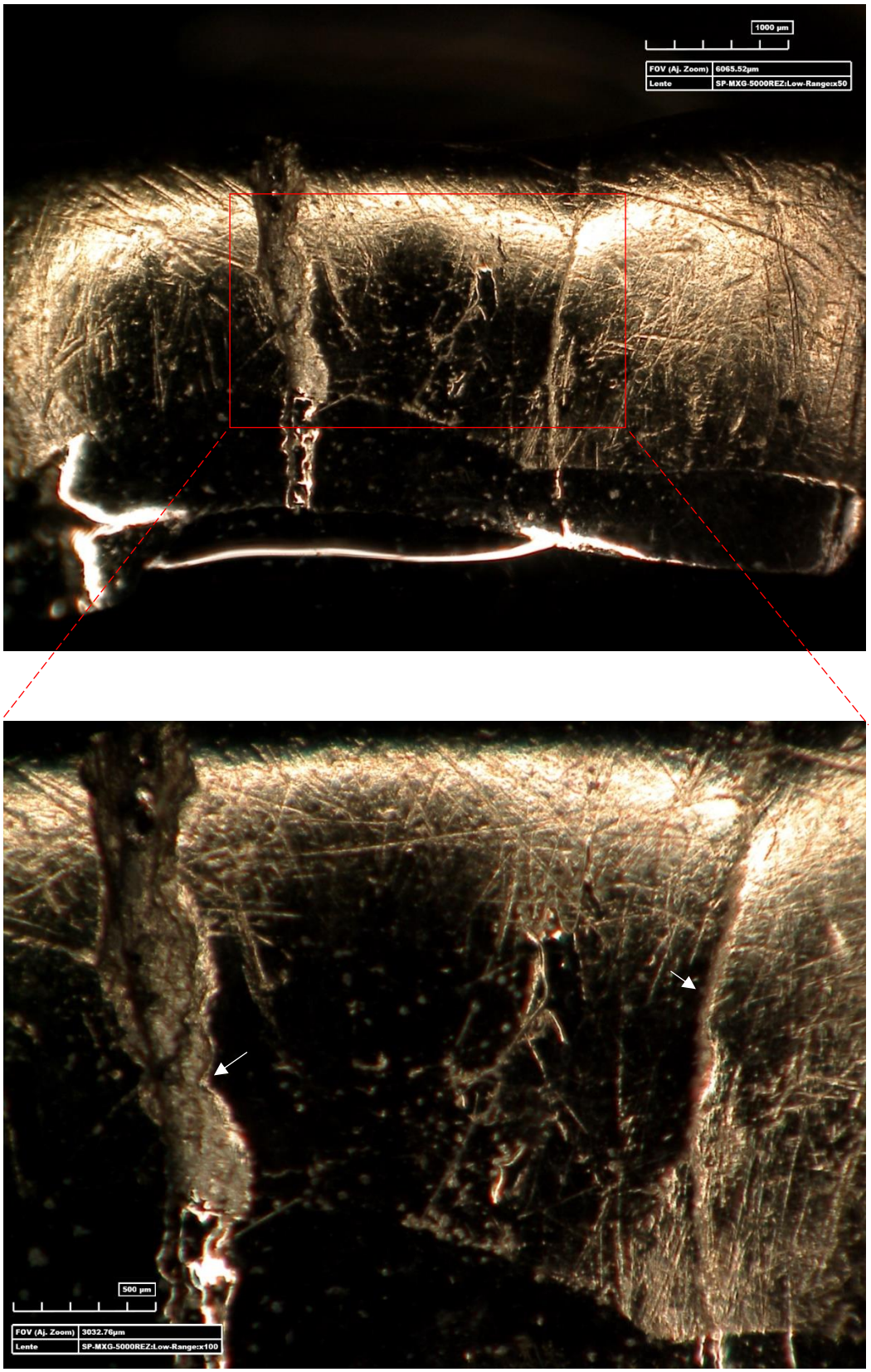

Figures 5.12 Above, Hirox capture image of the cast specimen *n.* CC20_13/4_F8_52 (Molar) buccal surface at 50x magnification (direct light). Below, focus on the medial area of the buccal surface of the tooth at 100x magnification (direct light), is possible to observe two enamel cracks (white arrows) probably caused by a taphonimic event. Photos taken by M. Mattera using a Hirox KH-8700 3D Digital Microscope located in the Lithic laboratory of IPHES (Tarragona, Spain) (April 2023).

Figures 5.13 Above, Hirox capture image of the cast specimen *n.* CC21_13/7_G8_433 (Molar) buccal surface at 35x magnification (direct light). Direct light here allows to observe both paleo-dietary features and enamel fractures. Below, focus on the medial area of the buccal surface at 100x magnification (transverse light). Is interesting notice that the transverse light enhances the enamel crack (white arrow). Photos taken by M. Mattera using a Hirox KH-8700 3D Digital Microscope located in the Lithic laboratory of IPHES (Tarragona, Spain) (April 2023).

Post-mortem abrasion and pitting: the analyzed sample also reveals many features related to erosive abrasion by sedimentary particles. Several experimental analyses have shown that post-mortem physical processes usually tend to erase or distort antemortem microwear features (King et al., 1999). A noticeable case was recognized between the middle third and incisal third labial' areas of the specimen *n*. CC19_13/3_E8_74 (incisor). Specifically, a large set of long scratches, with a particular morphology, where detected by using several types of microscopes. It is important to underline that these features were already clearly visible to the naked eye just by looking at the dental surface of the cast, this had initially led to the assumption that they might potentially be marks left by para-masticatory activities. Accurate analysis of the traces with ESEM (27x and 85x magnification) (Fig. 5.14) allowed to detect a set of signs with a chaotic pattern, even if three main larger scratches showed an apparent parallel disposition that might suggest an ante-mortem origin. Specifically, these three larger scratches show a curved orientation and a very large width/length ratio. 3D images of this area were also captured by both Hirox (50x and 100x magnification – direct light) and Zeiss (50x magnification) microscopes, in general the images captured with the Hirox seem to be slightly blurred in the internal structure of the scratches, but the superimposed lines are better defined (Fig. 5.15). While the internal structure is very well defined using the Zeiss (even if a reflection phenomenon is clearly visible) (Fig. 5.16 below). With the Hirox it was also possible to measure the degree of depth of these post-depositional features using a surface measuring instrument, in fact, as can be seen from the graph (Fig. 5.16 above), the line is almost straight, that indicates very shallow scratches. The surface measurements of the three striations were obtained using ImageJ software on the focused Hirox image (x100 magnification): maximum width of the scratches correspond to a Mean (M) of 69.625 μm and to a Standard deviation (SD) of 10.976 μm, while maximum length correspond to a Mean (M) of 1.640.450 μm and to a Standard deviation of 704.154 μm (Table 5.1).

Pits features and pitting surfaces are other common traces related to dental microwear analysis. But, other times, these features can be confused with post-depositional physical or chemical erosion that tends to emulate the diet signs as was demonstrated by King et al. (1999). This type of abrasion has been seen during the analysis of the facet 9 (occlusal area) on the specimen *n*. CC21_13/7_G8_433 (Fig. 5.17). The pitting pattern was initially interpreted as related to chewing actions, which on the occlusal surface are quite common when is related to the consumption of hard food and abrasive diets in general. For this reason, this surface was analyzed in the protocol of the diet-related features and, therefore, it will be described accurately in that section (paragraph 5.4). In a second stage of the analysis, because of certain characteristics that were recognized, this area was subsequently interpreted as being exposed to a post-depositional acidic or mechanical action more than a hard foodstuff consumption (see Discussion section).

CC19_13/3_E8_74	Length	Width
Striation 1 (left)	2.442.324 μm	57.692 μm
Striation 2 (middle)	1.444.809 μm	71.892 μm
Striation 3 (right)	1.034.216 μm	79.290 μm
Mean	1.640.450 μm	69.625 μm
Standard deviation	704.154 μm	10.976 μm

Table 5.1 surface measurements of three post-depositional labial scratches detected on the middle third right side of the specimen *n.* CC19_13/3_E8_74 using ImageJ software.

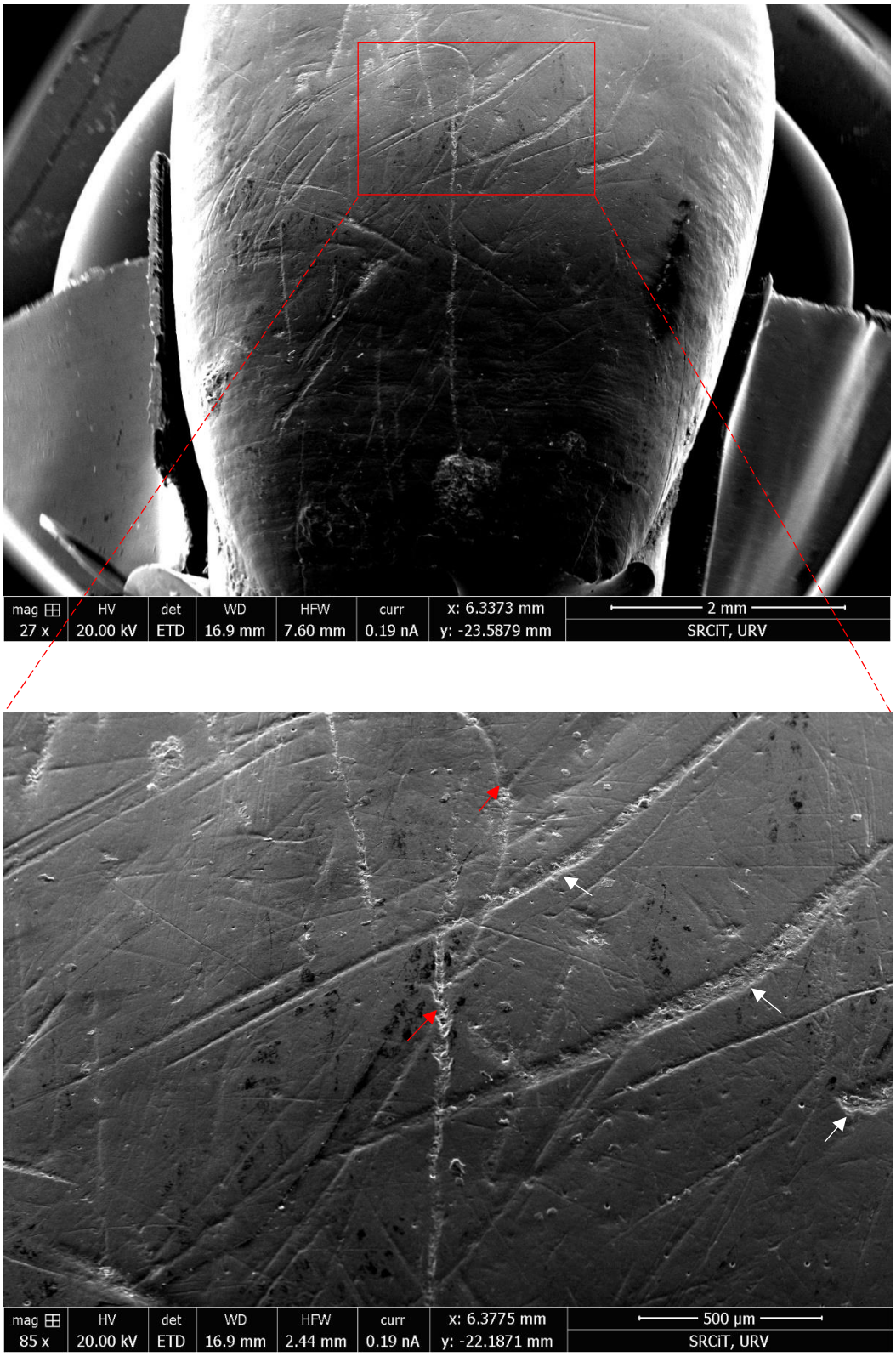

Figures 5.14 Above, ESEM capture image of the cast specimen *n.* CC19_13/3_E8_74 (incisor) labial area at 27x magnification. Below, focus on the middle/incisal third' labial area at 85x magnification. Is possible to observe the curved orientation of the largest scratches (white arrow) and their internal structure. Other superimposed and chaotic features are clearly visible (red arrows). Photos taken by M. Mattera and M. Lozano using the FEI QUANTA 600 environmental scanning electron microscope (ESEM) at the Universitat Rovira i Virgili - scientific and technical resources Department (March 2023).

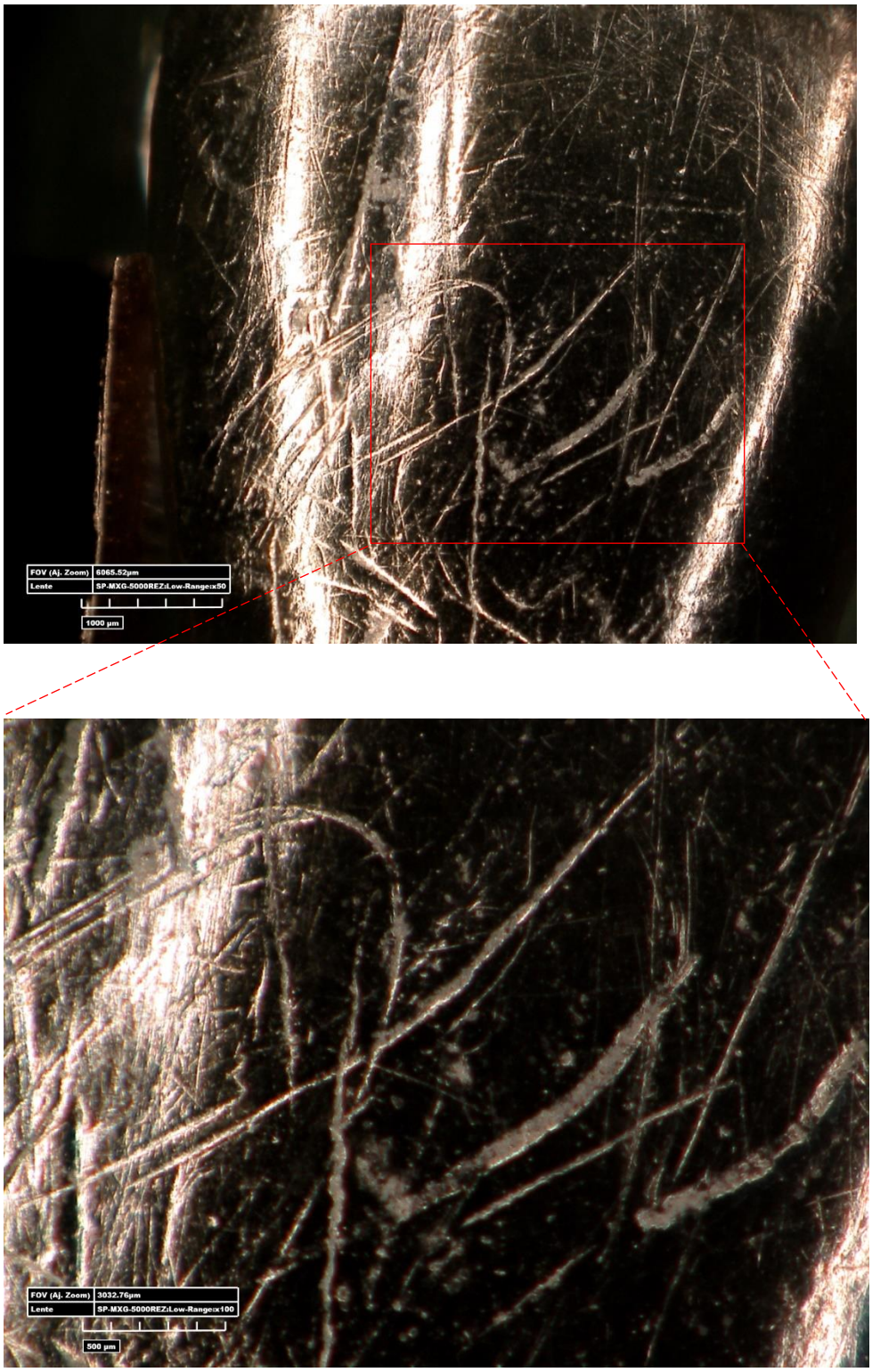

Figures 5.15 Above, Hirox capture image of cast specimen *n.* CC19_13/3_E8_74 (incisor) labial area at 50x magnification (direct light). Below, focus on the middle/incisal third' labial area at 100x magnification (direct light). Hirox lenses allow to better observe the superimposed scratches, but the internal structure of the features is blurred compared to ESEM and Zeiss. Photos taken by M. Mattera using a Hirox KH-8700 3D Digital Microscope located in the Lithic laboratory of IPHES (Tarragona, Spain) (April 2023).

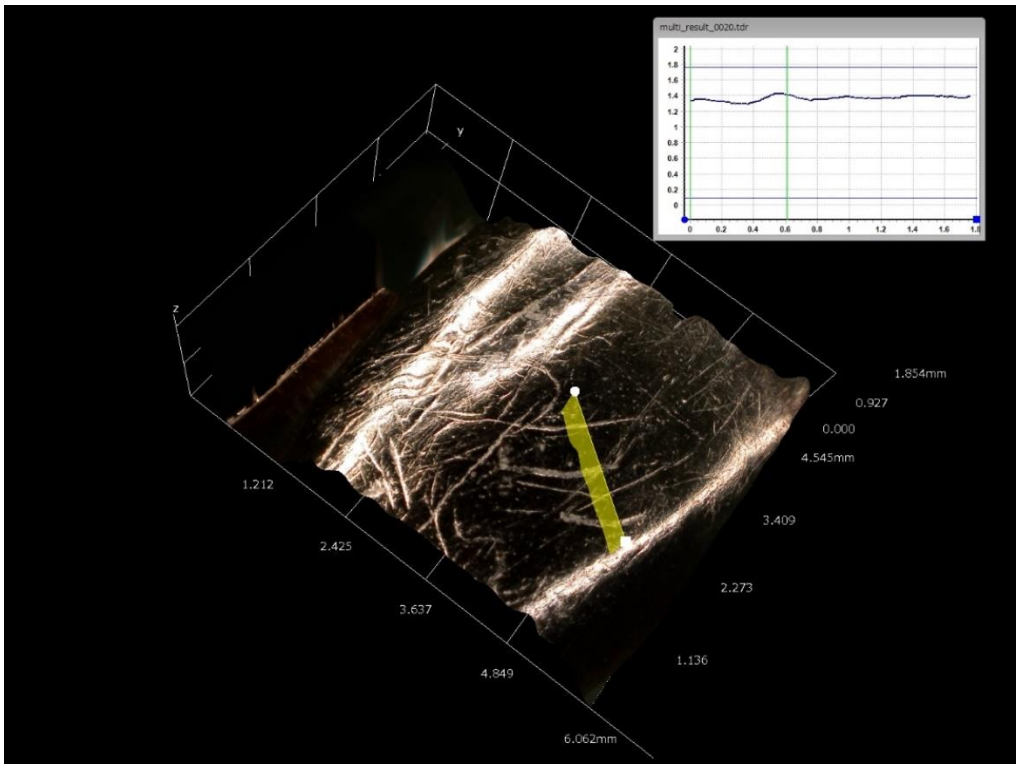

Figures 5.16 Above, Hirox 3D model and measurements graph of cast specimen *n.* CC19_13/3_E8_74 (incisor) labial area at 50x magnification (direct light). The measurement graph shows a relatively straight line, this indicates that the scratches are shallow. Below, Zeiss capture image focus on the middle/incisal third' labial area at 50x magnification. Zeiss lenses allow to better observe the inner part of the scratches, but the reflection of light/darkness is problematic. Photos taken by M. Mattera using a Hirox KH-8700 3D Digital Microscope and a Zeiss Axioscope A1 optical microscope located in the Lithic laboratory of IPHES (Tarragona, Spain) (April 2023).

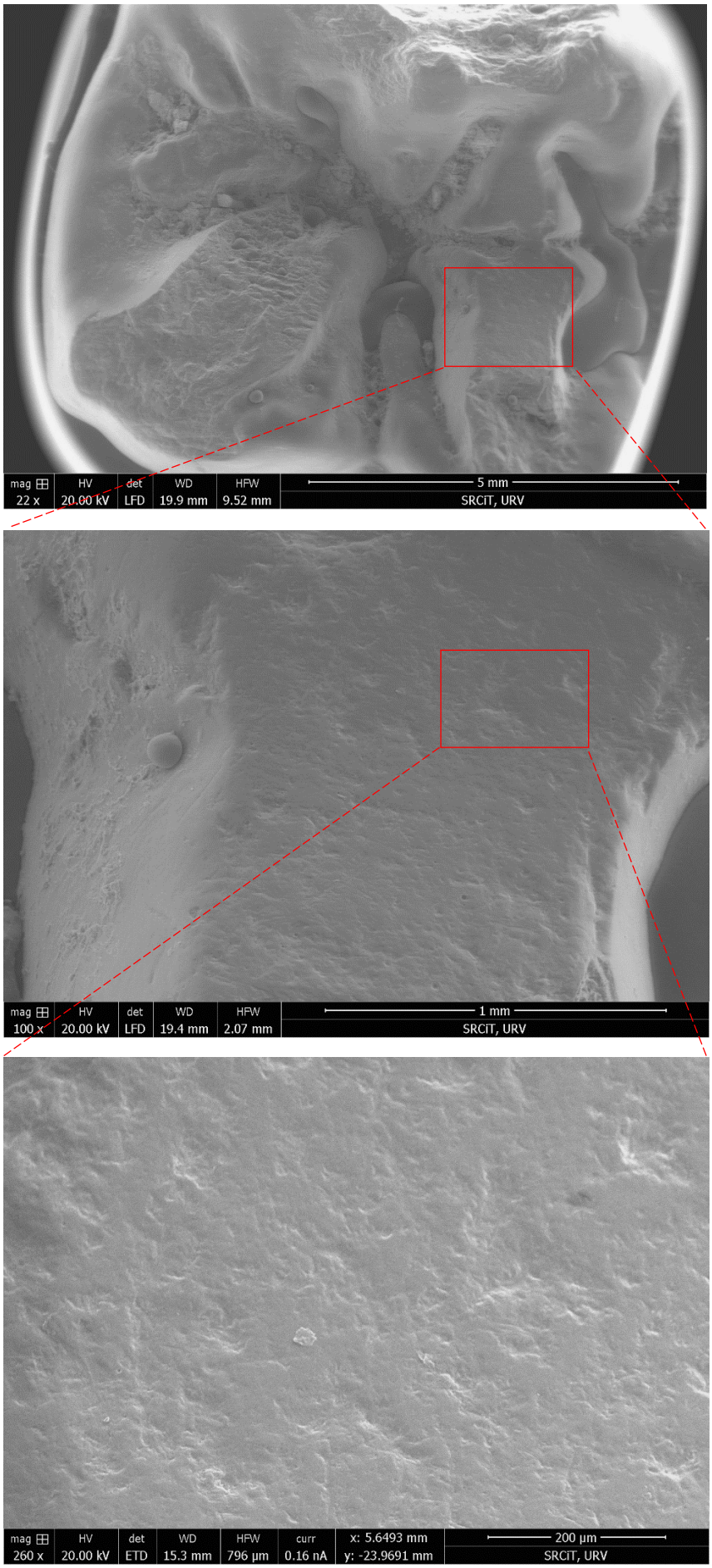

Figures 5.17 Above, ESEM capture image of the cast specimen *n.* CC21_13/7_G8_433 (molar) occlusal area at 22x magnification. Middle, focus on the facet 9 area at 100x magnification. Is possible to observe the pitting pattern along the surface. Below, further focus on the facet 9 area at 260x magnification. The pits are showed in detail by ESEM. Photos taken by M. Mattera and M. Lozano using the FEI QUANTA 600 environmental scanning electron microscope (ESEM) at the Universitat Rovira i Virgili - scientific and technical resources Department (March 2023).

5.3 *Detecting Ante-mortem alterations and Para-masticatory activities*

The previous section focuses on the identified taphonomic alterations, thus various methodologies for recognizing postmortem from antemortem processes (in microwear analyses) were discussed. The current paragraph, on the other hand, will show results obtained from the detected antemortem traces found on the Ciota Ciara's dental specimens and, among them, which features allowed to recognize possible activities of cultural/para-masticatory origin. Antemortem features were studied and described based on the previous methodological section (see paragraph 4.3.3), following the methodologies designed by different authors (i.e. Bonfiglioli et al., 2004; Lozano et al., 2008), the identified features were divided into the following categories:

Ante-mortem dental chipping: As already mentioned for the post-mortem chipping analysis on the Ciota Ciara's sample, even the antemortem dental chipping was not properly recorded because the recognition protocols must be carried out by observing the originals teeth and following a standard methodology. Otherwise, these features were detected, observing the casts under the microscopes, on two dental specimens (both incisors). Specifically, an antemortem enamel chipping was identified on the right part of the incisal third lingual area of specimen *n*. CC21_13/8_H7_36 (Incisor) (Fig. 5.18, 5.19, and 5.20). An important characteristic to distinguish postmortem from antemortem chipping is related to the breaking edges' shape, since a tooth chipped antemortem remains in functional occlusion for the life of the individual, the edges become smoothed or blunted. Therefore, the captured ESEM images at x24 and x80 magnification (Fig. 5.18) show blunted edges contours that seem to create almost a single surface with the adjacent enamel, while the most internal area of the break shows clear signs of incomplete reabsorption with partial exposure of the underlying dentin (Fig. 4.18 below). In addition, it can be seen that the lingual enamel area is completely smooth and has apparently not suffered any kind of surface alteration (Fig. 5.18 below). In fact, the lingual surfaces do not even show diet-related features in general. In the following image taken at x50 magnification (transverse light) with the Hirox microscope, it was possible to select (in red color) the whole area affected by this phenomenon (Fig. 5.19, above) and it was also possible to measure the surface anisotropy; in fact, as can be seen from the graph, the abrupt curved line show an anisotropy of the dental surface as a clear indication of an enamel remotion event (Fig. 5.19, below). On the contrary, the captured Zeiss image at 50x magnification, on the same area, displayed a more defined difference between the preserved enamel and the damaged area (Fig. 5.20). The surface measurements of the feature were taken using ImageJ software on the focused ESEM image (x80 magnification): the max length correspond to 1.64 mm, the max width correspond to 1.41 mm, and the total area corresponds to 1,591 mm^2; based on the methodological reference of Bonfiglioli et al. (2004), the antemortem chipping of this specimen can be scored as grade 3.

Another type of antemortem chipping was identified on the left occlusal surface side of the specimen *n*. CC19_13/3_E8_74 (incisor) (Fig. 5.21, 5.22, and 5.23). It is possible to notice, from the ESEM images taken at 38x and 100x magnification, that the identified dental chipping is smaller in size when compared to the previous one (Fig 5.21, below); moreover, it is possible to observe that the occlusal surface of the incisor is worn, thus the difference of mineral composition between the enamel (external) and the dentine (internal) is clearly shown in the microscopes images. Unfortunately, both the images taken with the Hirox microscope (50x and 100x magnification) (Fig. 5.22) and with the Zeiss microscope (50x magnification) (Fig. 5.23), focused on the same area, didn't show properly this feature because some reflection and shadow problems occurred. The surface measurements of the feature were taken using ImageJ software on the focused ESEM image (x100 magnification): the max length corresponds to 0,135 mm, the max width corresponds to 0,058 mm, and the total area

corresponds to 0,007 mm^2. Based on the methodological reference of Bonfiglioli et al. (2004), the ante-mortem micro-chipping of this specimen can be scored as grade 1.

Possible para-masticatory labial striations: Some scratches, morphologically different from the standard dietary traces, were detected also on the Ciota Ciara's sample. Specifically, these features were observed on the middle third left side of the specimen *n*. CC19_13/3_E8_74 (incisor). The ESEM images taken at 27x and 80x magnification (Fig. 5.24) displayed a set of three long scratches that are: well-defined, parallel to each other along most of their length, and with a right oblique orientation. Considering these characteristics and their position on the incisor, they were found to be excellent candidates to be considered as traces of cultural/para-masticatory origin (see Discussion section). The measurements of the scratches were obtained using imageJ software on the focused ESEM image (x80 magnification): the maximum width corresponds to a Mean (M) of 37.591 μm and a Standard deviation (SD) of 7.364 μm; while the maximum length corresponds to a Mean (M) of 835.942 μm and a Standard deviation (SD) of 82.393 μm; finally, for the orientation, the measured angle corresponds to a total Mean (M) of 50.833° and a Standard deviation (SD) of 3.349° (Table 5.2), in according to the orientation table developed by Pérez-Pérez et al. (1994), these scratches are oriented mesio-cervical to disto-occlusal (DM). 3D images, of the same area, were also captured by both Hirox (50x and 100x magnification – direct light) (Fig. 5.25) and Zeiss (50x and 100x magnification) (Fig. 5.26). In general, these images captured with the optical microscopes seem to be in low definition because the anatomical curvature of the incisor tends to create problems of reflected light with very bright and dark areas on tridimensional images.

CC19_13/3_E8_74	Length	Width	Angle
Striation 1 (left)	924.431 μm	30.591 μm	50.389°
Striation 2 (middle)	821.961 μm	36.910 μm	47.728°
Striation 3 (right)	761.433 μm	45.272 μm	54.382°
Mean	835.942 μm	37.591 μm	50.833°
Standard deviation	82.393 μm	7.364 μm	3.349°

Table 5.2 surface measurements of three possible para-masticatory labial scratches detected on the middle third left side of the specimen *n.* CC19_13/3_E8_74 using ImageJ software.

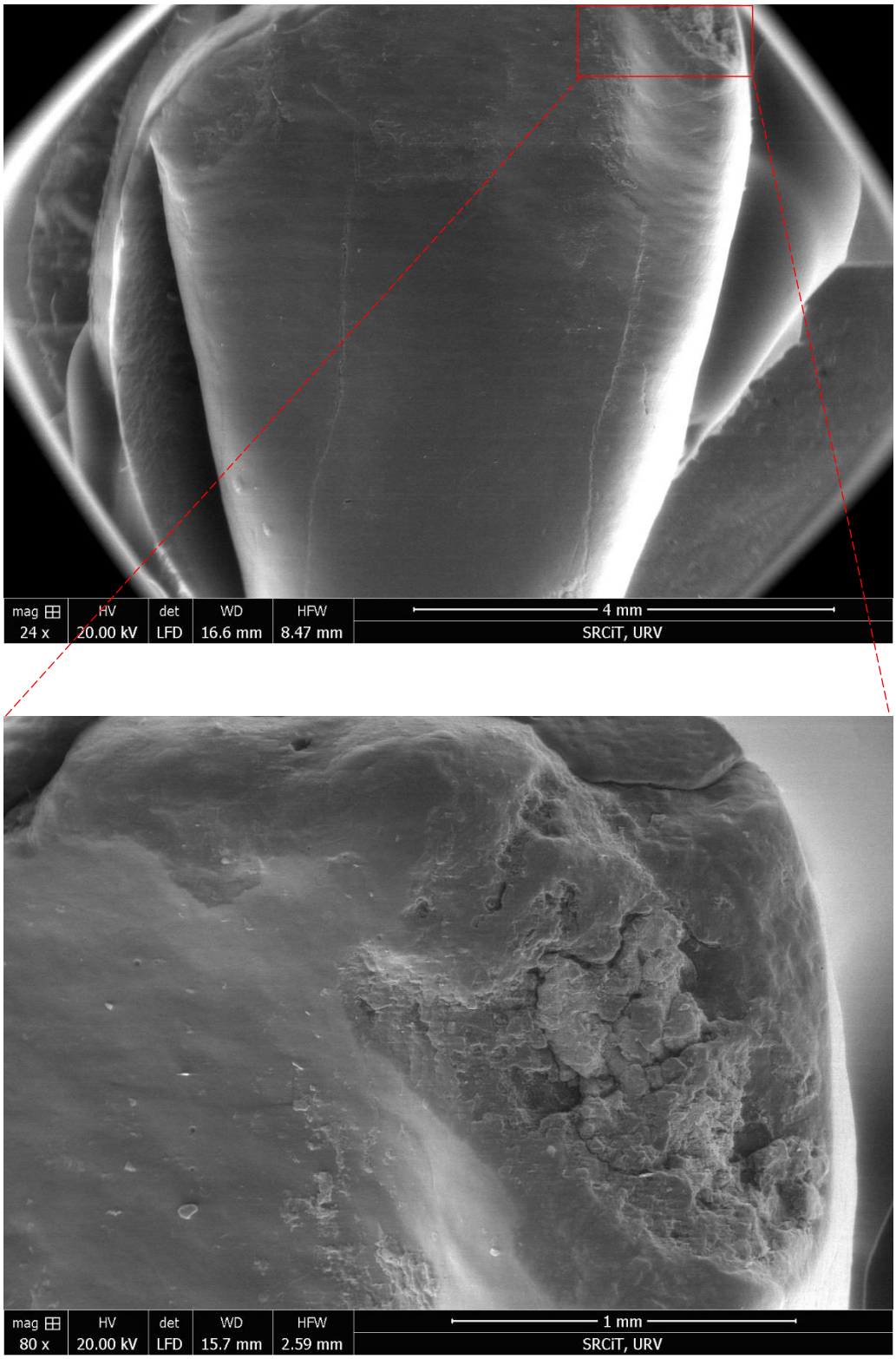

Figure 5.18 Above, ESEM capture image of the cast specimen *n.* CC21_13/8_H7_36 (Incisor) lingual surface at 24x magnification. Below, focus on the incisal third lingual area at 80x magnification. Is possible to observe the ante-mortem chipping area (right) and the smoothed enaml surface (left). Photos taken by M. Mattera and M. Lozano using the FEI QUANTA 600 environmental scanning electron microscope (ESEM) at the Universitat Rovira i Virgili - scientific and technical resources Department (March 2023).

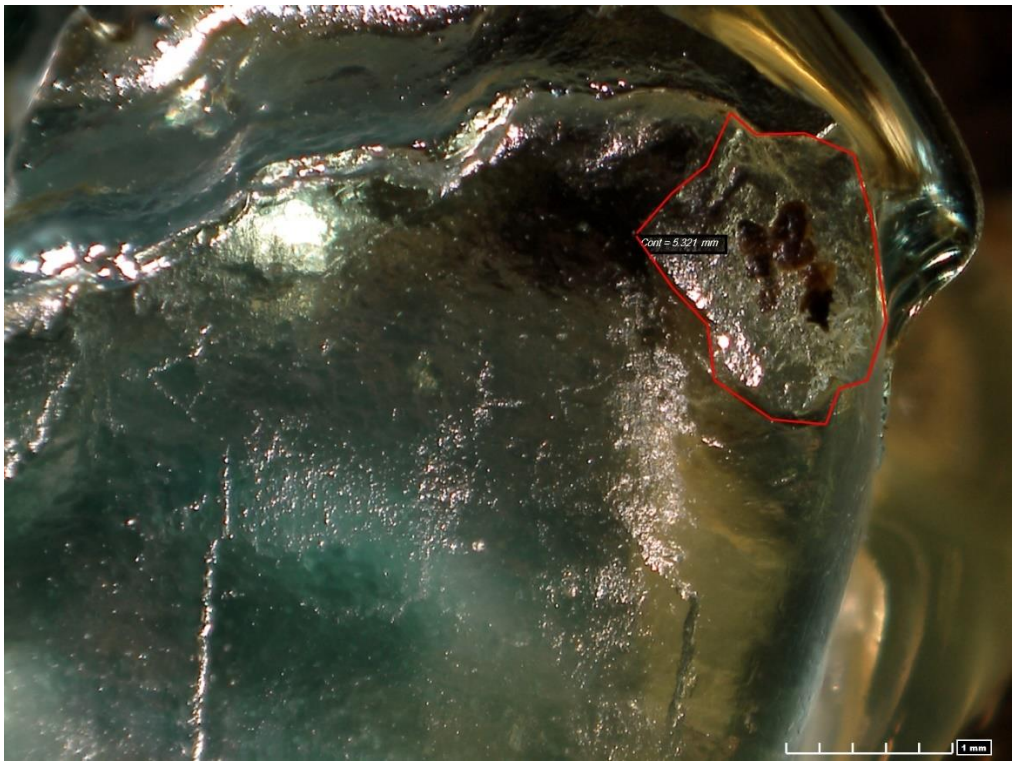

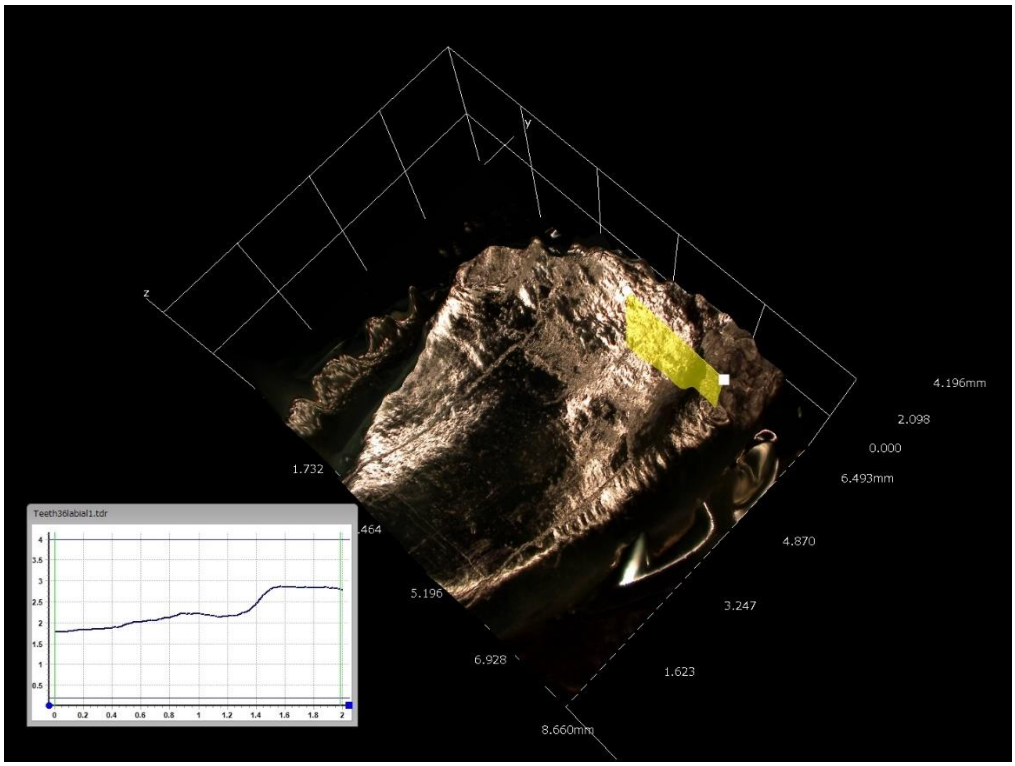

Figure 5.19 Above, Hirox capture image of the cast specimen *n.* CC21_13/8_H7_36 (Incisor) incisal third lingual surface at 50x magnification (transverse light). The chipping area was selected in red. Below, Hirox 3D model and measurements graph of cast specimen *n*. CC21_13/8_H7_36 (Incisor) lingual surface at 50x magnification (direct light). The measurement graph shows an abrupt curved line that correspond to an anisotropy of the surface on the chipping area. Photos taken by M. Mattera using a Hirox KH-8700 3D Digital Microscope located in the Lithic laboratory of IPHES (Tarragona, Spain) (April 2023).

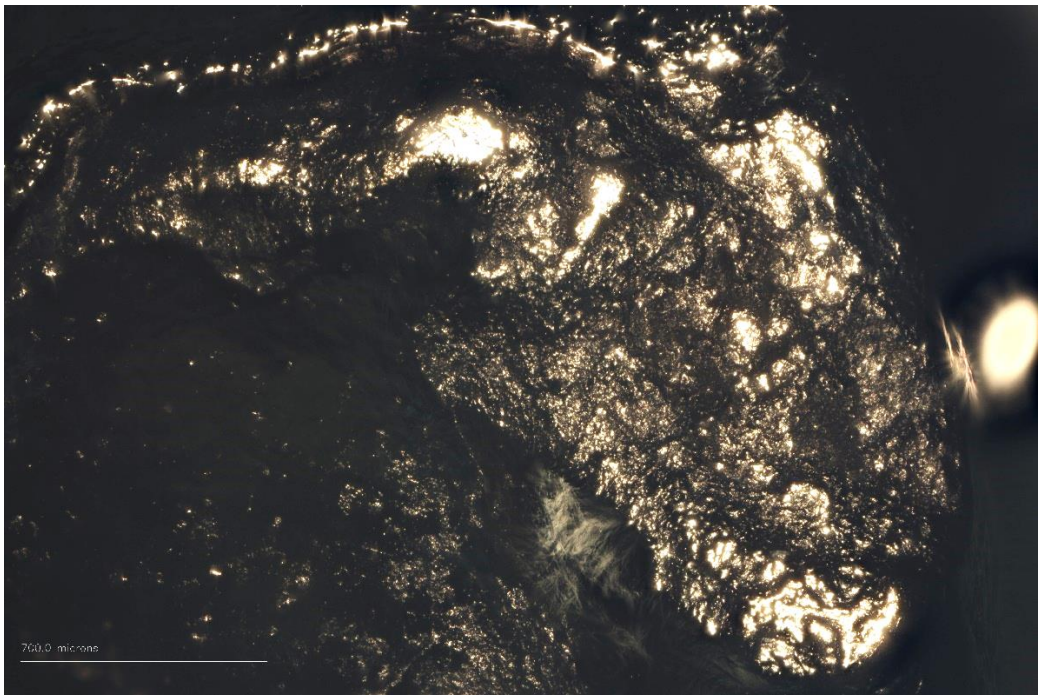

Figure 5.20 Zeiss capture image of the cast specimen *n.* CC21_13/8_H7_36 (Incisor) incisal third lingual surface at 50x magnification. Zeiss lenses allow to underline a marked difference between the chipped area (right) and the smooth enamel surface (left). Photo taken by M. Mattera using a Zeiss Axioscope A1 optical microscope located in the Lithic laboratory of IPHES (Tarragona, Spain) (April 2023).

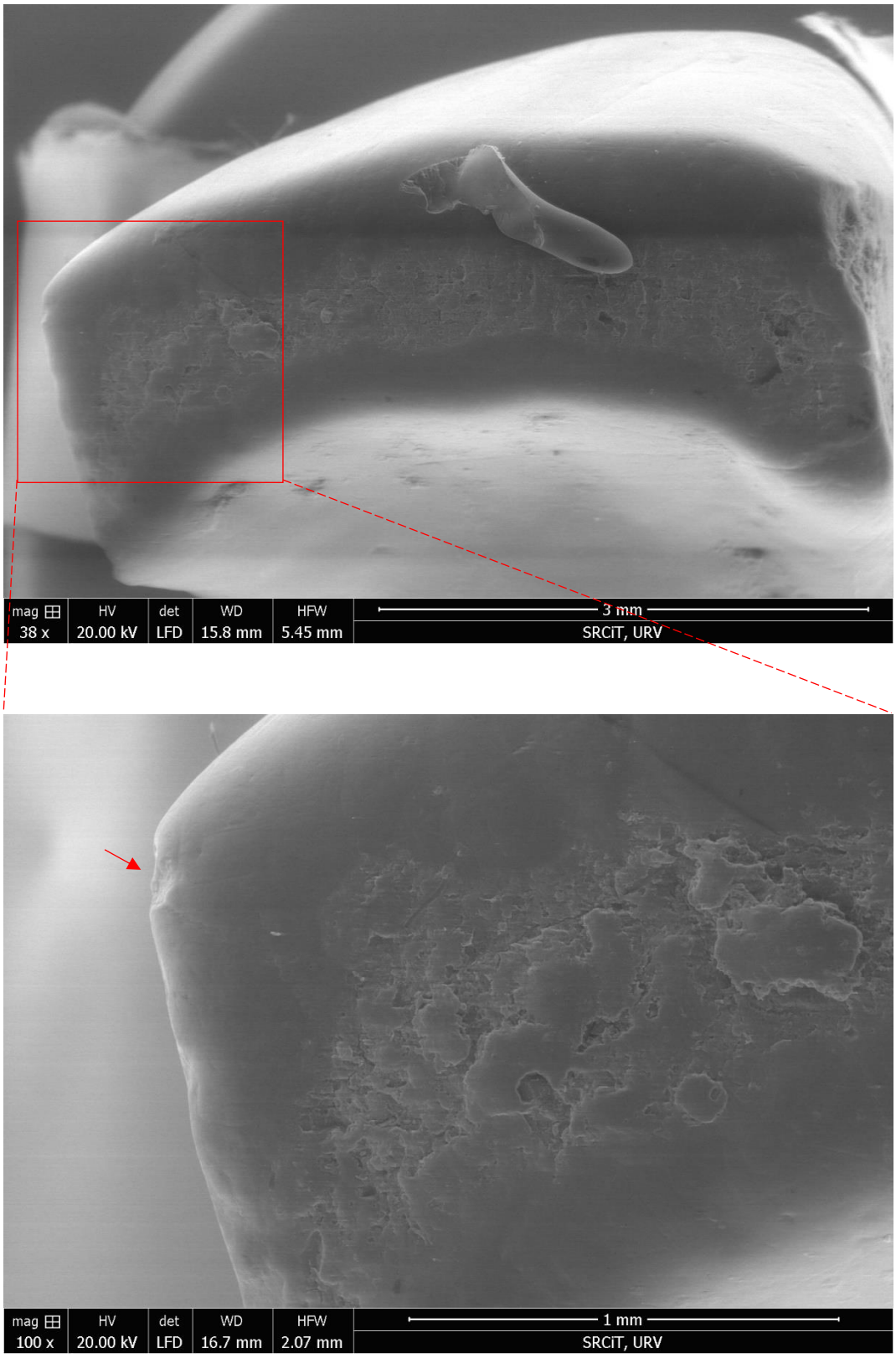

Figure 5.21 Above, ESEM capture image of the cast specimen *n.* CC19_13/3_E8_74 (incisor) occlusal surface at 38x magnification. Below, focus on the left occlusal side at 100x magnification. Is possible to observe the ante-mortem micro-chipping (red arrow) and the difference between the external enamel and internal dentine' composition. Photos taken by M. Mattera and M. Lozano using the FEI QUANTA 600 environmental scanning electron microscope (ESEM) at the Universitat Rovira i Virgili - scientific and technical resources Department (March 2023).

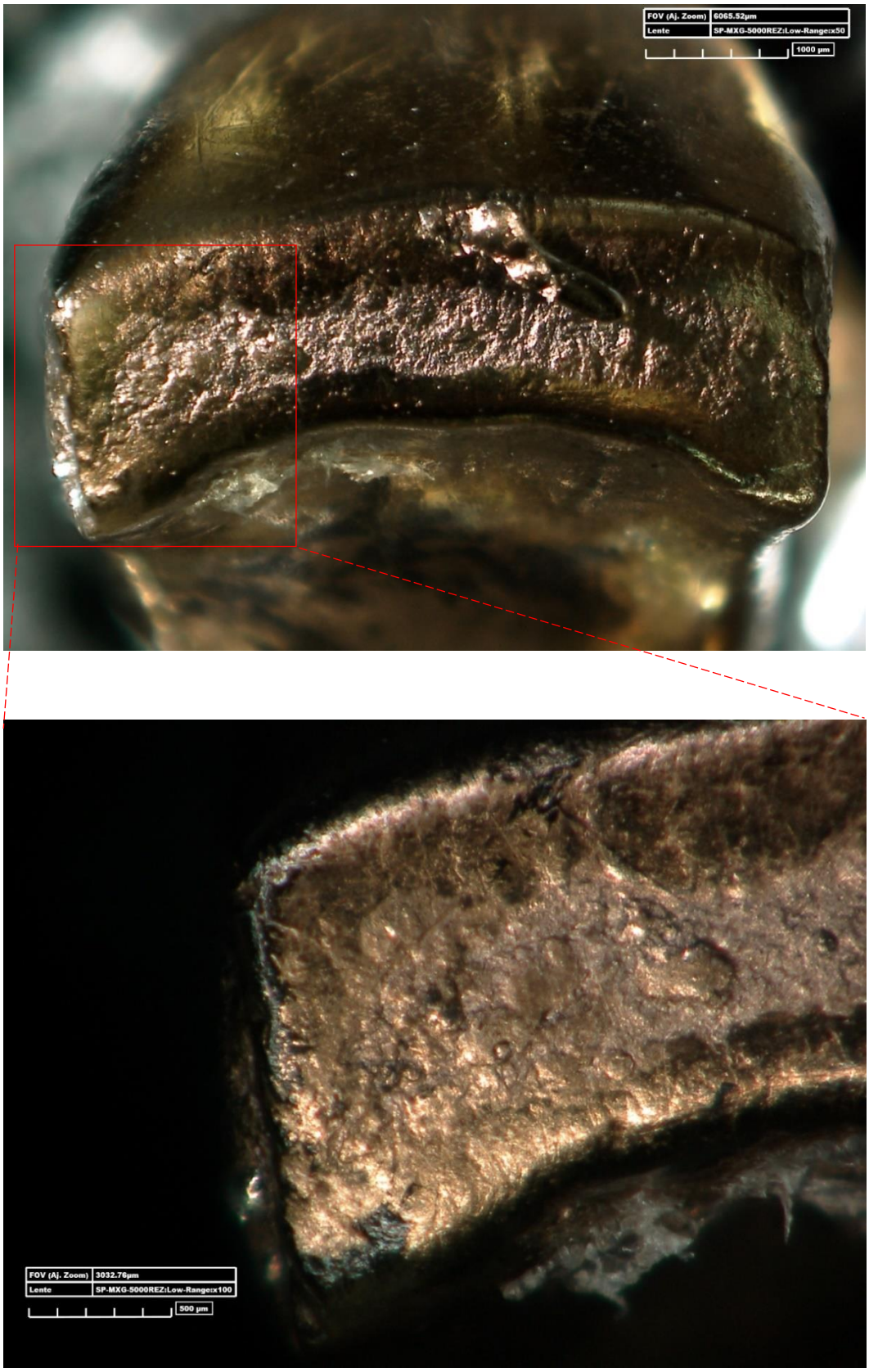

Figure 5.22 Above, Hirox capture image of cast specimen *n.* CC19_13/3_E8_74 (incisor) occlusal area at 50x magnification (transverse light). Below, focus on left occlusal side at 100x magnification (direct light). Hirox doesn't allow to properly observe the micro-chipping here, but the difference related to the different crystalline composition is clear. Photos taken by M. Mattera using a Hirox KH-8700 3D Digital Microscope located in the Lithic laboratory of IPHES (Tarragona, Spain) (April 2023).

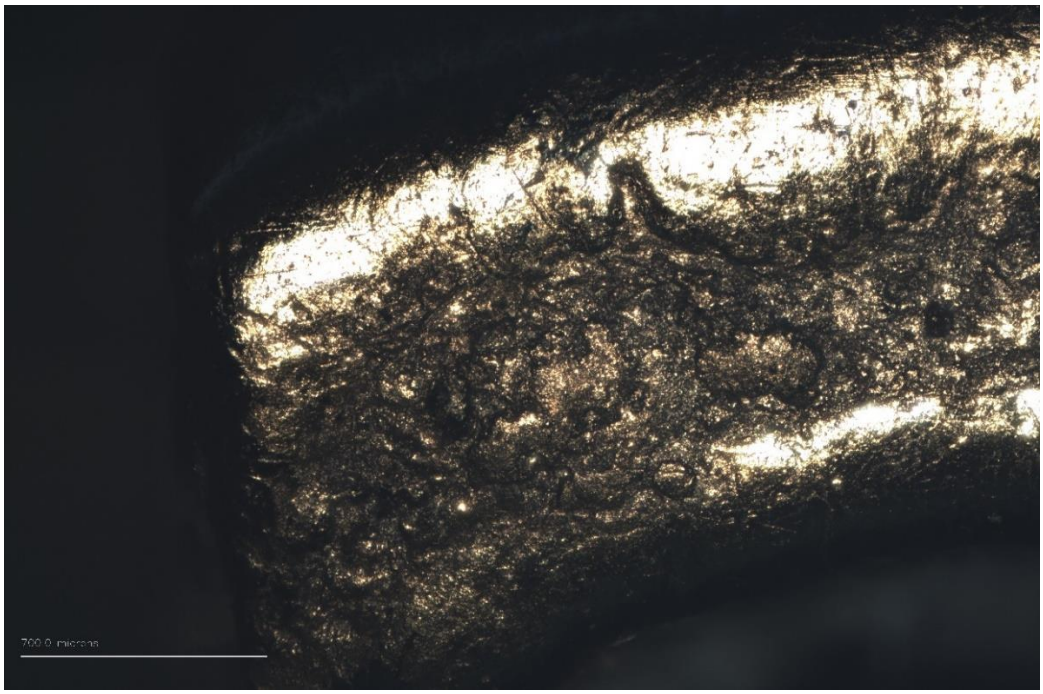

Figure 5.23 Zeiss capture image of the cast specimen *n.* CC19_13/3_E8_74 (incisor) left occlusal side at 50x magnification. Even Zeiss, as for Hirox doesn't allow to properly observe the micro-chipping here, but the difference related to the different crystalline composition is clear. Photo taken by M. Mattera using a Zeiss Axioscope A1 optical microscope located in the Lithic laboratory of IPHES (Tarragona, Spain) (April 2023).

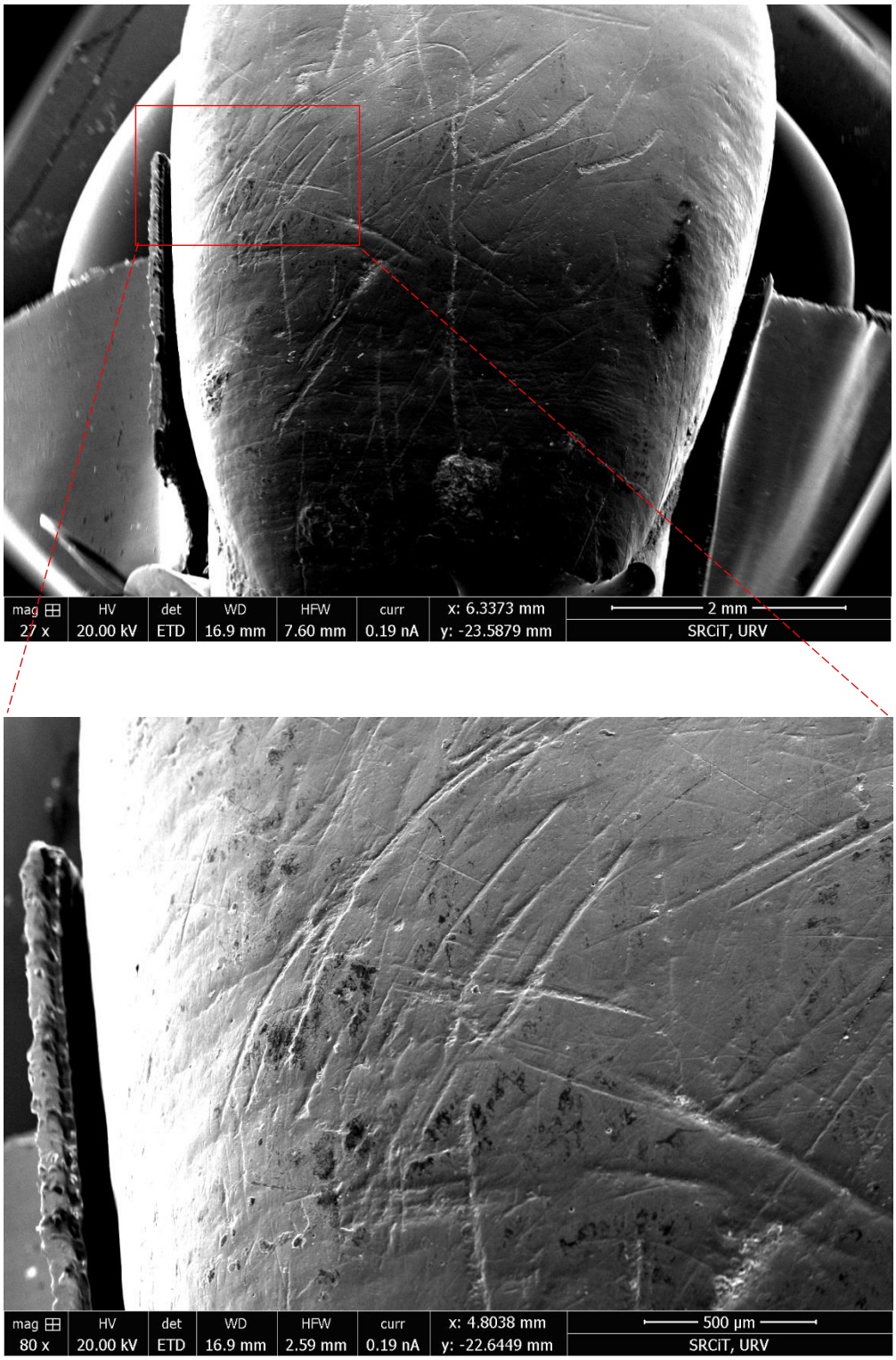

Figure 5.24 Above, ESEM capture image of the cast specimen *n.* CC19_13/3_E8_74 (incisor) labial surface at 27x magnification. Below, focus on the middle third left side at 80x magnification. Is possible to observe three well-defined and parallel scratches. Photos taken by M. Mattera and M. Lozano using the FEI QUANTA 600 environmental scanning electron microscope (ESEM) at the Universitat Rovira i Virgili - scientific and technical resources Department (March 2023).

Figure 5.25 Above, Hirox capture image of cast specimen *n.* CC19_13/3_E8_74 (incisor) labial area at 50x magnification (direct light). Below, focus on the middle third left side at 100x magnification. Is possible to observe the same three scratches underlined in red color. Photos taken by M. Mattera using a Hirox KH-8700 3D Digital Microscope located in the Lithic laboratory of IPHES (Tarragona, Spain) (April 2023).

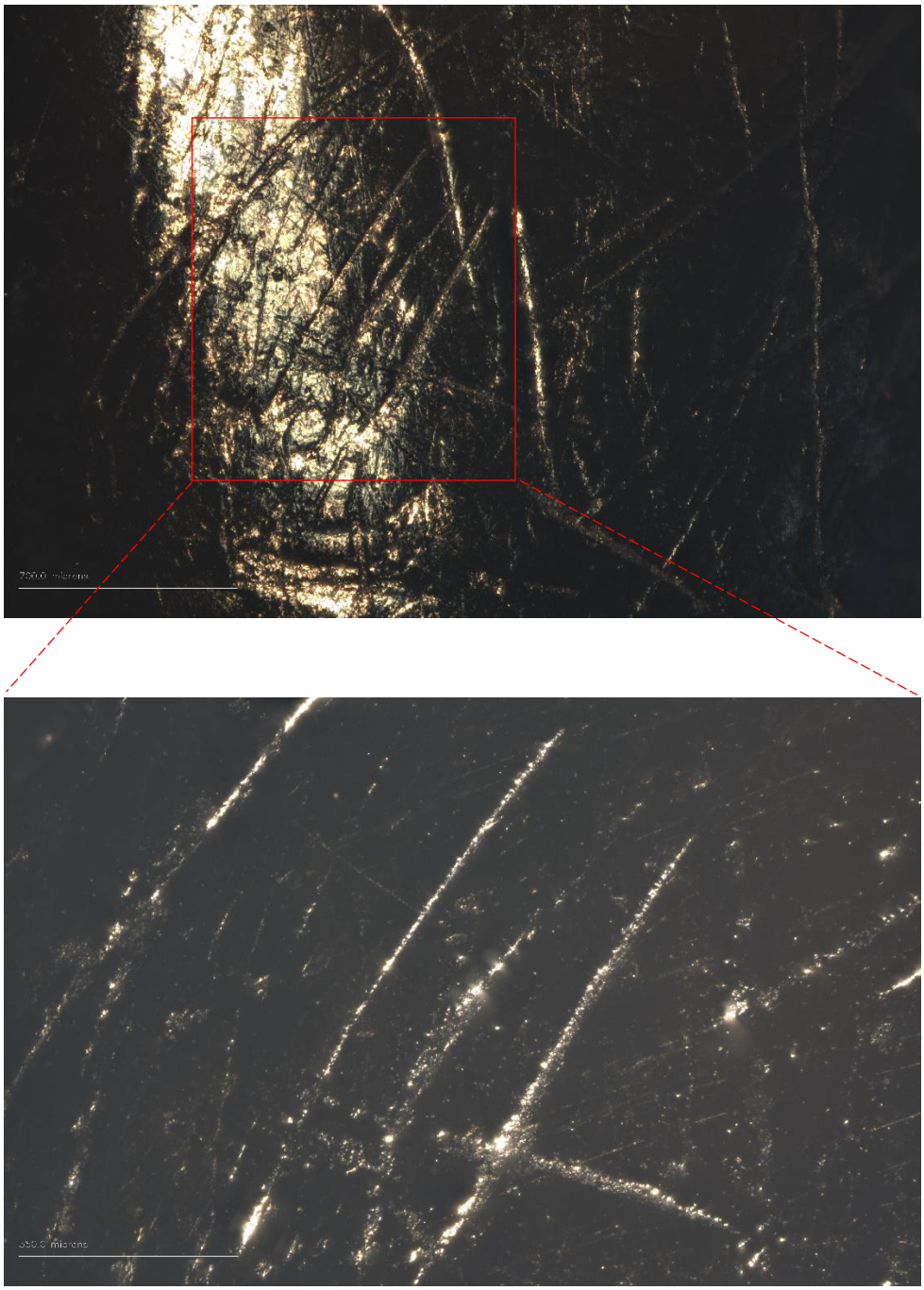

Figure 5.26 Zeiss capture image of the cast specimen *n.* CC19_13/3_E8_74 (incisor) labial left side at 50x magnification. Below, focus on the middle third left side at 100x magnification. Is possible to observe the same three scratches related to light reflection issues in their inner part. Photo taken by M. Mattera using a Zeiss Axioscope A1 optical microscope located in the Lithic laboratory of IPHES (Tarragona, Spain) (April 2023).

5.4 *Methodological Comparison of Diet-related Micro Features*

From the 7 samples selected for this analysis, one of them (tooth *n.* CC19_13/3_E8_74 – incisor) show several ante and post-mortem modifications on the labial surface; for this reason, the quantification of microwear dietary-related features was not possible to measure. Therefore, the specimen was formally excluded from the current comparative study, but its alterations were still documented for ante and post-mortem reference in the previous section (paragraphs 5.2-5.3). The other 6 samples were used for the microwear quantification, then graphical and numerical results were compared between each microscope. Specifically, no standard protocols were applied in the selection of the same areas to be analyzed for the anterior teeth because there are no formal procedures for the microwear feature analysis. Images were selected based on the greatest amount of microwear traces that it was possible to observe and quantify; moreover, the following analysis has a purely comparative function, thus different locations of the investigated areas do not alter the result. Regarding molar specimens, on the other side, the methodological protocols (paragraph 4.3.3) were properly followed to select the correct location on both buccal and occlusal surfaces. This is mostly due to the fact that standardized procedures were already developed for molars, but also because the other work aim is to obtain a preliminary analysis on diet reconstruction that can be comparable with previous studies addressing the same issue (paragraph 5.5). Unfortunately, some key areas for molar analysis did not return the expected results. In fact, two occlusal surfaces (specimens *n.* CC20_13/4_F8_52 and CC22_13/5_F9_134) were completely worn preventing proper visualization of "facet 9" area; moreover, the buccal surface of tooth *n.* CC21_13/7_G8_433 yielded no useful traces that could be linked to dental microwear. As mentioned earlier, each tooth area was divided by numbered graphical tables in order to observe the quantifications graphically between each microscope on the same detected surface. While the numerical results obtained from the measurements were insert into tables containing: absolute number of counted striations, average length mean, average length standard deviation, max length recorded, min length recorded, average angle mean, average angle standard deviation, max angle recorded, min angle recorded. The list (divided for specimen) with each surface analyzed and compared, based on the methodological description in the previous chapter 4, will follow:

Graphic Table 1° "*Specimen n. CC21_13/7_G8 (Incisor) - Labial surface, cervical third area*": Examining the different labial areas of sample *n.* CC21_13/7_G8, it was noted that the surface that gave the most dental microwear striations was the middle part of the cervical third area. This surface was first investigated by using the ESEM from which a 100x magnification image was captured, then additional images were acquired from both the Hirox and the Zeiss, in the same area, following the equivalence among the magnifications (Mag) and the horizontal field of view (HFOV) described in the table (Table 4.1) taken from Martín-Viveros & Ollé (2020). The analyzed area clearly shows diet-related marks of various lengths and orientations, the only inconvenient is a limited area of pitting on the right side that partially obliterated the scratches. The number of striations counted with the ESEM correspond to 89; while a smaller number of them were observed with Hirox (65) which corresponds to a decrease of -26.97%, and with Zeiss (63) which corresponds to a decrease of -29.21% (Tables 5.3). But is interesting to notice that the average length recorded from the OM microscopes (403.309 μm from Hirox and 346.476 μm from Zeiss) results greater when compared to ESEM (204.131 μm). While the average angle shows an orientation trend that slightly drops when measured with the Zeiss, but in general the measured orientations do not change significantly from one microscope to another. As can be seen from the comparative images, the area to the left of the tooth tends to be dark when observed through optical microscopes; this effect is due to the physiological curvature of the incisor

that creates areas of shadow on the surface. The lower number of striations counted here with the optical microscopes is mainly due to this phenomenon.

Graphic Table 1°	ESEM	Hirox	Zeiss
Counted Striations	89	65	63

Graphic Table 1°	Average length (ESEM)	Average length (Hirox)	Average length (Zeiss)	Average angle (ESEM)	Average angle (Hirox)	Average angle (Zeiss)
Mean	204.131 µm	403.309 µm	346.476 µm	91.335°	97.199°	79.581°
SD	150.188 µm	231.984 µm	223.381 µm	38.949°	41.682°	44.838°
Min	55.937 µm	104.065 µm	76.059 µm	7.461°	11.254°	8.270°
Max	937.551 µm	1.327.323 µm	1.229.958 µm	166.464°	174.738°	171.038°

Tables 5.3 Above, table showing the difference of counted striations using three different microscopes (ESEM, Hirox and Zeiss) on the same tooth area of cast specimen n. CC21_13/7_G8 (Incisor) - Labial surface, cervical third area. Below, table showing other comparative variables measured with ImageJ software on the images showed in Graphic Table 1°.

Graphic Table 1°

• *Specimen n. CC21_13/7_G8 (Incisor) – Labial surface, cervical third area*

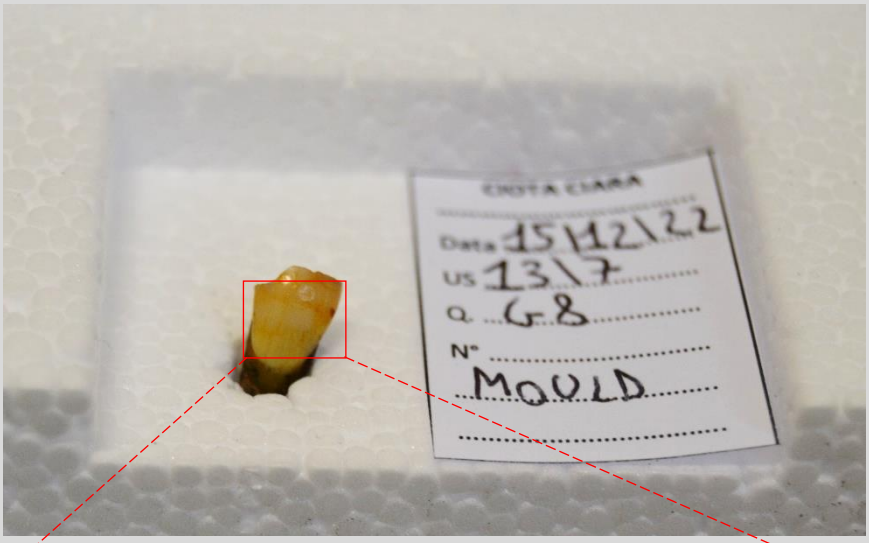

Original Neanderthal specimen n. CC21_13/7_G8 during the molding process.

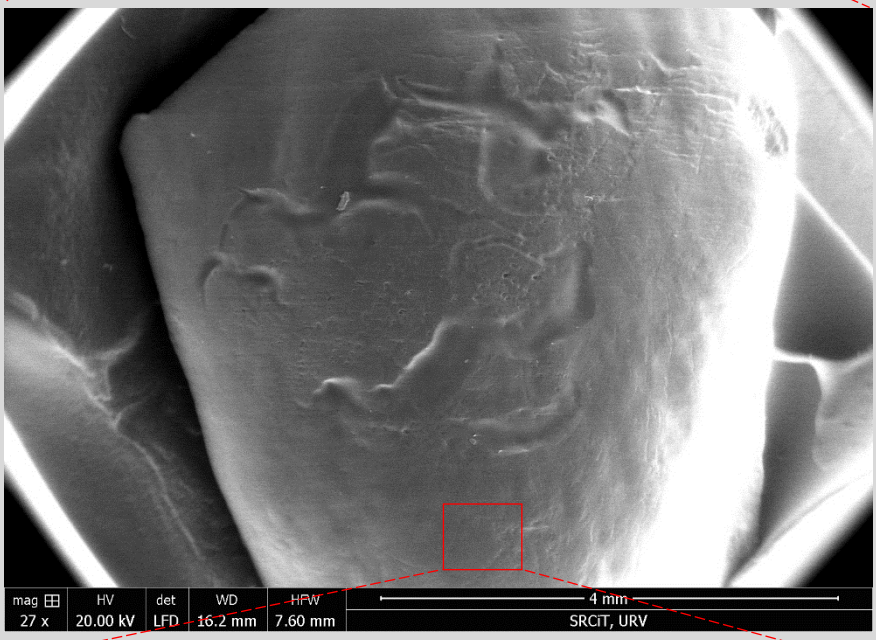

Capture ESEM image at 27x magnification of cast specimen n. CC21_13/7_G8 – Labial surface.

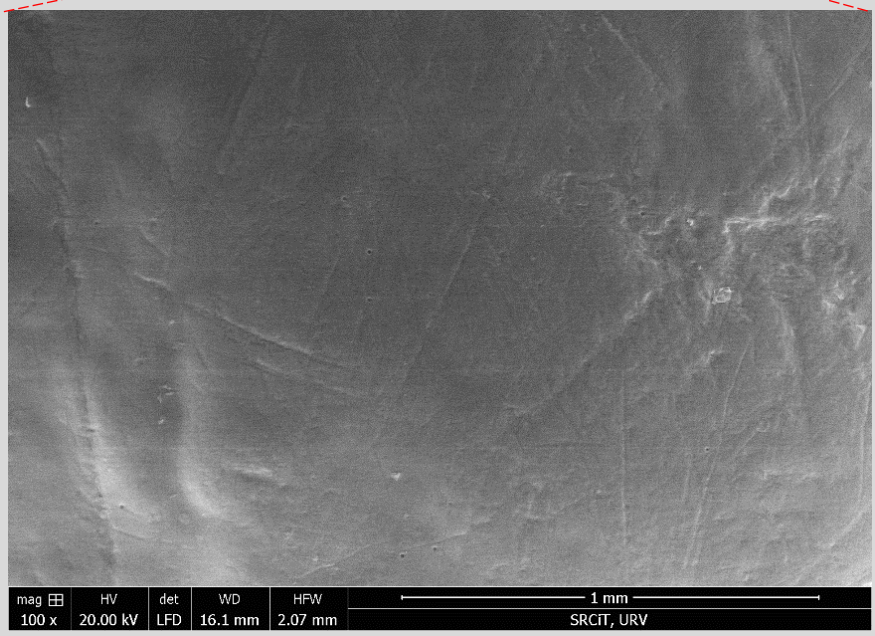

Capture ESEM image at 100x magnification of cast specimen n. CC21_13/7_G8 – Labial surface, cervical third area.

Dental microwear comparison – Labial surface

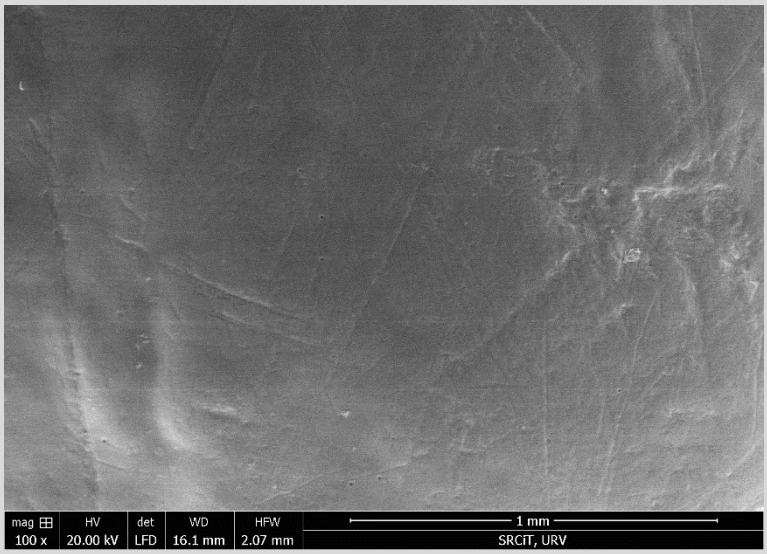

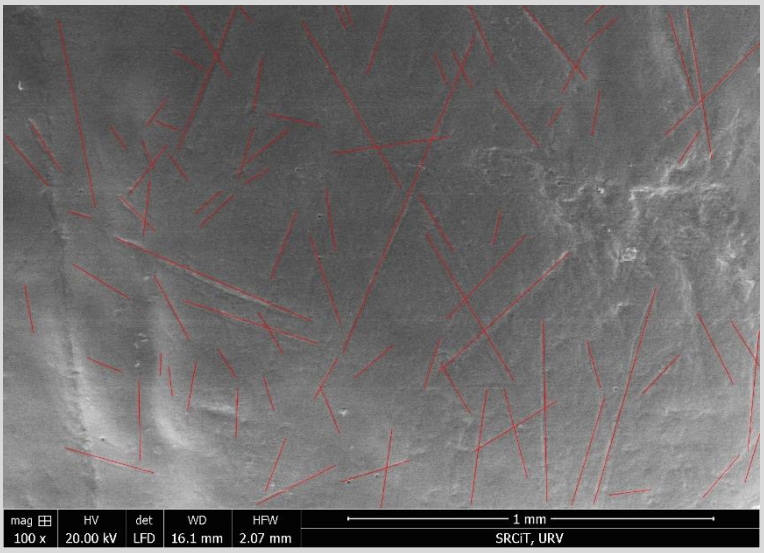

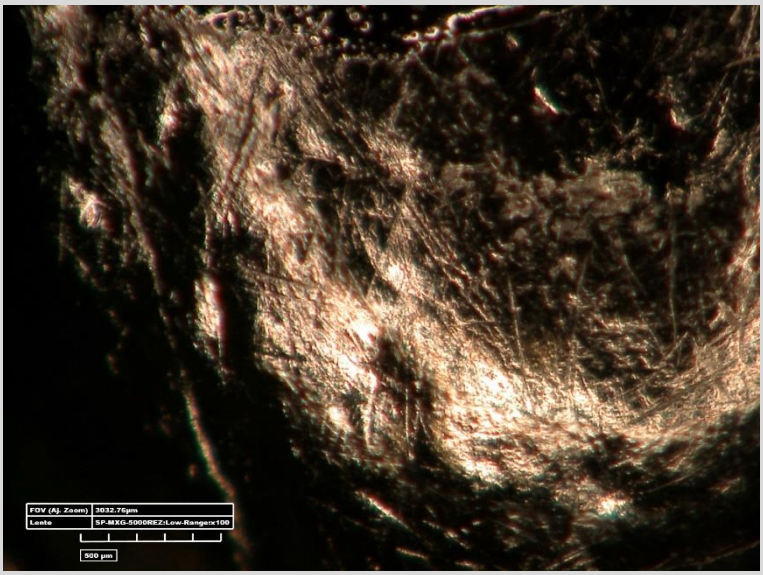

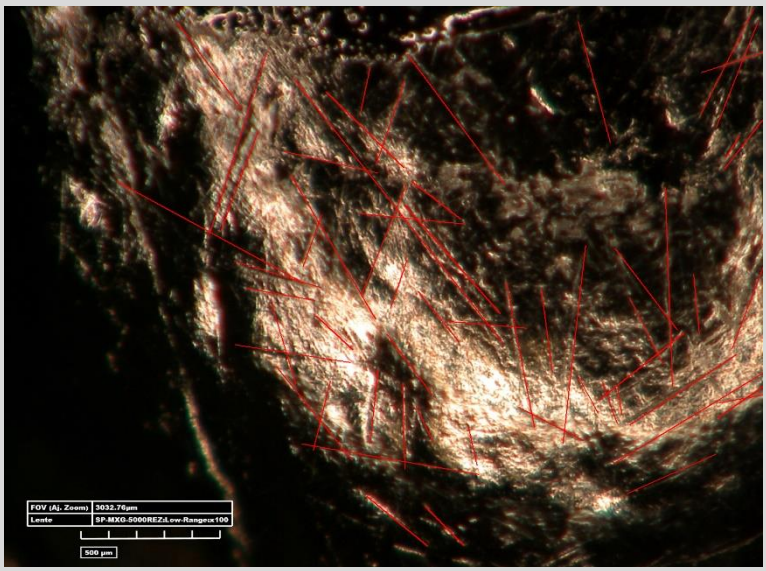

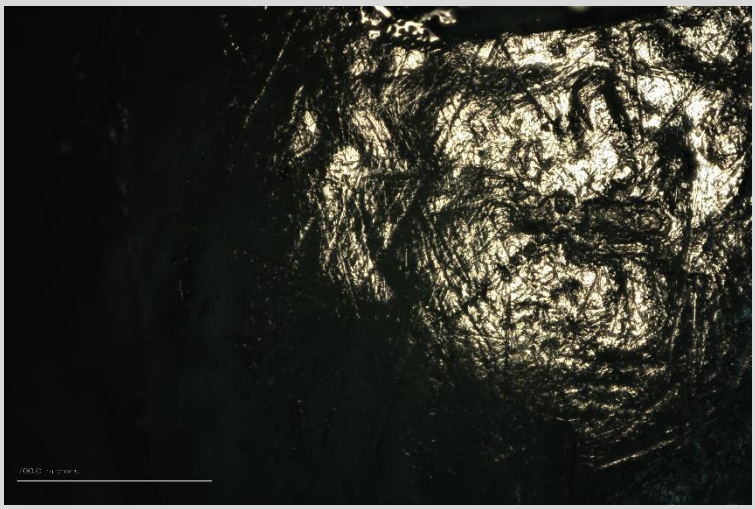

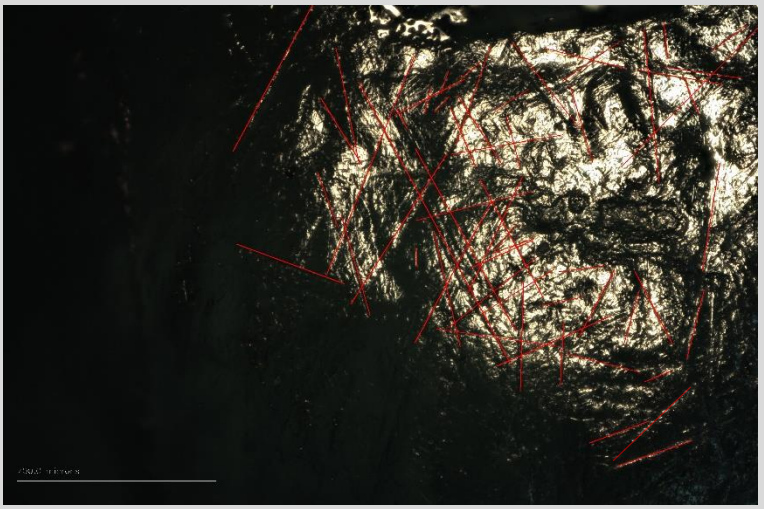

Dental microwear comparison between three different microscopes following the methodology previously described (paragraph 4.3.3). Above, ESEM capture images (x100). Middle, Hirox captured images (x100). Below, Zeiss captured images (x50). Images on the left refer to the original microsocopes' shots, images on the right refer to the processed microscopes' shots with the microwear striations measured (in red color) using imageJ software; these quantitative data are showed in tables 5.3

Graphic Table 2° "*Specimen n. CC21_13/8_H7_36 (Incisor) – Labial surface, middle third area*": Observing the different labial areas of sample *n.* CC21_13/8_H7_36, in general it does not yield many microwear striations. However, it was noted that the surface that gave the most dental microwear features was the central-left part of middle third area. This surface was first investigated by using the ESEM from which a 100x magnification image was captured, then additional images were acquired from both the Hirox and the Zeiss, in the same area, following the equivalence among the magnifications (Mag) and the horizontal field of view (HFOV) described in the table (Table 4.1) taken from Martín-Viveros & Ollé (2020). The entire surface has been affected by micro-bubbles (occurred during the molding phase) that have partially altered the visualization of the microwear traces. The number of striations counted with the ESEM correspond to 40; while a greater number of them were observed with Hirox (71) which corresponds to an increase of 43.66%, and with Zeiss (62) which corresponds to an increase of 34.48% (Tables 5.4). The ESEM image appears more blurred and this results in fewer displayed features. Even in this case, is interesting to notice that the average length recorded from the OM microscopes (340.424 µm from Hirox and 328.439 µm from Zeiss) results slightly greater when compared to ESEM (315.032 µm). While the average orientation shows an increased angle trend when measured with the Zeiss (103.623°). As can be seen from the comparative images, the lateral sides of the images tend to be dark when observed through optical microscopes for the physiological curvature of the incisor; but despite of that, it was still possible to observe a greater number of dental microwear features with OM microscopy.

Graphic Table 2°	**ESEM**	**Hirox**	**Zeiss**
Counted Striations	40	71	62

Graphic Table 2°	**Average length (ESEM)**	**Average length (Hirox)**	**Average length (Zeiss)**	**Average angle (ESEM)**	**Average angle (Hirox)**	**Average angle (Zeiss)**
Mean	315.032 µm	340.424 µm	328.439 µm	74.969°	103.623°	89.791°
SD	246.753 µm	263.539 µm	291.638 µm	44.767°	29.980°	41.559°
Min	50.449 µm	72.542 µm	57.452 µm	1.534°	2.498°	5.839°
Max	1.176.077 µm	1.627.555 µm	1.486.493 µm	158.569°	155.772°	165.630°

Tables 5.4 Above, table showing the difference of counted striations using three different microscopes (ESEM, Hirox and Zeiss) on the same tooth area of cast specimen n. CC21_13/8_H7_36 (Incisor) – Labial surface, middle third area. Below, table showing other comparative variables measured with ImageJ software on the images showed in Graphic Table 2°.

Graphic Table 2°

• *Specimen n. CC21_13/8_H7_36 (Incisor) – Labial surface, middle third area*

Original Neanderthal specimen n. CC21_13/8_H7_36 during the molding process.

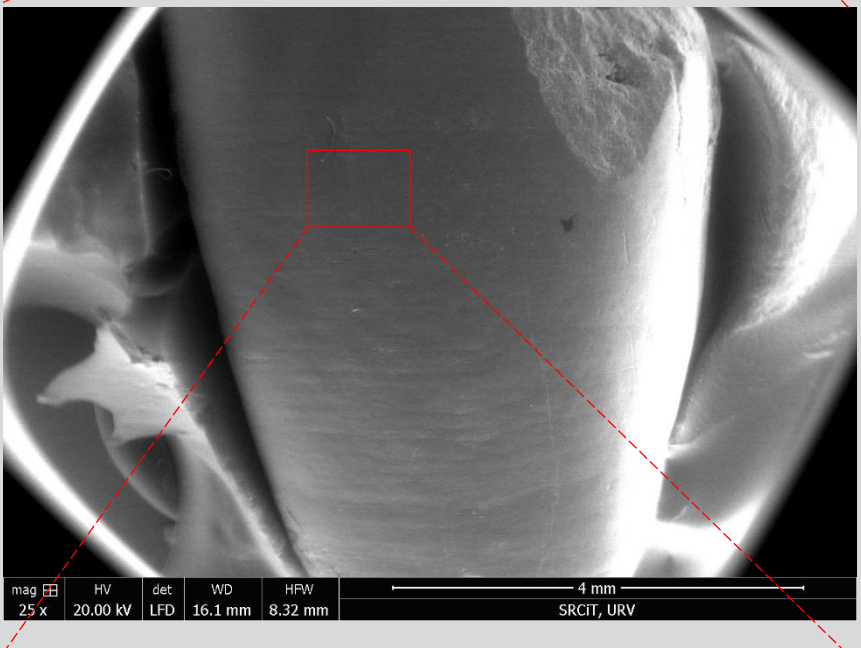

Capture ESEM image at 25x magnification of cast specimen n. CC21_13/8_H7_36 - Labial surface.

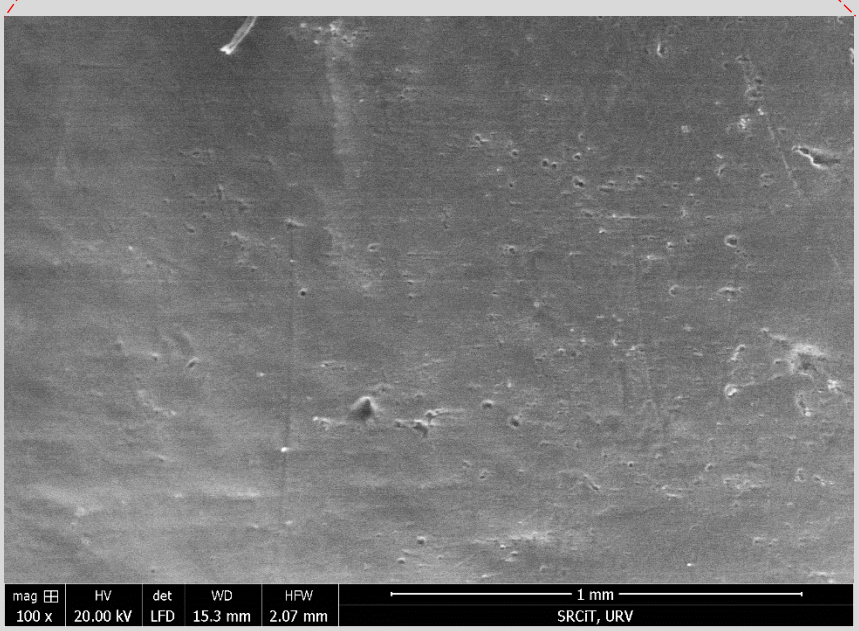

Capture ESEM image at 100x magnification of cast specimen n. CC21_13/8_H7_36 - Labial surface, middle third area.

Dental microwear comparison – Labial surface

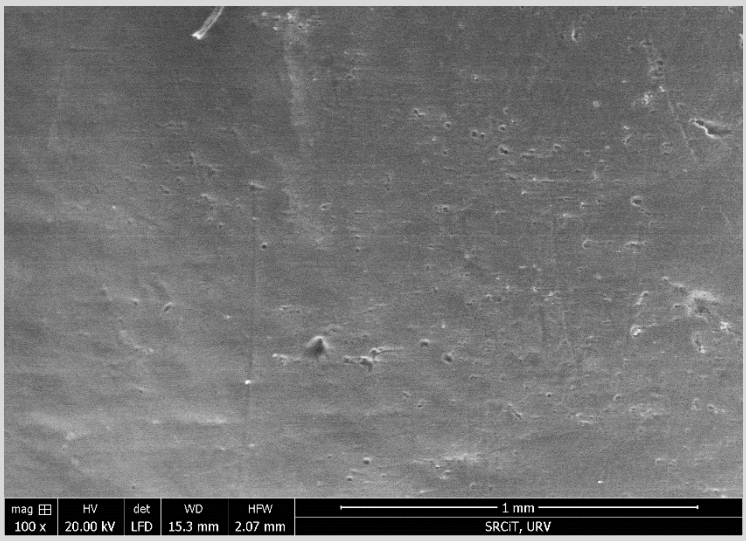

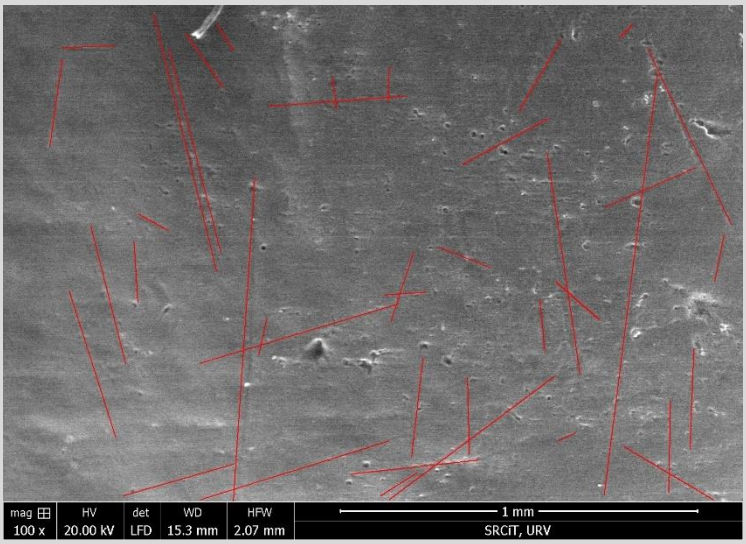

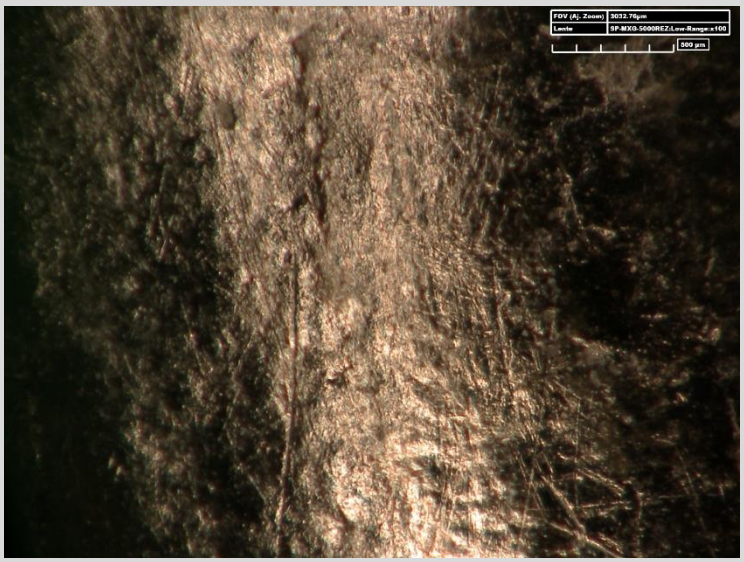

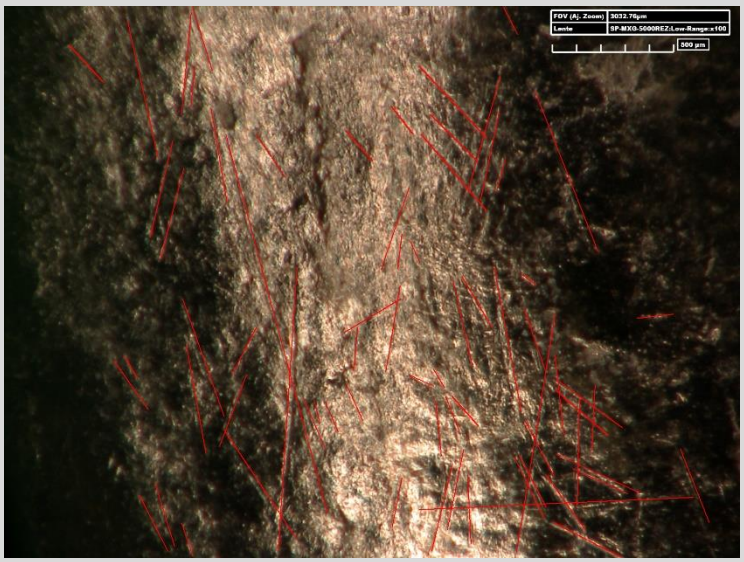

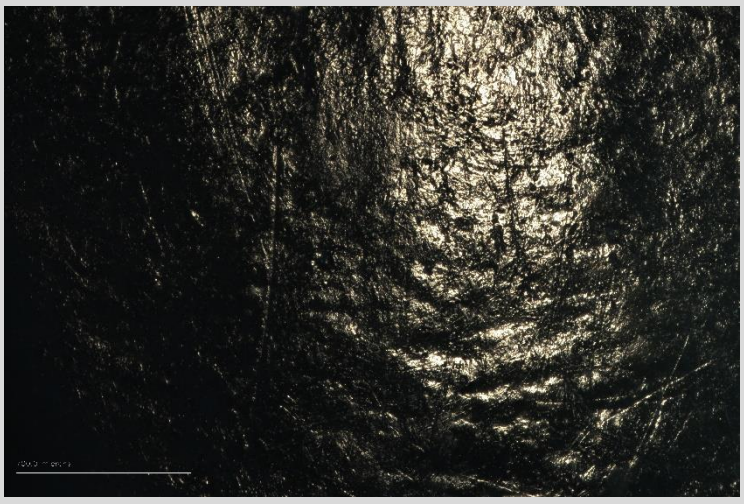

Dental microwear comparison between three different microscopes following the methodology previously described (paragraph 4.3.3). Above, ESEM capture images (x100). Middle, Hirox captured images (x100). Below, Zeiss captured images (x50). Images on the left refer to the original microsocopes' shots, images on the right refer to the processed microscopes' shots with the microwear striations measured (in red color) using imageJ software; these quantitative data are showed in tables 5.4

Graphic Table 3° "*Specimen n. CC20_13/7_G7_238 (canine) – Occlusal and Labial surfaces*": This specimen shows interesting dental microfeatures on both its occlusal and labial surfaces, specifically on the incisal third area. This occlusal side was first investigated by using the ESEM from which a 100x magnification image was captured, while the incisal third area was observed at 140x magnification; for this reason, only a comparison with Hirox (140x magnification) was possible. The occlusal surface shows several diet-related pits that has been counted on the ESEM image (Table 5.5); OM images of this area, unfortunately, doesn't allow to properly measure these pits because of light reflection issues. On the other side, the number of striations counted with the ESEM correspond to 60 and a similar number of them were observed both with Hirox (59) with Zeiss (66). The average angle tends to slightly increase for the Hirox striations, symptom of the fact that the counted features, even if almost in equal numbers, are not exactly counted in the same position on the three images. The morphological triangular shape of the occlusal canine' area results in a "light vs dark" visualization of the images in all the microscopes, above all for the OM's 3D images. On the other hand, the incisal third area shows a higher number of dental microfeatures on both microscopes at 140x magnification (ESEM:147 and Hirox:126). Even in this case is interesting notice that the average length recorded from the Hirox (251.558 µm) results greater when compared to ESEM (173.226 µm), while the general orientation was affected just by a slightly change (Tables 5.6).

Graphic Table 3°- Oc.	ESEM	Hirox	Zeiss
Counted Striations	60	59	66
Counted Pits	99	No data	No data

Graphic Table 3°- Oc.	Average length (ESEM)	Average length (Hirox)	Average length (Zeiss)	Average angle (ESEM)	Average angle (Hirox)	Average angle (Zeiss)
Mean	231.118µm	322.429 µm	229.820 µm	99.513°	113.032°	85.473°
SD	101.956 µm	197.670 µm	147.213 µm	55.290°	48.923°	44.838°
Min	69.761 µm	77.880 µm	44.112 µm	10.305°	7.044°	8.270°
Max	597.906 µm	964.944 µm	671.553 µm	179.708°	170.602°	171.038°

Tables 5.5 Above, table showing the difference of counted striations and pits using three different microscopes (ESEM, Hirox and Zeiss) on the same tooth area of cast specimen CC20_13/7_G7_238 – occlusal surface. Below, table showing other comparative variables measured with ImageJ software on the images showed in Graphic Table 3°- Occlusal surface.

Graphic Table 3°- Lab.	ESEM	Hirox
Counted Striations	147	126

Graphic Table 3°- Lab.	Average length (ESEM)	Average length (Hirox)	Average angle (ESEM)	Average angle (Hirox)
Mean	173.226 µm	251.558 µm	81.481°	91.376°
SD	116.710 µm	152.645 µm	49.565°	36.598°
Min	30.129 µm	45.325 µm	4.764°	6.303°
Max	670.176 µm	1.021.396 µm	179.226°	177.342°

Tables 5.6 Above, table showing the difference of counted striations using two different microscopes (ESEM and Hirox) on the same tooth area of cast specimen n. CC20_13/7_G7_238 - Labial surface, incisal third area. Below, table showing other comparative variables measured with ImageJ software on the images showed in Graphic Table 3°- Labial surface.

Graphic Table 3°

• *Specimen n. CC20_13/7_G7_238 (canine) – Occlusal and Labial (incisal third area) surfaces*

Original Neanderthal specimen n. CC20_13/7_G7_238 (canine) during the molding process.

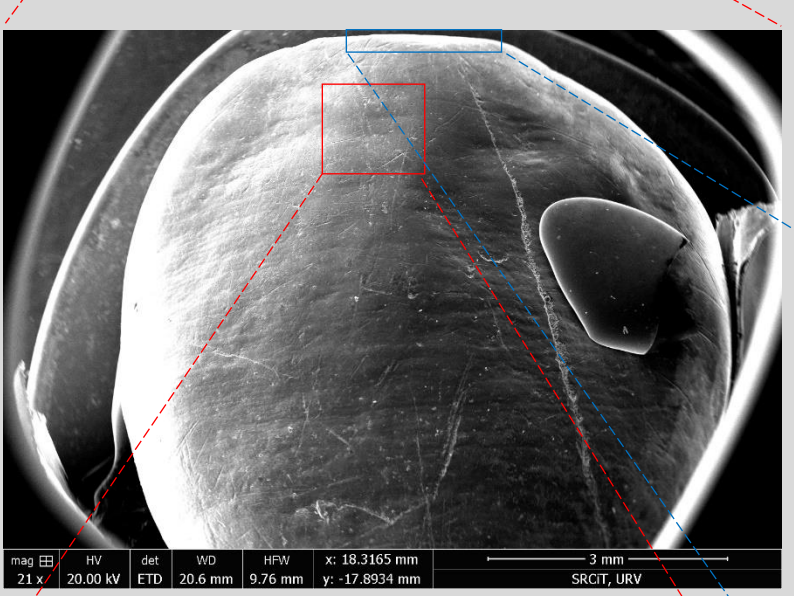

Capture ESEM image at 25x magnification of cast specimen n. CC20_13/7_G7_238 - Labial surface.

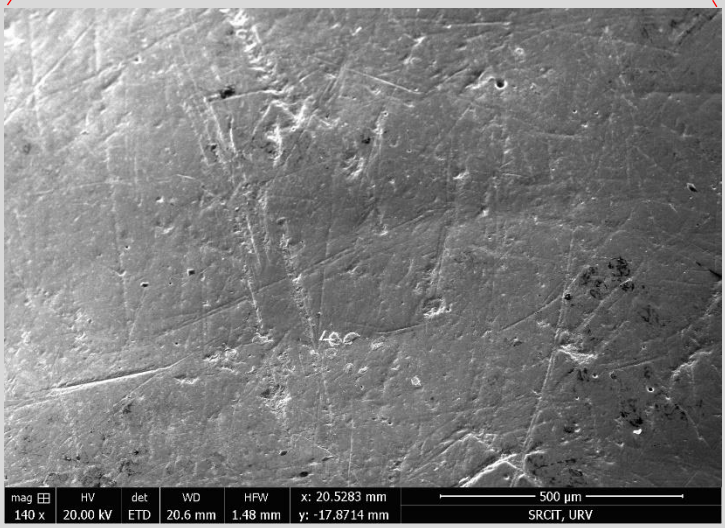

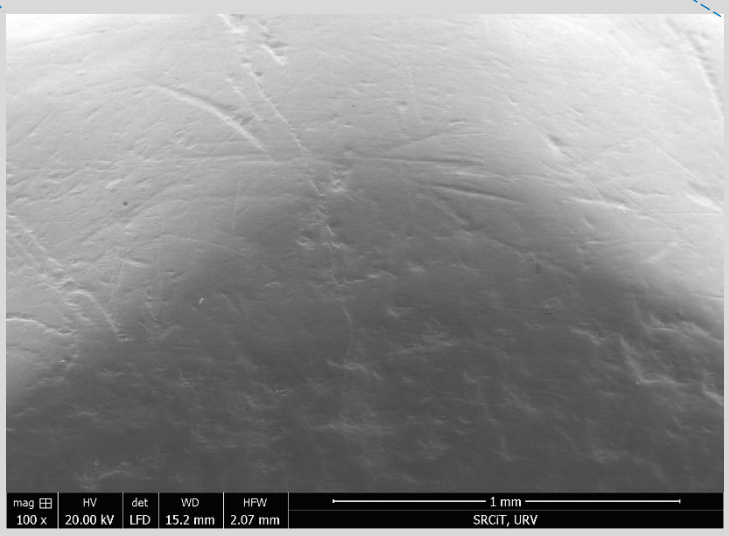

Left, capture ESEM image at 140x magnification of cast specimen n. CC20_13/7_G7_238 - Labial surface, Incisal third area. Right, ESEM capture image of the same tooth at 100x magnification – Occlusal area.

Dental microwear comparison – Occlusal surface

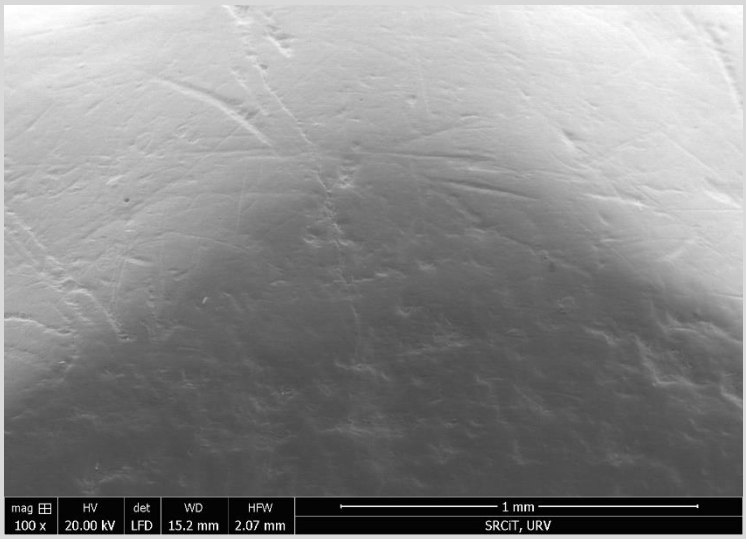

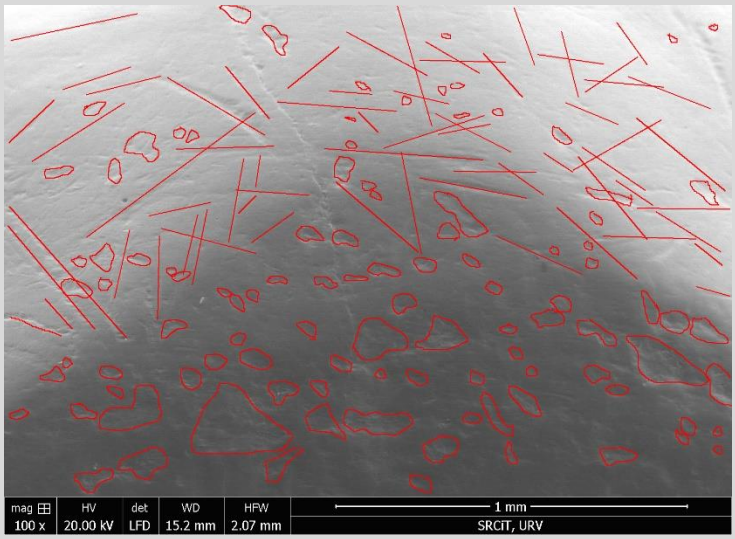

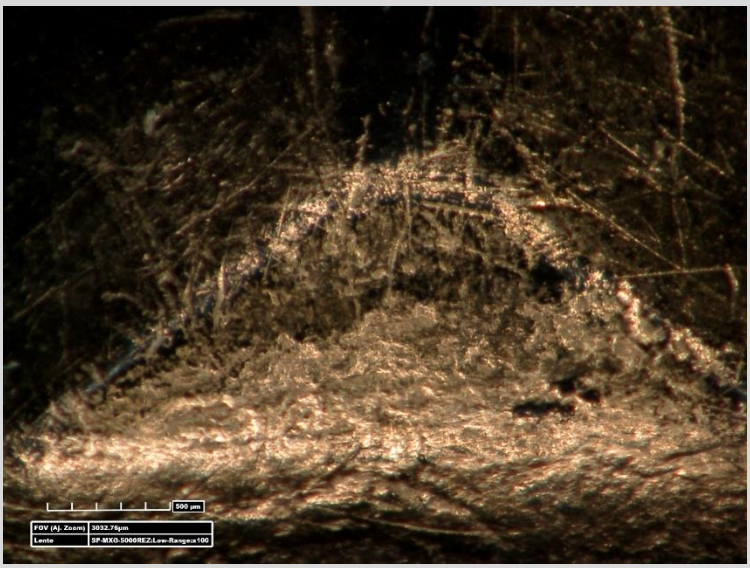

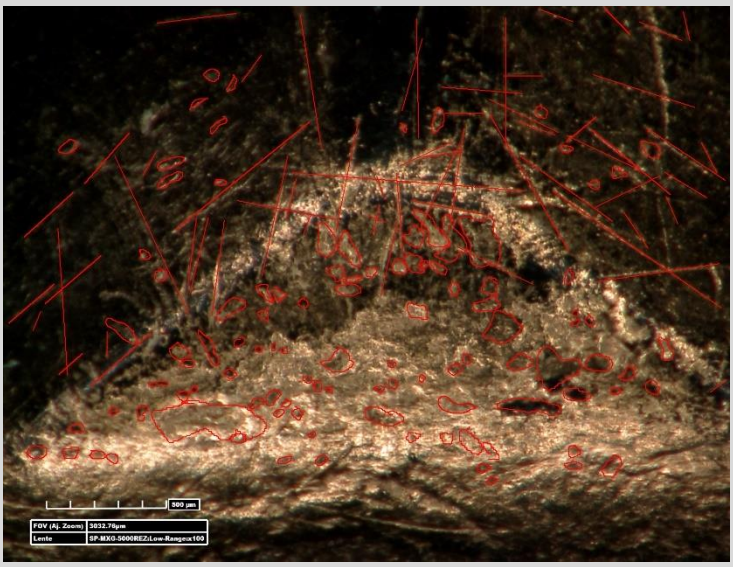

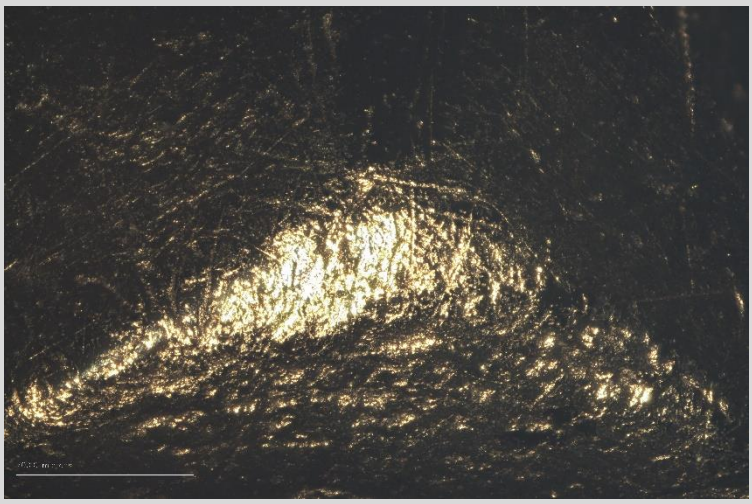

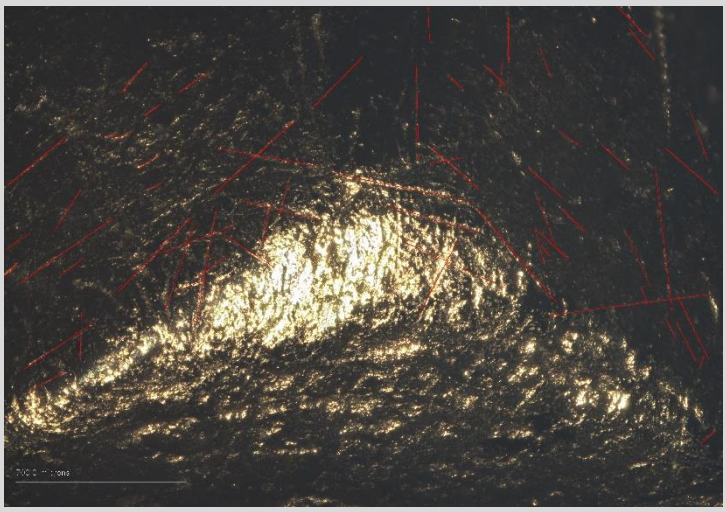

Dental microwear comparison between three different microscopes following the methodology previously described (paragraph 4.3.3). Above, ESEM capture images (x100). Middle, Hirox captured images (x100). Below, Zeiss captured images (x50). Images on the left refer to the original microsocopes' shots, images on the right refer to the processed microscopes' shots with the microwear striations measured (in red color) using imageJ software; these quantitative data are showed in tables 5.5

Dental microwear comparison – Labial surface

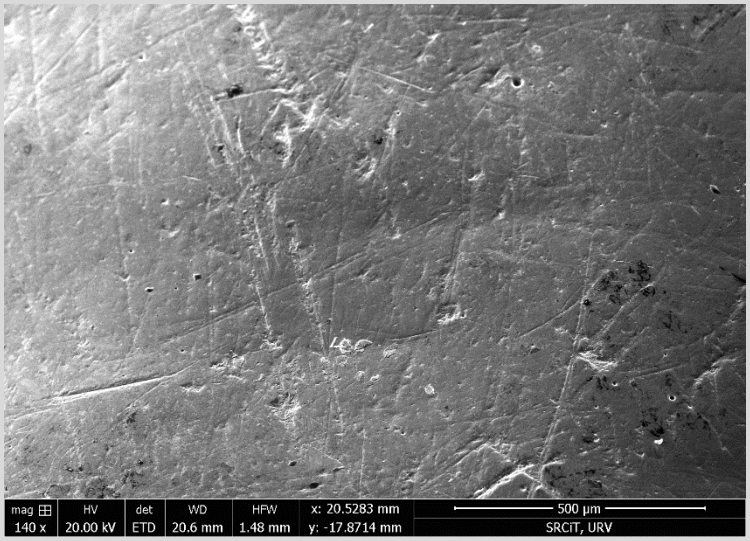

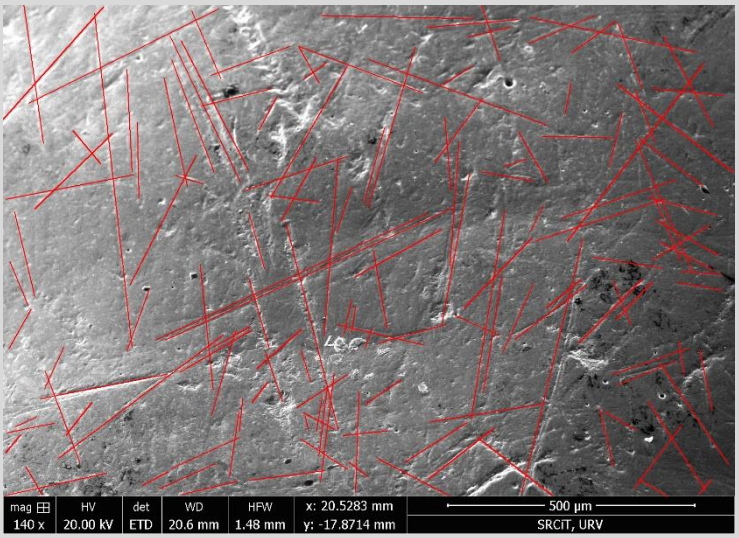

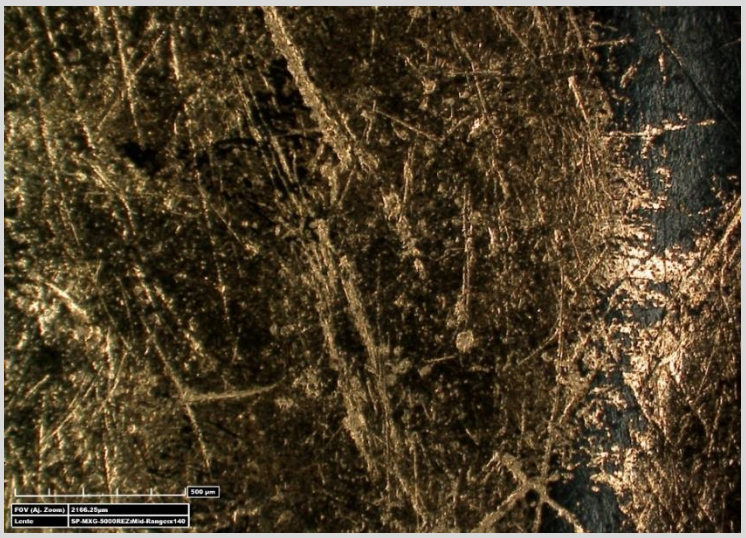

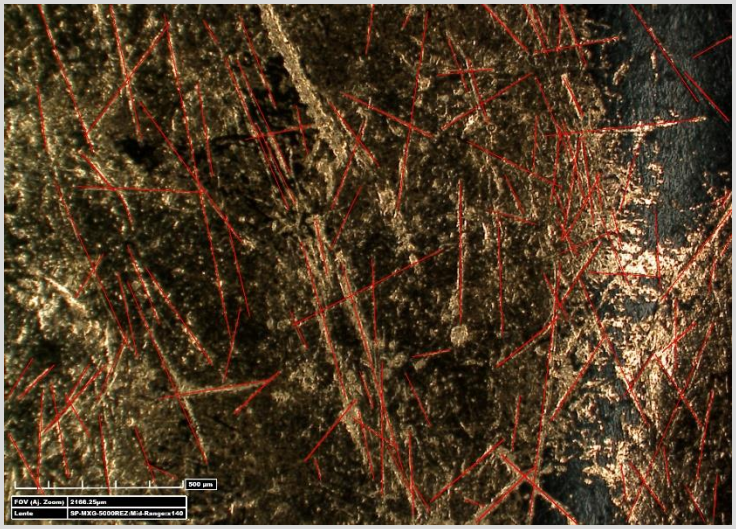

Dental microwear comparison between two different microscopes following the methodology previously described (paragraph 4.3.3). Above, ESEM capture images (x140). Below, Hirox captured images (x140). Images on the left refer to the original microsocopes' shots, images on the right refer to the processed microscopes' shots with the microwear striations measured (in red color) using imageJ software; these quantitative data are showed in tables 5.6

Graphic Table 4° "*Specimen n. CC20_13/4_F8_52 (molar) – Buccal surface, middle area*": As already mentioned earlier, the ESEM image was taken at 100x magnification on the medial area of the molar's buccal surface, avoiding both the occlusal and cervical thirds. In fact, following the methodology developed by Pérez-Pérez et al. (1994), this is the standardized area used for microwear analysis (on the buccal surface of teeth) to infer dietary habits that will be described in the next section (Paragraph 5.5). The microscopic investigation of the middle buccal area, as expected, yielded a great number of dental striations by using the three equipment. The only issue is represented by a post-depositional crack in the right side of the picture, but the remaining image's surface appeared very clear for microwear analysis. The number of striations counted with the ESEM correspond to 166; while a slight number of them were observed with Hirox (154) and a slight increase was observed with Zeiss (169) (Tables 5.7). Is interesting notice that the average length recorded from the ESEM (246.394 µm) and the Hirox (261.414) appear very similar, while the Zeiss value is slightly lower (200.027 µm). On the other hand, the average orientation shows an increased angle trend only when measured with the Hirox (113.032°). As can be seen from the comparative images, both Hirox and Zeiss yielded 3D pictures with dark areas probably due to the bulged curvature of the molar.

Graphic Table 4°	ESEM	Hirox	Zeiss
Counted Striations	166	154	169

Graphic Table 4°	Average length (ESEM)	Average length (Hirox)	Average length (Zeiss)	Average angle (ESEM)	Average angle (Hirox)	Average angle (Zeiss)
Mean	246.384µm	261.414 µm	200.027 µm	98.907°	113.032°	98.110°
SD	174.916 µm	182.748 µm	156.305 µm	47.953°	48.923°	37.761°
Min	39.282 µm	30.597 µm	30.061 µm	3.983°	11.004°	2.407°
Max	961.119 µm	1061.186 µm	940.312 µm	180.00°	180.00°	176.619°

Tables 5.7 Above, table showing the difference of counted striations and pits using three different microscopes (ESEM, Hirox and Zeiss) on the same tooth area of cast CC20_13/4_F8_52 (molar) – Buccal surface, middle area. Below, table showing other comparative variables measured with ImageJ software on the images showed in Graphic Table 4°.

Graphic Table 4°

• *Specimen n. CC20_13/4_F8_52 (molar) – Buccal surface, middle area*

Original Neanderthal specimen CC20_13/4_F8_52 (molar) during the molding process.

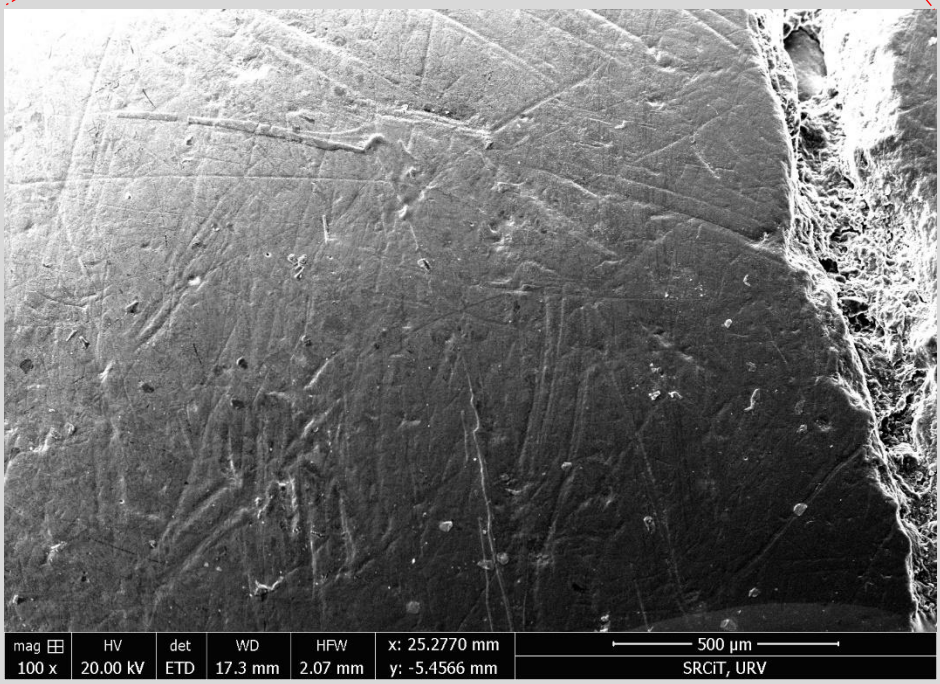

Capture ESEM image at 100x magnification of cast specimen n. CC20_13/4_F8_52 - Buccal surface, middle area.

Dental microwear comparison – Buccal surface

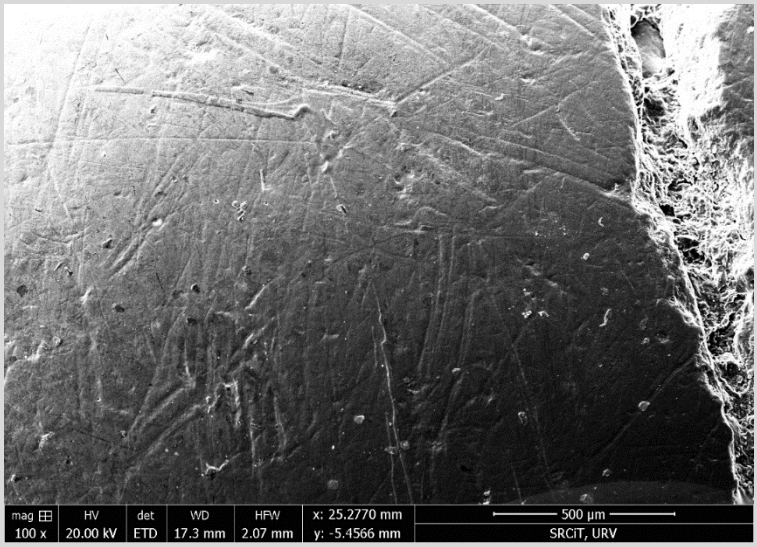

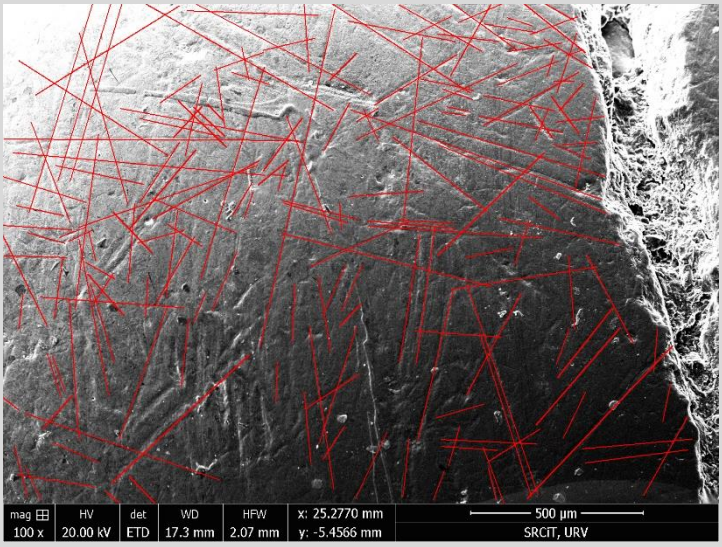

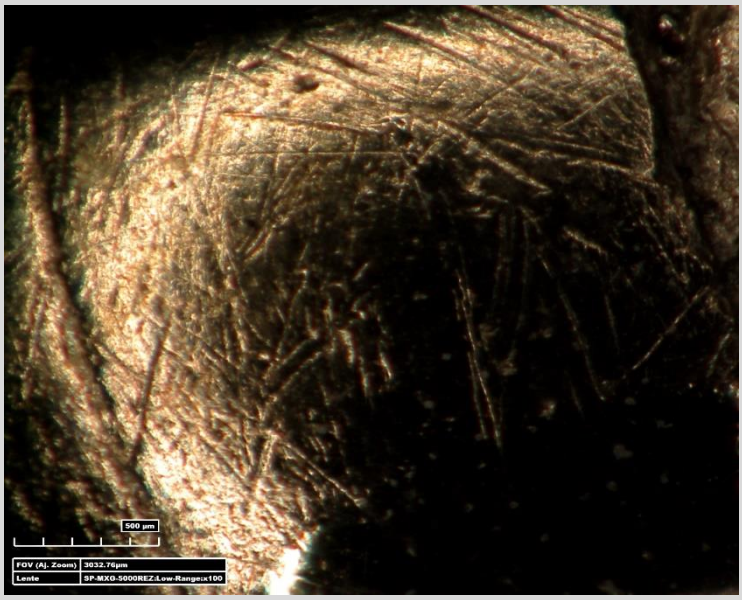

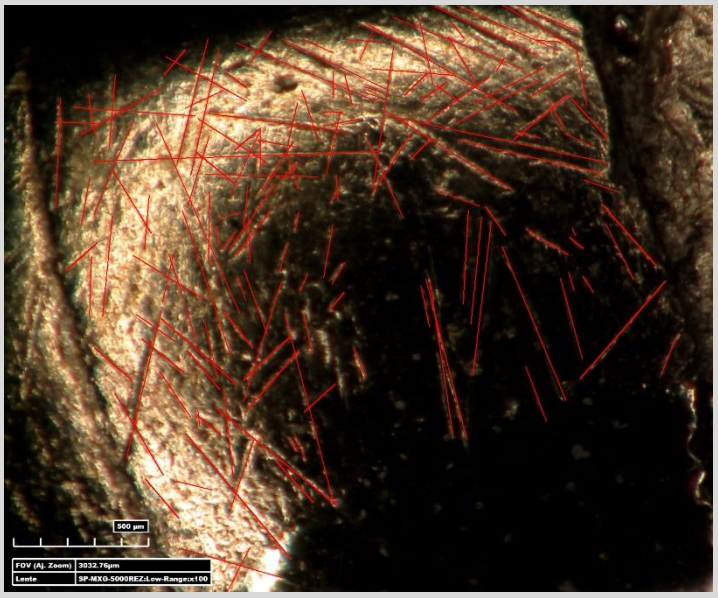

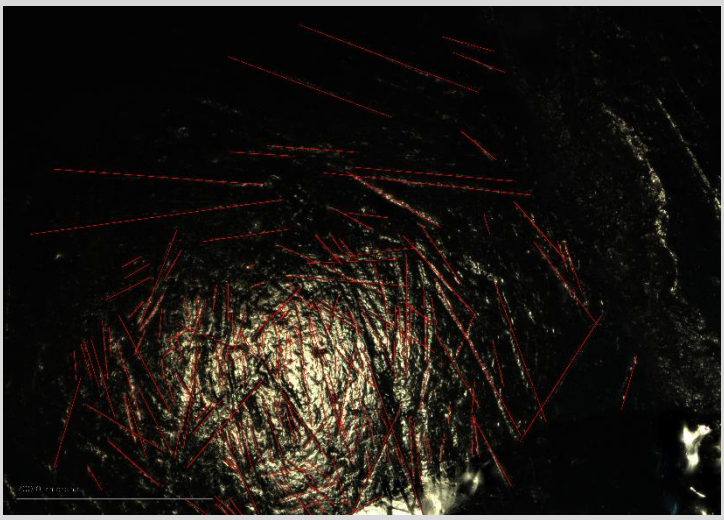

Dental microwear comparison between three different microscopes following the methodology previously described (paragraph 4.3.3). Above, ESEM capture images (x100). Middle, Hirox captured images (x100). Below, Zeiss captured images (x50). Images on the left refer to the original microsocopes' shots, images on the right refer to the processed microscopes' shots with the microwear striations measured (in red color) using imageJ software; these quantitative data are showed in tables 5.7

Graphic Table 5° "*Specimen n. CC22_13/5_F9_134 (molar) – Buccal surface, middle area*": The same precautions were applied for this molar as for the previous described specimen (CC20_13/4_F8_52 *)*: ESEM image was taken at 100x magnification on the medial area of the molar's buccal surface to infer dietary habits. The microscopic investigation of the middle buccal area, even here, yielded a great number of dental striations by using the three microscopes. The Images appear almost clear, even if some taphonomic features tend to be superimposed on the microwear striations. The number of striations counted with the ESEM correspond to 140; while a lower number of them were observed with Hirox (109) which corresponds to a decrease of 22.14%, but a higher number of features was observed with the Zeiss (237) which corresponds to an increase of 40.93% (Tables 5.8). Is interesting notice that the average length recorded from the ESEM (200.885 µm) is very low when compared to both and the Hirox (313.324) Zeiss (262.354 µm). On the other hand, the average orientation shows a decreased angle trend only when measured with the ESEM (56.309°). As can be seen from the comparative images, both Hirox and Zeiss yielded clearer and not dark images (if compared to the previous specimens), and it is possible to observe a high rate of differences for this sample.

Graphic Table 5°	ESEM	Hirox	Zeiss
Counted Striations	140	109	237

Graphic Table 5°	Average length (ESEM)	Average length (Hirox)	Average length (Zeiss)	Average angle (ESEM)	Average angle (Hirox)	Average angle (Zeiss)
Mean	200.885 µm	313.324 µm	262.354µm	56.309°	82.672°	81.857°
SD	128.309 µm	242.743 µm	233.173 µm	30.453°	49.692°	44.838°
Min	34.800 µm	27.944 µm	15.330 µm	4.618°	3576°	8.270°
Max	651.218 µm	1.574.525 µm	1.768.993 µm	174.289°	178.781°	171.038°

Tables 5.8 Above, table showing the difference of counted striations and pits using three different microscopes (ESEM, Hirox and Zeiss) on the same tooth area of cast specimen *n.* CC22_13/5_F9_134 (molar) – Buccal surface, middle area. Below, table showing other comparative variables measured with ImageJ software on the images showed in Graphic Table 5°.

Graphic Table 5°

• *Specimen n. CC22_13/5_F9_134 (molar) – Buccal surface, middle area*

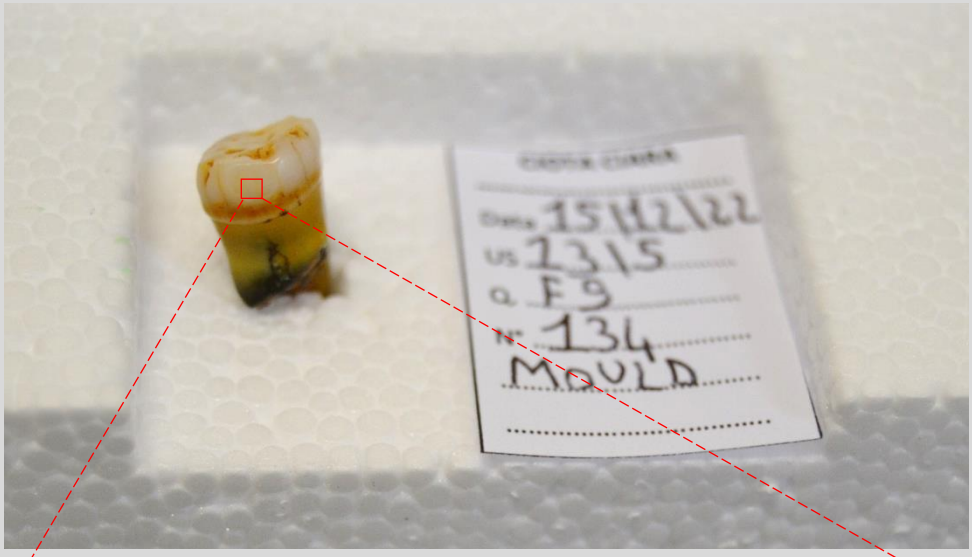

Original Neanderthal specimen n. CC22_13/5_F9_134 (molar) during the molding process.

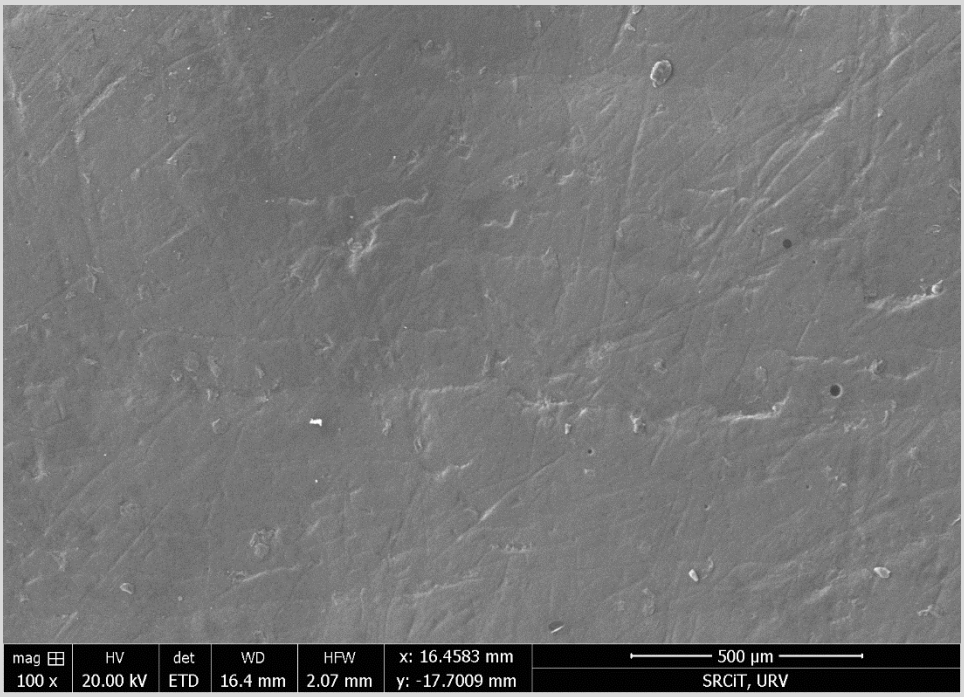

Capture ESEM image at 100x magnification of cast specimen n. CC22_13/5_F9_134 - Buccal surface, middle area.

Dental microwear comparison – Buccal surface

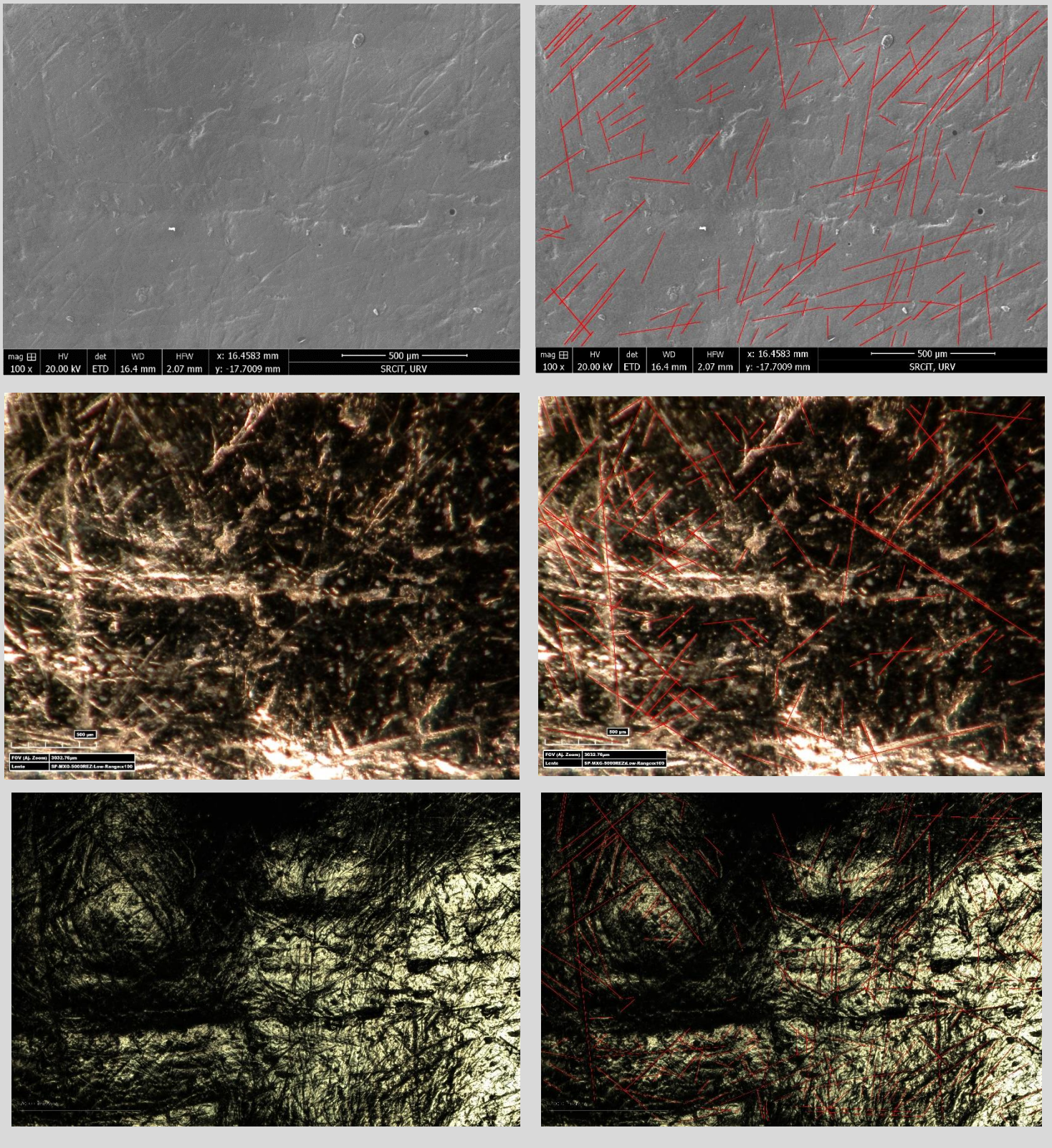

Dental microwear comparison between three different microscopes following the methodology previously described (paragraph 4.3.3). Above, ESEM capture images (x100). Middle, Hirox captured images (x100). Below, Zeiss captured images (x50). Images on the left refer to the original microsocopes' shots, images on the right refer to the processed microscopes' shots with the microwear striations measured (in red color) using imageJ software; these quantitative data are showed in tables 5.8

Graphic Table 6° "*Specimen n*. CC21_13/7_G8_433 *(molar) – Occlusal surface, facet 9*": unfortunately, the buccal surface of this specimen didn't yield dental scratches to infer dietary habits (Graphic table 6°), and, for this reason, the surface was discarded from the current analysis. On the other hand, the microscopic investigation of the occlusal surface, focused on the facet 9 area, showed a high density of pits. This pitted enamel was analyzed following the standard microwear methodology applied on occlusal surfaces but adjusted to the equivalence table among the magnifications (Mag) and the horizontal field of view (HFOV) described in the table (Table 4.1) and taken from Martín-Viveros & Ollé (2020). For this reason, the ESEM image of this area was captured a 510x magnification, while the Zeiss image was taken at 200x magnification. However, it was not possible to apply a lens that would achieve exactly 510x magnification with the Hirox microscope, so this equipment was excluded from the current sample analysis. The ESEM image appear clear, and each pit can be easily recognized, the number of counted features with this microscope correspond to 244 (Table 5.9). But unfortunately, the pitted surface was difficult to observe with the Zeiss at this magnification (200x) because of an intense reflection of light on this anisotropic surface, reason why it was not possible to measure and compare data from the optical microscope. As already mentioned in the previous section (paragraph 5.3). Considering the abnormal morphology of pits and the total absence of striations, it is much more probable that facet 9 of this tooth suffered damage caused by post-depositional effects. As a result of possible post-mortem origin of these dental features, no protocols for studying paleodiet at the occlusal surface level (e.g. pits percentage) have been applied.

Graphic Table 6°	ESEM	Zeiss
Counted pits	244	No data

Table 5.9 Table showing the difference of counted pits using two different microscopes (ESEM and Zeiss) on the facet 9 area of cast specimen *n.* CC21_13/7_G8_433 *(molar)* showed on Graphic table n. 6°

Graphic Table 6°

• *Specimen n. CC21_13/7_G8_433 (molar) – Occlusal surface, facet 9*

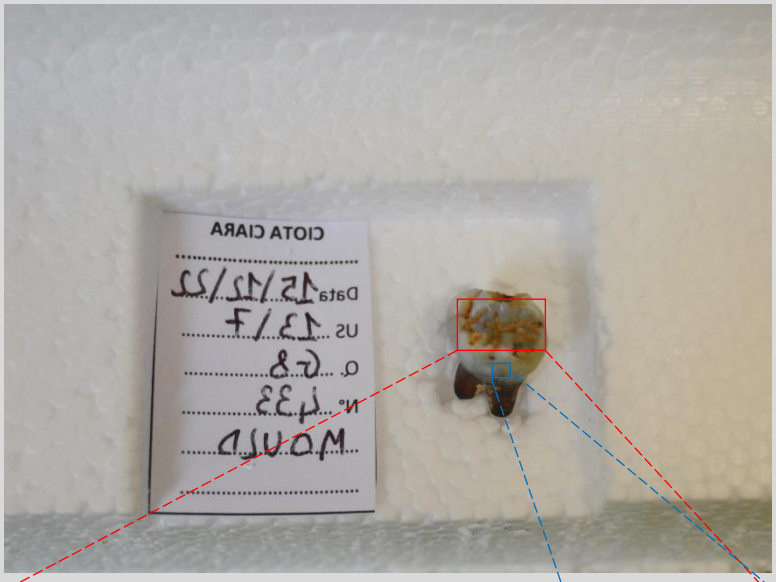

Original Neanderthal specimen n. CC21_13/7_G8_433 (molar) during the molding process.

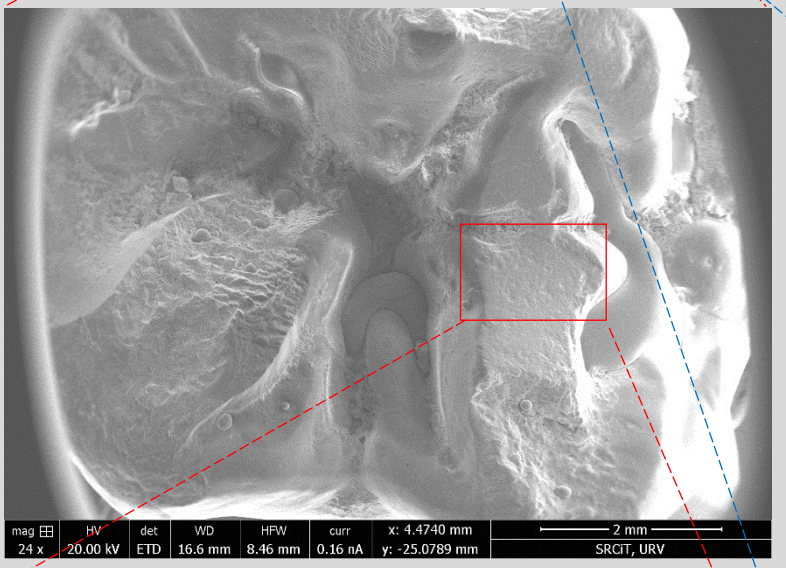

Capture ESEM image at 24x magnification of cast specimen n. CC20_13/7_G7_238 - Occlusal surface.

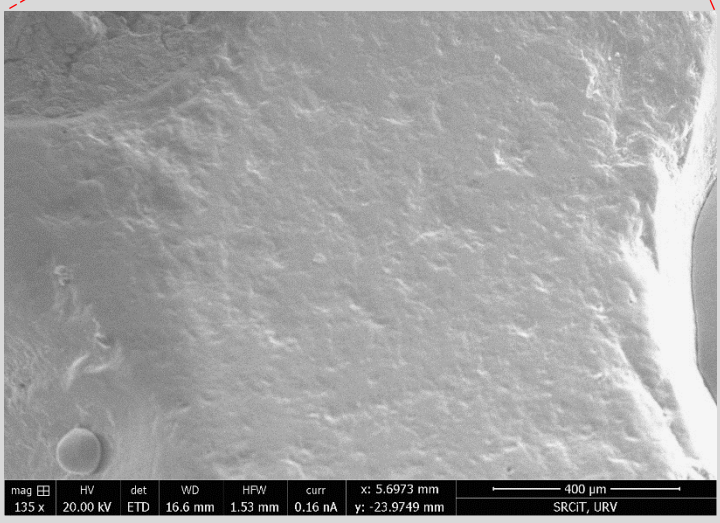

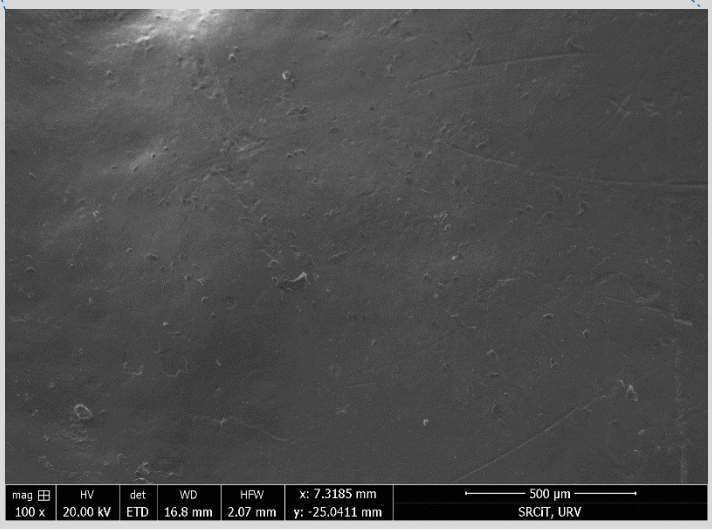

Left, capture ESEM image at 135x magnification of cast specimen n. CC20_13/7_G7_238 - Occlusal surface, facet 9. Right, ESEM capture image of the same tooth at 100x magnification – Buccal surface, middle area.

Dental microwear comparison – Occlusal surface, facet 9

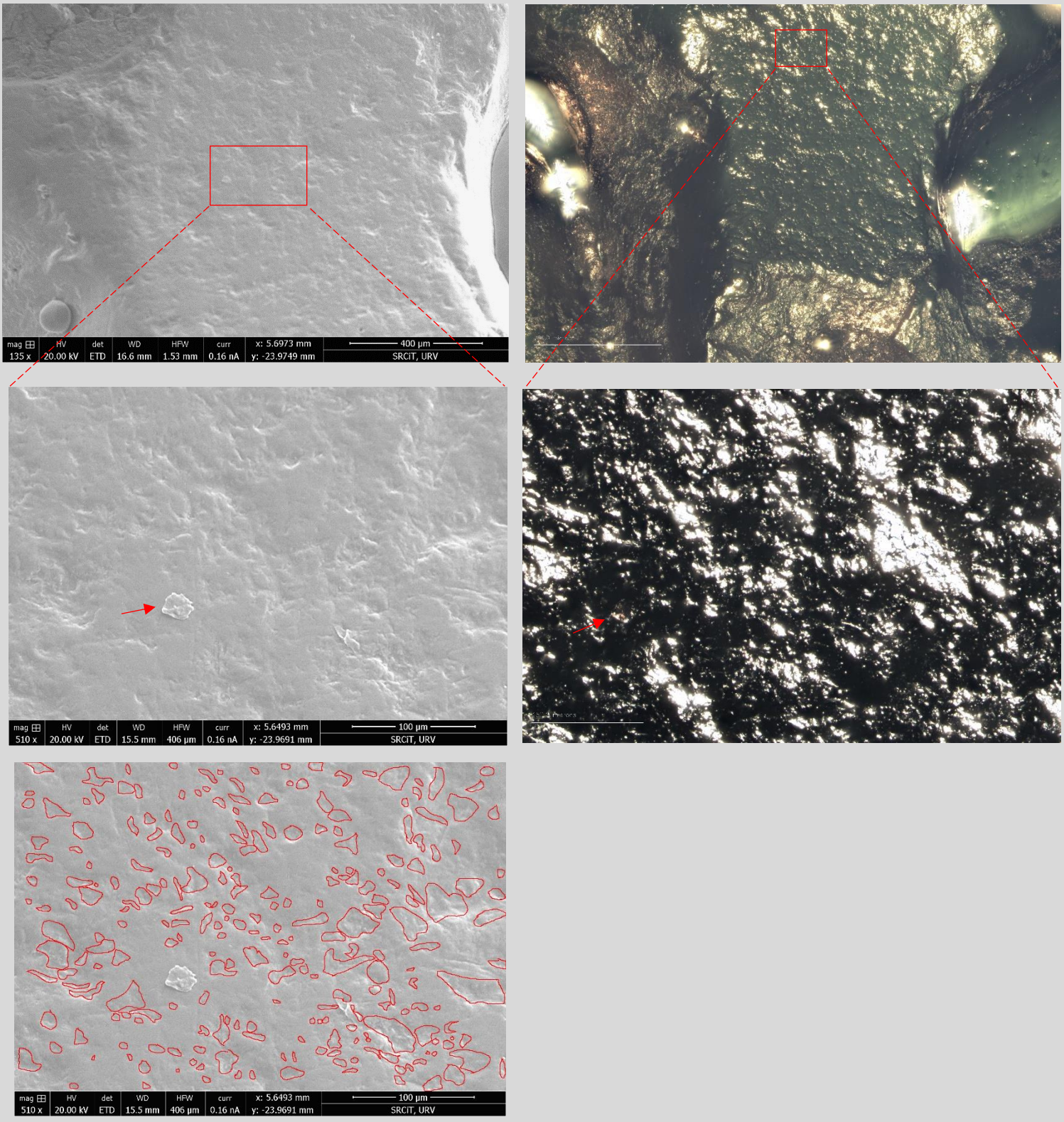

Dental microwear comparison between two different microscopes following the methodology previously described (paragraph 4.3.3). Above left, ESEM capture image of facet 9 (x135). Above right, Zeiss captured images (x50). Middle left, ESEM capture image of facet 9 (510x). Middle right, Zeiss captured image of Facet 9 (200x). Red arrows indicate the same particle used as landmark. Below right, ESEM image (x510) processed using imageJ software, no data can be obtained from the Zeiss image.; ESEM quantitative data are showed in table 5.9

Confocal Microscope: The current study also included the use of Confocal microscope to compare some of the previously analyzed surfaces. Unfortunately, the application of this equipment did not yield any results as the images of the dental areas appeared completely disfigured with a "dirty" effect covering the microwear traces. for this reason, the samples were further cleaned from possible particle residues with an acetone-based solution. Unfortunately, this process did not solve the problem. As can be seen from the image (Fig. 5.27), the dental surface appears to have a kind of “micro-peeling” effect that does not allow a proper observation of the tooth features. No data were obtained from the Confocal microscope for this analysis.

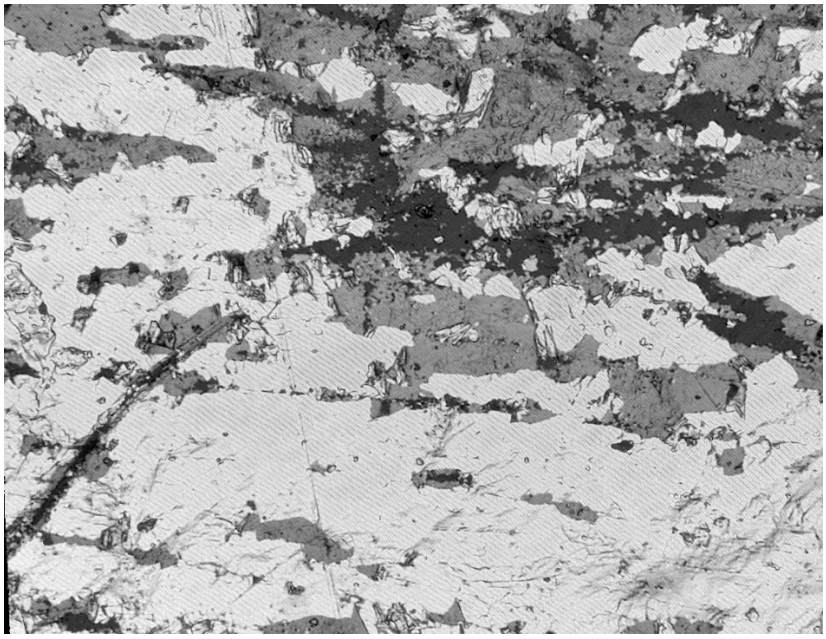

Figure 5.27 Confocal capture image of the cast specimen *n.* CC22_13/5_F9_134 (molar) – Buccal surface, middle area at 100x magnification. It is possible to observe a blurred and disfigured surface that doesn’t allow to record any kind of dental microfeature for the current comparative analysis. Photo taken by M. Mattera and Marina Lozano using a Confocal Microscope - Sensofar® S Neox 3D optical profilometer located in the Lithic laboratory of IPHES (Tarragona, Spain) (June 2023).

5.4 *Statistical analyses*

This last section of the chapter will discuss the statistical analyses performed for the current microwear study.

5.4.1 Statistical analysis of the comparative methodology: On the previous 6 analyzed dental surfaces (related to 1°-6° graphic tables), only those teeth' areas that showed dental striations and that were recorded (using the three microscopes) at the same magnification level (according to the methodologies explained in paragraph 4.3.3), were statistically processed. Therefore, the occlusal surface of dental specimen n. CC21_13/7_G8_433 (molar) was formally excluded because did not yield any striation pattern, while the labial surface of specimen n. CC20_13/7_G7_238 (canine*)* was discarded because the magnification used for this surface (140x – ESEM and Hirox) was different from all the others (100x - ESEM and Hirox, 50x – Zeiss). The remaining 5 surfaces were used for the quantification of microwear and the comparison of the performance of each microscope. Specifically, two pairs of tables were developed: one pair is related to the total number of striations recorded with each microscope (Table 5.10), while the second pair of tables is related to the mean of the total striation's length recorded with the same equipment (Table 5.11). The division in pairs will allow to observe the main difference observed between the ESEM - Hirox and between ESEM - Zeiss. Five main variables were analyzed and compared: total number of striations (NT), number of vertical striations (NV), number of horizontal striations (NH); number of mesio-occlusal to distocervical striations (NMD), number of disto-occlusal to mesiocervical striations (NDM). The differences between microscopes were evaluated by calculating the error (difference between the value recorded with OMs and SEM) related to a percentage of average increase (what percentage of the mean value of a variable on the SEM does the average error represent). The small sample size (n = 5) requires the use of non-parametric tests (U Mann-Whitney) for the inter-microscope results comparison of all variables, the obtained results that were underlined (light orange color) in the tables are considered as statistically significant. Each variable is related to a Boxplot that graphically expose the obtained comparative results (Graphs 5.1 and 5.2). It is important to mention that some numerical errors in the mean sums (regarding few microns of difference) are due to the fact that some outliers were removed. Is interesting to notice that, comparing the number of counted striations, the ESEM recorded a greater number of them when compared to the Hirox (excluding NMD variable), but a lower number of them when compared to Zeiss (excluding NH variable). The differences calculated, using U Mann-Whitney test, show a statistically significance value related to NT and NH variables between ESEM and Hirox, the same happens for the NV variable between ESEM and Zeiss (Tables 5.10). On the other hand, comparing the total length mean of the counted striations, all the OMs values show positive increase when compared to ESEM but only NMD variable yielded a statistical significance value (Tables 5.11).

Variables comparison ESEM-Hirox (Number of striations)

Variable	Counted striations ESEM	Counted striations Hirox	Striations error ESEM/Hirox	Percentage of increase ESEM-Hirox	Test U Mann Whitney: z-value	Test U Mann Whitney: p
NT	495	458	38	-7,47%	2,0465	0,040708
NDM	154	98	56	-36,36%	4,8637	1,1519E-06
NMD	84	138	54	+39,13%	4,8856	1,0312E-06
NH	94	64	30	-31,91%	3,4825	0,00004967
NV	163	158	5	-3,07%	0,47456	0,6351

Variables comparison ESEM-Zeiss (Number of striations)

Variable	Counted striations ESEM	Counted striations Zeiss	Striations error ESEM/Zeiss	Percentage of increase ESEM/Zeiss	Test U Mann Whitney: z value	Test U Mann Whitney: p
NT	495	597	102	+16,92%	4,8208	1,4299E-06
NDM	154	158	4	+2,53%	0,38599	0,6995
NMD	84	144	60	+41,67%	5,1861	2,1478E-07
NH	95	83	12	-12,63%	1,334	0,18222
NV	163	212	49	+23,11%	3,8374	0,00012434

Tables 5.10 Above, Table showing the difference of counted striations between ESEM and Hirox. Below, Table showing the difference of counted striations between ESEM and Zeiss. Underlined results display values of statistical significance. Graphical representations of these tables are showed in Graphs 5.1

Variables comparison ESEM-Hirox (Total Length Mean)

Variable	Total length mean ESEM	Total length mean Hirox	Length mean difference ESEM/Hirox	Percentage of increase ESEM/Hirox	Test U Mann Whitney: z-value	Test U Mann Whitney: p
NT	230,204 µm	313,228 µm	83,024 µm	+26,52%	6,928	4,2671E-12
NDM	210,727 µm	330,544 µm	119,817 µm	+36,36%	4,4653	7,9945E-06
NMD	206,808 µm	267,455 µm	60,647 µm	+22,85%	2,7325	0,0062855
NH	267,901 µm	319,900 µm	51,999 µm	+16,30%	1,4235	0,15458
NV	245,590	325,261	79,671 µm	+24,62%	4,1652	3,1109E-05

Variables comparison ESEM-Zeiss (Total Length Mean)

Variable	Total length mean ESEM	Total length mean Zeiss	Length mean difference ESEM/Zeiss	Percentage of increase ESEM/Zeiss	Test U Mann Whitney: z value	Test U Mann Whitney: p
TN	230,204 µm	265,351 µm	35,147 µm	+13,21%	1,0532	0,29226
NDM	210,727 µm	230,537 µm	19,81 µm	+8,70%	0,17478	0,86125
NMD	206,808 µm	232,441 µm	25,633 µm	+11,21%	0,73495	0,46237
NH	267,901 µm	328,279 µm	60,378 µm	+18,60%	1,649	0,099139
NV	245,590 µm	258,155 µm	12,565 µm	+5,04%	0,036518	0,97087

Tables 5.11 Above, Table showing the difference related to the total length mean between ESEM and Hirox. Below, Table showing the difference related to the total length mean between ESEM and Zeiss. Underlined results display values of statistical significance. Graphical representations of these tables are showed in Graphs 5.2

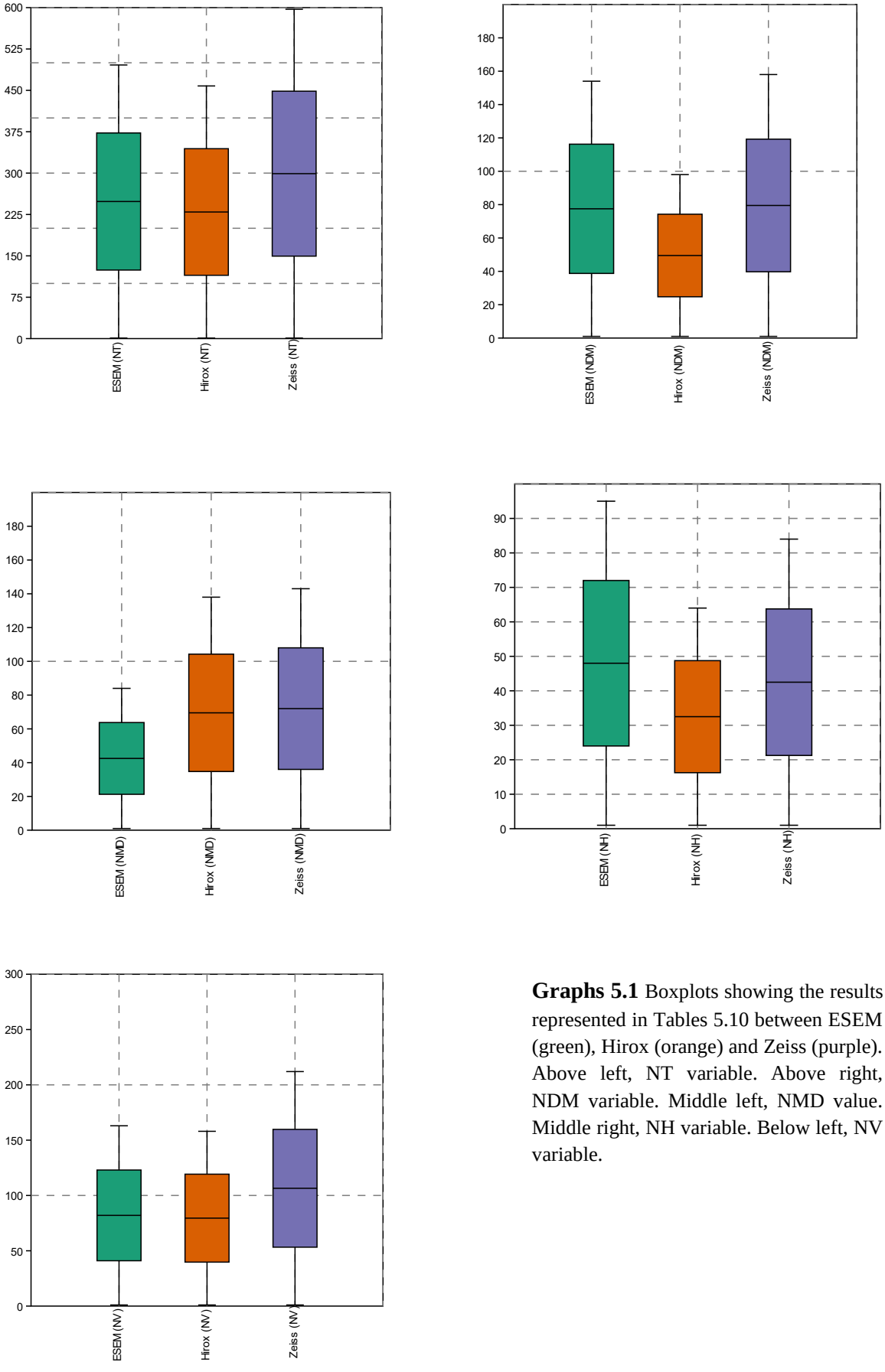

Graphs 5.1 Boxplots showing the results represented in Tables 5.10 between ESEM (green), Hirox (orange) and Zeiss (purple). Above left, NT variable. Above right, NDM variable. Middle left, NMD value. Middle right, NH variable. Below left, NV variable.

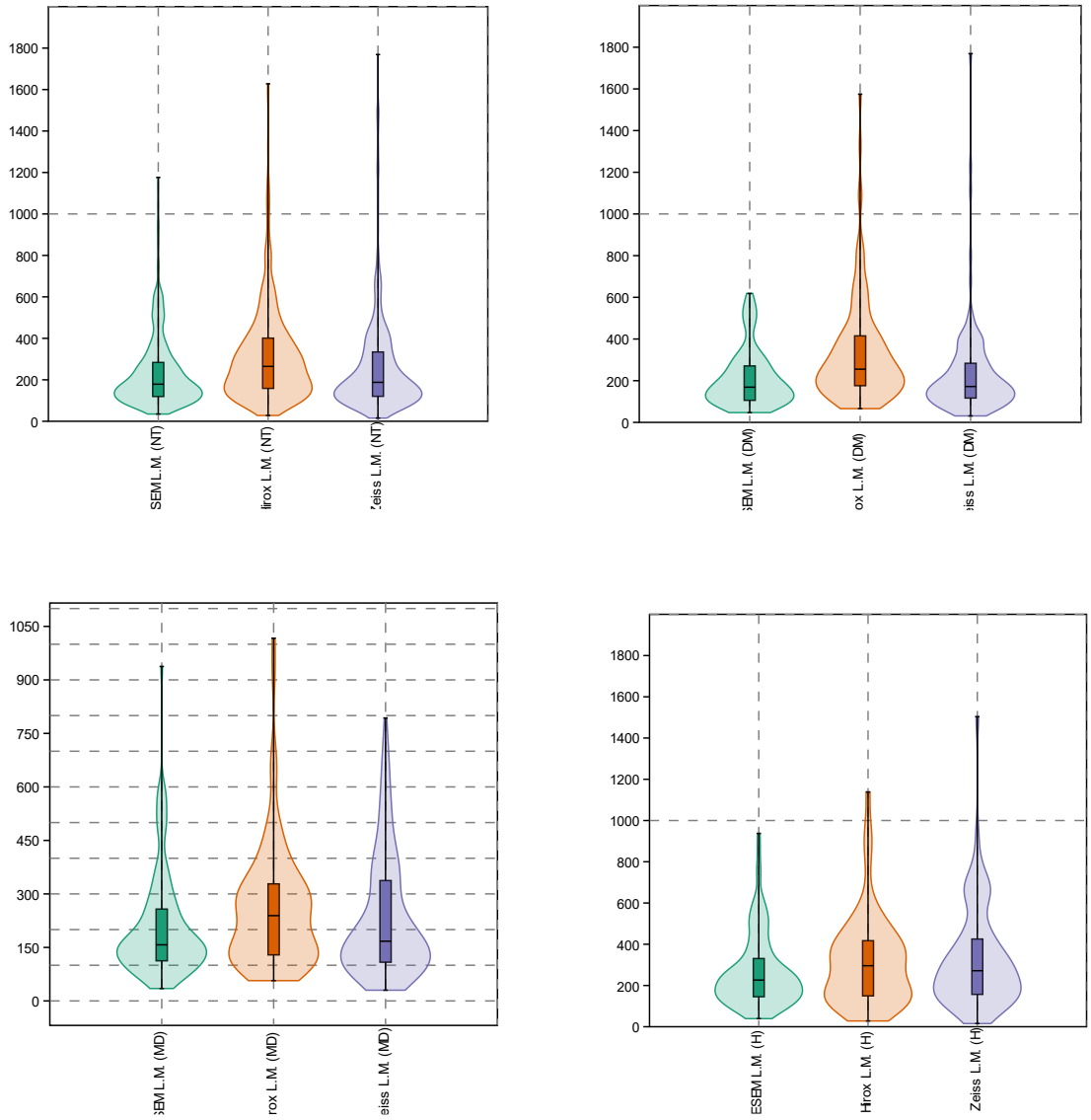

Graphs 5.2 Boxplots-Violin graphs showing the results represented in Tables 5.11 between ESEM (green), Hirox (orange) and Zeiss (purple). Above left, NT variable. Above right, NDM variable. Middle left, NMD value. Middle right, NH variable. Below left, NV variable.

5.4.2 Statistical analysis of the preliminary paleodietary reconstruction: As already mentioned in the methodological section (Paragraph 4.4.2), statistical analyses for a preliminary paleodiet reconstruction were performed on previously obtained quantitative data (only on molar buccal surfaces) following a standardized methodology derived by other similar microwear studies (e.g. Galbany et al., 2005; Pérez-Pérez et al., 1994; Pérez-Pérez et al., 1999, 2003). The only two preserved molar's buccal surfaces that yield a useful dietary-related microwear pattern are: the dental specimens *n.* CC20_13/4_F8_52 and *n.* CC22_13/5_F9_134, the obtained data are summarized in the following table (Table 5.12). The microwear pattern of each analyzed surface was characterized by 15 summary variables for the number, average length, and standard deviation of the length of the observed striations by groups of orientation: NT, total number of striations; NV, number of vertical striations; NH, number of horizontal striations; NMD, number of mesio-occlusal to distocervical striations; NDM, number of disto-occlusal to mesiocervical striations; NT, total number of striations; XV, average length of the vertical striations; XH, average length of the horizontal striations; XMD, average length of the mesio-occlusal to distocervical striations; XDM, average length of the disto-occlusal to mesiocervical striations; XT, average length of all striations; STDV, standard deviation of the length of the vertical striations; STDH, standard deviation of the length of the horizontal striations; STDMD, standard deviation of length of the mesio-occlusal to distocervical striations; STDDM, standard deviation of length of the disto-occlusal to mesiocervical striations; and STDT, standard deviation of the length of all the striations. These 15 quantitative variables constitute the buccal microwear pattern for the analyzed sample. Moreover, to compare the obtained results with other buccal microwear data, indexes of relative frequently of striations by orientation were calculated by dividing the number of horizontal and vertical striations by the total number of observed striations (NH/NT, NV/NT). An index of the number of horizontal to vertical striations (NH/NV) was also calculated. Data interpretation and comparisons with other published buccal microwear Neanderthals samples, will be discussed in the next chapter (Discussion).

Variable	Tooth *n.* CC20_13/4_F8_52	Tooth *n.* CC22_13/5_F9_134
NTN	166	140
NDM	27	3
NMD	40	78
NH	43	16
NV	56	43
XT	200.027 µm	200.885 µm
XDM	211.344 µm	223.038 µm
XMD	224,236 µm	194,168 µm
XH	215.150 µm	269.964 µm
XV	264.33 µm	185.819 µm
STDT	156.305 µm	128.309 µm
STDDM	160,064 µm	134,361 µm
STDMD	135,903 µm	125,132 µm
STDH	207.233 µm	169.9433 µm
STDV	189.940 µm	111,513 µm
Indexes		
NH/NV	0,767	0,372
NV/NT	0,293	0,307
NH/NT	0,331	0,114

Table 5.12 Table showing the quantitative data and calculated indexes obtained from the two molars buccal surface of the Ciota Ciara sample following the methodology developed by Pérez-Pérez et al. (1999)

CHAPTER 6: Discussion

This Chapter will discuss the interpretative reliability of the previous results by comparing them with the current scientific bibliography related to dental microwear analysis. Specifically, other published studies conducted on several Neanderthal's (and other hominins) dental fossils will be examined in order to compare them with the features previously observed and recorded on the Ciota Ciara's teeth. A section will be devoted to the interpretation of post-mortem and ante-mortem/para-masticatory activities (Paragraph 6.1), a second paragraph will explain the validity of the methodological comparison between different microscopes (Paragraph 6.2), and, finally, an interpretation of the preliminary paleodietary reconstruction will be presented (Paragraph 6.3)

6.1 Interpretation of Post-mortem and Ante-mortem/Para-masticatory Traces

One of the purposes of this work was to identify ante-mortem traces on teeth to detect the actual presence of possible para-masticatory indicators. Obviously, for this reason, it was necessary to methodologically recognize and separate ante-mortem from post-mortem features in order to not fall into interpretive errors. Moreover, as seen in section 5.1, the identification of methodological mistakes (made during the stages of the dental microwear protocol) was crucial to not confuse possible moulding/casts processing aberrations from the effective dental traces found on the original Neanderthal's teeth. It is important to remember that the meticulous analysis of errors made during the microwear process is a key step for the correct interpretation of dental micro-features.

1) Post-mortem alterations: Currently, there are no specific studies that have dealt with post-depositional alterations uniquely and exclusively focused on Neanderthal dental specimens. On the other hand, there are several comparative and experimental works that have addressed this issue on both human dental specimens in general (e.g Fox & Pérez-Pérez, 1994; King et al., 1999; Martìnez & Pèrez-Pèrez 2004) and other animal fossil taxa (e.g. Micó et al., 2023; Uzunidis et al., 2021), in fact specific post-depositional processes have been shown to cause recognizable post-mortem traces in some experimental studies (i.e. King et al., 1999), moreover Teaford (1988) demonstrated that the post-mortem effects of taphonomic agents could be distinguished clearly from ante-mortem dental microwear and, above all, from food-related features (scratches and pits) (Teaford, 1988). Actually, no association between the type of erosive agent (dust, ash, sand or phytoliths) and the microwear pattern has been recorded, neither for the width of striations or their orientations (Martìnez & Pèrez-Pèrez, 2004). Erosive effects, both physical (mainly abrasive particles) and chemical (mainly acids), tend to erase and distort the food-related traces that formed during lifetime, rather than to produce new formations or secondary alterations (King et al., 1999). Since the current work is a dental microwear analysis, the previous evaluation of post-depositional processes was focused particularly on the surfaces of dental enamel; in fact, enamel, due to its bio-structural composition, reacts differently to mechanical and chemical stresses than other dental structures (dentin, cementum). Therefore, is important to remember that the scientific literature on post-depositional effects on different tooth structures is extremely abundant. As already seen in the previous chapter, the most common and detectable post-mortem features observed on the Ciota Ciara's enamel surfaces were: enamel removal as chipping, enamel cracks, non-dietary related physical abrasion on the enamel surfaces, post-mortem pitting as erosive effect; but no enamel prism exposure was recorded. The agents responsible for these events can be of different origins (as trampling, weathering, transport, precipitation of chemical compounds, different fossilization processes, etc.); in fact, all chemical and

mechanical alterations are inextricably associated to the sediment 'characteristics where the fossils lay. Usually, well-preserved surfaces had a clear striation pattern with scratches running in different orientations and lengths; for that reason, when other dental alterations are observed during a microwear protocol, it is necessary to identify the cause in order to not fall into interpretative errors.

Post-mortem enamel chipping: On the previous results, a clear post-mortem enamel chipping was identified only on the right part of the incisal third labial area of specimen *n*. CC21_13/8_H7_36 (Incisor) (Fig. 5.9-5.10). Post-depositional processes can easily cause enamel splintering or chipping. In fact, post-mortem chipping is generally characterized by exposed enamel that is whiter than adjacent surfaces. As enamel is brittle but dentine is not, the enamel frequently fractures at the level of the dentine, which is generally dull yellow in color. As for appearance, post-mortem chipping results in exposed enamel with sharp and well-defined edges (G. R. Scott & Winn, 2011). The study of the dental chipping gets complicated because the blows that produce enamel flakes can have an ante-mortem or post-mortem origin which can be recognized based on specific characteristics. Since a tooth chipped ante-mortem remains in functional occlusion for the life of the individual, the edges become smoothed or blunted (Scott & Winn, 2011). On the contrary, after death, the enamel matrix slowly dehydrates, this event decreases the strength of the crystalline structure to the point where the enamel chips or flakes easily. In fact, well-defined enamel removals with sharp edges (and not reshaped contours) are more likely caused by post-depositional events (Scott & Winn, 2011). Based on literature information compared with the description given in the previous section (paragraph 5.2), it is possible to confidently interpret this feature found on CC21_13/8_H7_36 (Incisor) as a clear example of post-depositional chipping.

Post-mortem dental fractures and cracks: Dental fractures or cracks are a quite common event that can be produced during life or by a post-mortem alteration Several Ciota Ciara's dental surfaces yielded examples of multiple fractures (paragraph 5.2), as specimens *n.* CC20_13/4_F8_52 (molar) (Fig. 5.11-5.12) and CC21_13/7_G8_433 (molar) (Fig. 5.13). Crack patterns are considered as a great source of information about the nature of the stresses to which teeth and dental structures have been subjected. Unlike bone, enamel preserves cracks as long as the hydroxyapatite structure itself survives, so the cracks are a complete record of the stresses that have exceeded the strength of the material, including post-mortem stresses (Rensberger, 1987). The scientific research on microcrack formation and propagation in human teeth is abundant both *in vivo* and on fossil samples, covering topics such as the fracture properties of different tooth tissues, thermal stress and fatigue of enamel and dentin, fracture behavior at the microstructure level, and dentin-enamel junction mechanical properties (Hughes & White, 2009: 263). Studies that are related to postmortem taphonomic alterations (e.g. Kruzic et al., 2003; Rasmussen et al., 1976), examine the biomechanical strength of hydrated (peri- and antemortem) versus dehydrated (postmortem) enamel/dentin that can produce various types of post-depositional fractures located in different position of the dental specimens. It has been demonstrated that fresh cracks in fossil enamel show very sharp edges and may suggest a diagenetic cause. While rounded edges are evidence of a reshape action, therefore these cracks may have been acquired during the lifetime (Rensberger, 1987). Another important difference is that post-mortem cracks usually appear wider and longer compared to ante-mortem ones. Considering the fracture features observed on the sample, Ciota Ciara's dental remains were probably affected by several post-mortem stresses. Specifically, fractures and cracks of different intensity were observed in this study, especially on molars where these features appear very deep. It can be seen that the recorded jagged edges of the cracks are compatible with a post-depositional stress, probably due to a compression on the occlusal or lateral area of the teeth.

Alteration effects by physical abrasion: In the results chapter, a large set of long scratches (with a particular morphology) where detected on the right labial side of specimen *n*. CC19_13/3_E8_74 (5.14 – 5.16). It is important to underline that these features were already clearly visible to the naked eye just by looking at the dental surface of the cast, this had initially led to the assumption that they might potentially be marks left by para-masticatory activities. Because of this particular curved morphology related to an anomalous width, it was initially hypothesized that these scratches might be impact blows that occurred ante-mortem, but subsequent observations have refused this first assumption. Very few experimental protocols have tested the effects of mechanical erosions on tooth enamel. Those experiments were designed to mimic the action of sediment abrasion. Specifically, Gordon (1984) tumbled several human dental specimens in four different types of soil, showing that that tumbling process only seems to erase food-related features (scratches and pits) rather than adding new ones (Gordon, 1984). Moreover, King et al. (1999) carried out a similar experiment, always with human teeth, using three types of materials: quartz pebbles, particles size: 2000–11,000 μm; coarse sand, particles size: 500–1,000 μm; medium sand, particles size: 250 and 500 μm This protocol yielded very close results to that of Gordon (1984). The article of King et al. (1999) is considered as a fundamental work for the analysis of post-mortem processes applied to dental microwear studies. But also very illustrative are the descriptions made by Martínez & Pérez- Pérez (2004), the paper shows several taphonomical processes that altered a hominin's dental surfaces sample from the Olduvai gorge site (Tanzania, Africa). Specifically, well-preserved hominin teeth can exhibit patches of slightly damaged enamel, or very clear enamel cracks that tended to erase the normal striation pattern. The combination of well-preserved and altered surfaces in the same dental specimens seems to be indicative of a moderate erosion that does not affect the whole tooth (Martínez & Pérez- Pérez 2004). In some other cases, under worse conditions, enamel eroded surfaces can show a high density of parallel scrapes, sometimes combined with enamel prisms exposure and pitting. These teeth probably rolled along the sediment in a post-mortem transport resulting in an intense pattern of parallel scrapes caused by the soil composition' hardness (Martínez & Pérez- Pérez 2004). The three larger scratches, found on specimen *n*. CC19_13/3_E8_74, show a curved orientation and a very large width that is incompatible with the standard identification of para-masticatory signs on the labial surfaces of anterior dentition (i.e. Lalueza-Fox & Pérez-Pérez, 1994; Lozano et al., 2008). Moreover, the internal structure of these features reveals morphological traits that would appear to be caused by a scraping action from mineral movements more than ante-mortem cut-marks; finally, additional scratches with a chaotic pattern are superimposed on them (Fig. 5.14, below), leading to the conclusion that abrasions seen on this labial area of the specimen may have been the result of a post-mortem alteration (most probably a physical abrasion by sediment). The differences in abrasion dimensions could be related to differences in the mineral composition or size of the particles. In addition, it was also possible to measure the degree of depth of these post-depositional features using a surface measuring instrument (with Hirox microscope), in fact, as can be seen from the graph (Fig. 5.16 above), the scratches are really very shallow and this reinforces the supposed mineral friction action' hypothesis.

Alteration effects by chemical agents: On the previous results section, a pitted abrasion pattern was recorded during the analysis of the facet 9 (occlusal area) on the specimen *n*. CC21_13/7_G8_433 (Fig. 5.17 and Graphic table n 6°). This pitting pattern was initially interpreted as related to chewing actions, which on the occlusal surface are quite common when is related to the consumption of hard food and abrasive diets in general. For this reason, this surface was analyzed in the protocol of the diet-related features (paragraph 5.4, Graphic table 6°). In a second stage of the analysis, because of certain characteristics that were recognized, this area was subsequently interpreted as being exposed to a post-depositional acidic or mechanical action more than a hard foodstuff consumption. Actually, the effect of chemical erosion of enamel was investigated by many researchers (e.g King et al., 1999;

Puech et al., 1985; Teaford, 1994; Weber et al., 2022). Dental specimens with enamel erosive features, due to chemical attacks, are easy to identify; but, as argued by King et al. (1999), it is necessary to understand whether the apparent acid etching had occurred during the individual's life as a result of an ante-mortem event (i.e., through the ingestion of acidic fruits) or as a result of post-mortem exposure to an acidic condition of the sediment (King et al., 1999). Experimental protocols conducted by these authors demonstrate that acids do affect enamel and dental microwear by removal, in varying degrees, of the features and exposure of enamel prisms composition. Specifically, hydrochloric acid caused heavy erosion of the microwear features and the enamel prisms network is frequently exposed, while citric acid produces a lighter erosion of the dental surfaces (King et al., 1999). When the chemical erosion is intense, it is usual to observe a generalized exposition of growth lines or perikymata or other superficial dissolution, attributable to some type of chemical alteration due to the uniformity and large extension of the affected area (Martínez & Pérez- Pérez 2004: 40). It is also important to notice that, when prisms exposition is due to physical abrasion, the prisms are mainly observed only in reduced and prominent areas (Martínez & Pérez- Pérez 2004). When the chemical dissolution is slight, it can be result in a uniform pitted surface with no prism exposure. In fact, considering the abnormal morphology of pits and the total absence of striations, it is much more probable that facet 9 of this tooth suffered damage caused by this type of post-depositional effects.

Almost all the data, about the mechanisms and consequences of post-mortem effects on dental microwear features, has been replicated and compared through experiments (previously described). But it is unknown how well natural alteration processes can be experimentally simulated, in fact artificial post-mortem alteration can hardly recreate processes that act on geological timescales. Thus, some authors (i.e. Weber et al., 2022) tested how comparable simplified experimentally induced post-mortem wear alteration is to naturally induced alteration.

2) Ante-mortem alterations and Para-masticatory activities: A theoretical reference has already been made for ante-mortem dental alterations (paragraph 2.2.2), in fact dentition were also used as a tool for the manipulation of non-diet related materials. These activities produce some features on dental enamel and dentine known as cultural or non-alimentary dental wear. Tooth features associated with cultural activities are mostly described as: vestibular striations, vestibular-lingual striations, dental chipping (or enamel flakes), and polished enamel (Lozano et al., 2008). Recognizing this type of traces required an optimal dental enamel preservation condition, since (exactly as for the dietary-related traces) the ante-mortem microwear features may be easily eroded by subsequent post-depositional processes. The scientific literature is quite rich in examples of para-masticatory activities recognized and linked to Neanderthals. Below it will be possible to see if the Ciota Ciara samples also yielded these types of dental traces.

Ante-mortem dental chipping: In the results section, two Ciota Ciara's incisors yielded traces of possible ante-mortem dental chipping: on the incisal third lingual area of specimen *n*. CC21_13/8_H7_36 (Fig. 5.18-5.20) and on the occlusal surface of specimen *n*. CC19_13/3_E8_74 (Fig 5.21-5.23). Very few studies had specifically dealt with ante-mortem chipping of *Homo neanderthalensis* species, a comprehensive and methodologically detailed study was published by Belcastro et al. (2018) on the Neanderthal dental specimens from Krapina (Croatia). Other studies, more focused on the description of other dental characteristics (e.g. morphology, pathology etc.), have mentioned the presence of chipping (Bailey & Hublin, 2006; Estalrrich & Rosas, 2015; Lalueza-Fox & Frayer, 1997; Lozano et al., 2013; Lumley-Woodyear, 1973), but there have been few systematic investigations related to Neanderthals' ante-mortem dental chipping. Other studies report on tooth ante-mortem enamel removals in modern humans (e.g. Belcastro et al., 2007; Bonfiglioli et al., 2004; Scott & Winn, 2011) or on other Pleistocene hominins such as, *Homo naledi* (Towle et al., 2017),

and genus Paranthropus & Australopithecus (Constantino & Konow, 2021; Towle et al., 2021). Ante-mortem dental chipping occurs when a tooth contacts a hard object with enough force to fracture the enamel (in other words: when the strength of enamel is surpassed by bite force pressure) (Constantino et al., 2010). It is defined as an "Ante-mortem irregular crack, involving enamel or enamel and dentine, situated on the buccal, lingual or interproximal edge or crest of the tooth" (Bonfiglioli et al., 2004: 449). Different dietary items can cause enamel splintering (in the lifetime) at different rates and sizes, from soft fruits that rarely cause chipping to hard seeds and nuts that may lead to large chips. However, the propensity of some foods for dental chipping is more difficult to discern (Towle et al., 2017). Environmental contaminants may also be important, such as grit incorporated into the diet (Belcastro et al., 2007). However, even non-masticatory behaviors were also found to be a potentially cause of ante-mortem chipping, with different activities leading to a variety of patterns. The size and shape that an object must be to cause ante-mortem chipping are still subjects of debate between scholars. Ante-mortem chipping can be easily separate from post-mortem chipping (previously described) by looking at some peculiar characteristics; in fact, Lozano et al. (2008) argue that: "Enamel ante-mortem microfractures can be recognized due to a smoothed contour of the break made by the active action of saliva, tongue movements, and functional use of teeth during the individual's life. Moreover, this type of chipping is often located on the incisal part of the labial surface in the contact zone between the labial and the occlusal surfaces" (Lozano et al., 2008: 720). All the traits related to CC21_13/8_H7_36's feature (described in paragraph 5.3), support the hypothesis that it may be an ante-mortem dental chipping whose causes cannot be easily understood. Since this is a lower (first or second) incisor, it is possible that the cause of chipping may have been due to either hard food processing or extra-masticatory activities. The partial resorption and the fact that the Zeiss image shows a more pronounced difference in composition (Fig 5.23) can indicate that the tooth chipping may have occurred shortly before the individual's death. Or the other hypothesis is related to a post-mortem event, therefore is important to remember that the occlusal surface of this specimen is very eroded and, even in its labial side, a chipping of clear post-depositional origin was shown (Fig. 5.9-5.10).

The second detected ante-mortem chipping was identified on the left occlusal surface side of the specimen *n*. CC19_13/3_E8_74. From the ESEM images taken at 100x magnification, it was noticed that this dental chipping was smaller in size when compared to the previous one; moreover, it is possible to observe that the occlusal surface of the incisor is worn, thus the difference of mineral composition between the enamel (external) and the dentine (internal) is clearly shown in the microscope images (Fig. 5.21). Typically, this type of dental micro-chipping in the occlusal areas of the anterior teeth are usually described as ante-mortem features that have been systematically used, by several authors, as a proof of hard food consumption (Constantino & Konow, 2021). In fact, in dental anthropology field, is well know that the incisors are typically the first teeth to contact foods during feeding, specifically the anterior teeth are used to ingest portions of different food which are then masticated by the post-canine dentition (Calhoun et al., 2022). For this reason, the accurate analysis of anterior teeth' features may yield fundamental clues on human feeding behaviors. Ante-mortem fractures to access hard foods were already documented in other works on Neanderthals teeth (i.e. Belcastro et al., 2018), then is possible to support that forceful bites of their anterior dentition to process this food can reflect significantly greater incisor wear and dental ante-mortem micro-chipping like this one documented on the occlusal surface of Ciota Ciara's tooth *n.* CC19_13/3_E8_74.

Possible para-masticatory labial striations: As already mentioned in the previous section (paragraph 2.4.2), the presence of long scratches on the labial surface of anterior teeth (obliquely oriented and visible to the naked eye) has been reported in various Neanderthal and Pre-Neanderthal hominins from different European and Near-east sites (e.g. Estalrrich & Rosas, 2015; Lalueza-Fox & Frayer, 1997; Frayer et al., 2010; Lozano et al., 2004, 2008, 2017; Lumley-Woodyear, 1973; Trinkaus, 1983). Previous analysis tested the similarity between the traces found on fossils and the labial scratches experimentally made on modern human samples (Lozano et al., 2004). Moreover, ethnographic evidence indicate that Eskimos and Australian aborigines use their anterior dentition for several tasks, leading to a result very similar to that observed on fossil's teeth (Lozano et al., 2004). These comparisons allowed the researchers to hypothesize a para-masticatory/cultural origin of the scratches found on the hominin's anterior dentition. These features show a specific morphology that clearly differentiates them from the standard dietary striations. Some similar scratches were also observed on the middle third left side of the Ciota Ciara's specimen *n*. CC19_13/3_E8_74 (incisor) (Fig 5.24-5.26). The ESEM images (previously analyzed) displayed a set of three long scratches that are: well-defined, parallel to each other along most of their length, and with a right oblique orientation (Fig 5.24). Considering these characteristics and their position on the incisor, they were found to be excellent candidates to be considered as traces of cultural/para-masticatory origin. In fact, based on the definition of Lozano et al. (2008), the edges of these labial striations are linear, well-defined, and parallel to each other along most of their length. The lower part of the striations usually displays a ''V''-shaped transverse section and is ploughed by several parallel microscratches (Lozano et al., 2008: 718). Triangular liftings, or fractures in the borders of the striations called Hertzian cones, have sometimes been documented. These cones are the result of the interaction between the pressure exerted by the action of cutting and the resistance offered by the surface to be cut (Lozano et al., 2008: 718). The morphological traits of labial striations are exactly the same as those displayed by cutmarks on bone, that is linear and parallel borders, the presence of Hertzian cones, grooves with a ''V''-shaped section, and microscratches on the bottom of the striation. The orientation of striations is an important diagnostic characteristic because right oblique (RO) and vertical (V) orientations are the most common (Lozano et al., 2008: 718). Actually, the measured Mean of both length and width (Table 5.2) of the previous three scratches found on the specimen *n*. CC19_13/3_E8_74 (incisor), falls within the standard variability related to para-masticatory traces on labial teeth measured for Australian aborigine and Sima de los Huesos specimens (see Lozano et al., 2008: 718). Moreover, analyzing the orientation of the previous labial striations (see table 5.2 for the angle measurements), it has been verified from experimental studies (i.e. Lozano et al., 2017)that these oblique marks are typically produced by a right-handed action. This information is interesting since Lozano et al., (2017), analyzing several Neanderthals labial surfaces (NMI = 36) from different European sites, detected a frequency of 88.9% right-handed individuals; and, by adding the pre-Neandertal data from Sierra de Atapuerca, the frequency of right-handed Pleistocene Europeans rises to 92.2% (Lozano et al., 2017). Thus, the Ciota Ciara individual (of incisor *n*. CC19_13/3_E8_74) could be included in the variability of European Neanderthals related to a right-handed specialization. Despite all these evidence in favor of an extra-masticatory hypothesis, the state of the enamel on the labial surface of this tooth is extremely compromised. in fact, other post-depositional scratches had been found on the right side of the specimen (as already seen before). To further test the hypothesis of a no-alimentary and no-taphonomic origin of these traces, the lingual area of the tooth was also investigated. Unfortunately, as can be seen from the ESEM image, the lingual area had also been altered by post-depositional processes (Fig 6.1) that suggest refusing the previous para-masticatory hypothesis. However, in conclusion, these three striae have many features in favor of being ante-mortem features (cut marks), but it would be preferable to conduct more accurate analyses and comparisons, in the future, to validate this hypothesis with reliability.

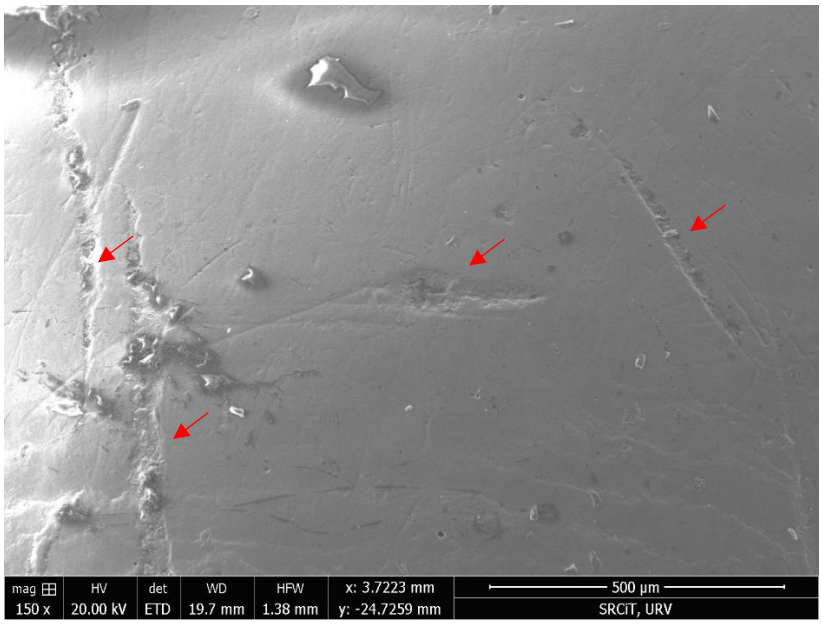

Figure 6.1 ESEM capture image of the cast specimen *n.* CC19_13/3_E8_74 (incisor) lingual surface at 150x magnification. It is possible to observe several large features of post-depositional origin (red arrows).

6.2 Validity of the Methodological Comparison between Different Microscopes

The main aim of the current work was to methodologically evaluate the applicability of optical microscopy (joined and compared to the standardized Scanning Electron Microscopy protocols) for buccal and occlusal dental microwear analysis. As already mentioned on the methodological section (paragraph 4.3.3), previous studies that replaced traditional SEM with OM equipment have run into a series of incongruences that included limited depth of field, problems with reflecting enamel surfaces, and resolution issues; these methodological limitations, mixed with the physiological curved surface of the teeth, made it very difficult to analyze the microwear features with optical microscopy since much of the field of view was out of focus on the 3D images. However, few recent publications encouraged the integration of the OM research application not only related to dental microwear studies (i.e. Calandra et al., 2019; Hernando et al., 2020), but even for the traceology field. The common objective of both approaches is the observation of wear traces, and several methodological crossovers also exists (Hernando et al., 2020). The focus of the previous analyses was basically evaluating the applicability of optical microscopy for dental microwear analysis, following the standardized traceology protocols that were established in parallel with recent developments in OM technology (against established SEM procedures); therefore, the problems that initially led to the replacement of OM for dental microwear studies are no longer the obstacle they once were. The intention of this thesis was to continue the explorative line of research developed by Hernando et al. (2020) to test the potential and limitations of their comparative approach in the current development of microwear analysis techniques.

Several differences implemented in the current work must be taken into consideration. In fact, the number of samples that it was possible to compare methodologically is far less (N=5) than in the original Hernando et al. (2020)' research (N=16). This is also related to the fact that other hominin teeth (such as *Homo neanderthalensis* in this case) are significantly rarer than recent anatomically modern humans; therefore, it was necessary to work with the available materials. However, given this constraint, it was decided to enlarge the number of optical microscopes to be used, not only the Zeiss (applied by Hernando et al. 2020) but also the Hirox equipment. The original project also included

the use of the Confocal microscope, but due to several inherent problems related to cast specimens and the limited worktime, this type of analysis was not possible to perform. Finally, the statistical analyses that were conducted on the comparisons between the different instrumentations are fewer in number and less elaborate than those carried out by Hernando et al. (2020) research, since the main objective was to give an overview of the results obtained.

Aside from that, the comparative analyses returned very interesting results that were partially different from the previous research. First, the higher mean total number of striations (TN) observed with the Zeiss (+16,92%) compared to ESEM, agrees with the previous research line. This event can be strictly related to the image characteristics of the OM, which has a better qualitative resolution and a three-dimensional appearance facilitated by improvements with the extended focus. Since the equivalence of the magnifications between microscopes is based on a previous calibration where the size of the field of view dimensions for each acquisition system is known, the field of view of both microscopes are equivalent. Therefore, the difference in striation count is not due to a difference in field of view between microscopes and reflects a real difference in the ability of a single user to detect more striations using Zeiss. On the contrary, the other OM equipment (Hirox microscope) recorded a slight negative value (-7,47%), for the same TN mean variable, when compared to ESEM. And it was demonstrated to be statistically significant between the two instrumentations. This event could be related to the variation of intensity in the illumination system, in fact it was noticed that by changing the direction (direct vs transverse) and intensity of light, often some dental micro-features tended to be less visible and even obliterated. Being able to adjust the illumination system, to not get reflection/darkness effects, is not always an easy task with this type of instrumentation. Sometimes, in fact, the images yielded by this microscope were slightly out of focus. However, this hypothesis needs to be furtherly tested by observing more dental samples. In a second step, by dividing each striation for its own orientation, it was noted that the most different mean was apparently related to a higher number of mesio-distal striations (NMD) recorded in both the OM microscopes when compared to ESEM: Hirox +39,13% and Zeiss +41,67%. But the statistical test did not yield a significant value for the MD variable. On the other hand, the number of horizontal striations counted with both OM microscopes was surprisingly low, while the Zeiss NV variable (vertical striations) is higher. Specifically, the recorded Hirox NH value (-31,91%) was more than doubled respect to Zeiss NH value (-12,63%) and it was considered statistically significant. This result was unexpected because it contrasts with what has been observed in the previous research by Hernando et al. (2020), in which the observed horizontal lines were statistically significant but for a positive increasing value (+17,65%). After all, it should be added that only the results recorded with the Hirox turn out to be very different for the NH variable, so the hypothesis is that the differences between the two optical microscopes also need to be tested because, apparently, they do not give similar results when compared to ESEM. This difference between the two OM microscopes can also be seen from the results displayed in the table related to the total length mean. In fact, all the optical microscope variables recorded positive increasing values compared to ESEM, but comparing the results between Zeiss and Hirox it was possible to observe a trend in which the values of the Hirox are almost duplicated compared to the Zeiss (excluding the total length value for the NH variable). Is also interesting notice that the only one significant value, from a statistical point of view, is related to the mesio-distal (NMD) striations total length (+22,85%) recorded with the Hirox that was also the only one positive recorded value, for this equipment, in the previous table (counted striations). Hernando et al. (2020)'s research compared only ESEM and Zeiss, so these new data between Zeiss and Hirox

should be furtherly investigated maybe by using a larger sample to reduce the errors. Regarding the striations' comparison between the two OM and ESEM equipment, the conclusions of the current analysis are in agreement with what has already been expressed by Hernando et al. (2020), in fact it is not possible to assume that the variables concerning absolute striation counts and total length mean, are equivalent between methods. This conclusion suggests that the use of data from SEM-based microwear analysis cannot be used as a comparative reference for the interpretation of the same variables collected with OM for dietary inferences except in a very general sense. However, regarding the comparison between different microscopes, the OM equipment applied to microwear analysis exhibit a variety of advantages when compared to the traditional SEM protocols: optical microscopes are faster in terms of sample preparation and image acquisition, time-consuming sample preparation processes are avoided, these instrumentations require much less physical space, are generally much lower in initial cost to purchase and maintenance. The current work did not analyze originals teeth, but is important to mention that they could be directly observed with OM without additional preparation or modification of equipment parameters. In conclusion, even if OM-based microwear analysis cannot totally replace the traditional ones, are still configured as a supportive and friendly comparative methodology.

6.3 Interpretation and Comparison of the Preliminary Paleodietary Reconstruction with other Published Works

Several buccal dental microwear studies have been involved in paleodietary reconstructions of fossil hominins both related to Pre-Neanderthal (e.g. Pérez-Pérez et al., 1999) and Neanderthal groups (e.g. Lalueza-Fox et al., 1996; Pérez-Pérez et al., 2003). Although, as was already mentioned in chapter two (paragraph 2.4), the most popular line of research at the moment, for paleo-diet reconstruction, is the analysis of occlusal surfaces by DMTA method using Toothfrax software. For the present study, this type of analysis was impossible to carry out because the Toothfrax software was not available; on the other hand, a preliminary paleodietary reconstruction analysis, based on the buccal variables analyzed in the previous section (paragraph 5.4), has been successfully performed. It is important to mention that the sample from the Ciota Ciara cave, for the current paleodietary reconstruction, is small (NMI= 1 or 2) and that inter-population comparisons between other Neanderthal and non-Neanderthal groups will be taken from other published studies. In fact, the purpose of this section is only to give an initial and general idea about the diet typology of Neanderthal individuals in this geo-chronological context, but it will be necessary to explore this topic with further and more accurate analyses in the future.

It has been demonstrated that the buccal microwear pattern seems to be conservative within individuals, independent of the analyzed tooth, and the interindividual variability seems to be significantly larger than the intraindividual variability. Moreover, the buccal microwear pattern needs a longer period of time to be fully attained, and therefore slight seasonal variations in dietary habits may not significantly affect it (Pérez-Pérez et al., 1994). These observations suggest that the study of the buccal striation pattern may be successfully applied to the study of the diet of past human populations (Pérez-Pérez et al., 1994). In general, previous studies underlined an existing tendency toward fewer striations in general and a higher proportion of vertical striations in the carnivorous groups than in the vegetarian ones. Specifically, the high frequency of vertical striations observed in the carnivorous groups may reflect the biomechanics of meat eaters, with predominantly vertical movements of the mandible; in contrast, the mastication of hard and fibrous materials, such as

vegetables, may need more horizontal movements. An important comparative study was conducted by Lalueza-Fox et al. (1996), the analyzed sample of this study includes specimens classified as archaic *H. sapiens* (Broken Hill, Banyoles, Montmaurin, La Chaise-Suard, La Chaise-Bourgeios et Delaunay), Neanderthal (La Quina V, Gibraltar 2, Tabun 1 and 2, Amud 1, Malarnaud, St. Cesaire, Marillac), and anatomically modern *H. sapiens* (Skhul 4, Qafzeh 9, Cro-Magnon 4, Abri-Pataud, Veyrier, La Madelaine, Rond-du-Barry) (Table 6.1). Basically, the obtained results indicate that some of the Neanderthal specimens have a microwear pattern close to that of the carnivorous extant populations (such as Inuit and Fueguians), suggesting that these groups follow a predominately hunter strategy. On the contrary, archaic *H. sapiens* and anatomically modern humans seem to have a more abrasive diet, probably more depending on vegetable intake, than the Neanderthals (Lalueza-Fox et al., 1996). In this case, the paleodietary reconstruction by comparison was mainly made by plotting in a graph the obtained NV/NT (Y axis) and NH/NT (X axis) indexes of each specimen to check in which dietary range they fall into (Graph 6.1). These values for the Ciota Ciara specimens are: 0,293 (NV/NT) and 0,331 (NH/NT) for molar *n.* CC20_13/4_F8_52, then 0,307 (NV/NT) and 0,114 (NH/NT) for molar *n.* CC22_13/5_F9_134. Lalueza-Fox et al. (1996) argued that, with respect to the NV/NT index, the carnivorous groups tend to have low values (Vancouver Islanders, 0.19; Inuit, 0.28; Fueguians, 0.33), due to the major presence of vertical scratches. The more vegetarian groups have higher values of this index (Tasmanians, 0.60; Australians, 0.64; Bushmen, 1.19; andamanese, 1.20; Veddahs, 1.31; Hindus, 2.60). The Neanderthal specimens have low NV/NT values (carnivorous like) ranging from 0.19 to 0.47, except for St. Cesaire (0.64) and Marillac (0.66), which have values similar to the mixed-diet hunter-gatherer samples Lalueza et al. (1996). Plotting the NV/NT values from the Ciota Ciara cave, it possible to observe that both falls into the range of the carnivorous diet-related groups due to a higher presence of vertical striations (N=56 for CC20_13/4_F8_52 and N=43 for CC22_13/5_F9_134) than horizontal ones. But is interesting notice that tooth n.CC20_13/4_F8_52 shows a high number of horizontal striations (43) compared to the other molar (only 16). As already mentioned in the materials section (Paragraph 3.2), it is unclear whether the two molars, given the similar degree of wear, belonged to the same individual or not (this will have to be tested with future analyses). But the differences that were observed, at the micro-wear level, could suggest at least two individuals related to a different striations pattern. Therefore, these data could be very important because, in spite of indicating that different individuals could have different types of food intake (maybe a division by sex or age group could be a hypothesis), it also suggests that for the individual related to tooth n. CC20_13/4_F8_52, a diet that was more abrasive in terms of vegetable consumption is more plausible. In fact, looking at the NH/NT value, this specimen falls into the range of arid hunters-gatherer that correspond to a mixed-diet range. On the other hand, the same variable for the molar n. CC22_13/5_F9_134 shows a low value that automatically make it falls into the carnivorous-like range.

As argued by Lalueza-Fox et al. (1996) “There exists a considerable degree of heterogeneity in the microwear of these specimens, though, and no clear dietary trend, either temporal or phylogenetic, is present, with the exception, perhaps, of the Neanderthal group. Some of the Neanderthal fossils (Tabun 1, Tabun 2, Amud 1, and La Quina 5) are clearly distributed within or close to the carnivorous hunter-gatherer 95% dispersion range, suggesting that their diet was mainly meat dependent. This might be related to the existence of a subarctic environment in Europe during the Ice Age, which might have favored the development of a predominantly hunting strategy in the Neanderthals. However, the Neanderthal individuals from Marillac, St. Cesaire, and Malarnaud are distributed within the mixed-diet hunter-gatherers. This relatively large dispersion of the Neanderthals’ microwear is not surprising, as it may reflect the geographical and temporal diversity of this group” (Lalueza-Fox et al., 1996: 384). Is necessary to keep in mind that only two samples are very few in order to formulate robust paleodietary hypotheses. But these preliminary data obtained from the Ciota

Ciara samples are very interesting because allow to include this hominin group in the carnivorous-like range previously hypothesized for many European Neanderthalian populations. The information obtained from the buccal microwear analysis are totally in agreement with the previous archeozoological study conducted by Buccheri et al. (2016) (paragraph 3.1.2), in which hunting activities must have been one of the predominant subsistence strategies to gain high quantity of proteins. In addition, paleoclimatic and paleo-ecological analyses carried out by Berto et al. (2016) on the paleontological assemblage of the site (paragraph 3.1.2), revealed a high biodiversity paleoenvironmental context mostly dominated by a woodland zone. The surrounding area of mount Fenera, during this Middle Pleistocene phase, besides being rich in mammal wild fauna, must have provided an optimal supply of plants intake. This datum would be confirmed by the presence of a quite high number of horizontal striations found on molar *n.* CC20_13/4_F8_52, which would suggest a regular consumption of phytolith-rich plants. In addition, these data could suggest that some of the processed materials previously recognized in the lithic use-wear analysis made by Berruti & Arzarello (2012), could be part of the vegetal food resources that may have been exploited by the Ciota Ciara Neanderthals. From the DMTA comparative analysis made by El Zaatari et al., (2011), the authors conclude that: Neandertals from wooded habitats were found to have higher levels of surface complexity and heterogeneity compared to the other Neandertal groups. This suggests that the Neandertals from wooded environments had more of a mixed diet, probably consisting of higher proportions of plant foods, compared to the Neandertals from more open habitats; increased tree cover was found to be correlated with an increase in the levels of surface complexity and heterogeneity, likely reflecting a higher ingestion of hard items and an increase in the level of individual dietary variability (El Zaatari et al., 2011: 419). But is important to mention that these data reflect an occlusal microwear pattern, not buccal. Actually, another interesting microwear study, published by Pérez-Pérez et al. (2003), tried to compare the different density of buccal striations with the technological development of lithics to process food; in fact the authors argued that: "This Upper Paleolithic industry, which is certainly highly sophisticated, might have allowed for complex food processing techniques and widened dietary resources, whereas Late Pleistocene assemblages, much more limited in shapes and sizes, might have reflected functional activities with less food processing and, perhaps, more abrasive diets. The abrasive potential of edible materials might have decreased as a consequence of such technological evolution, though the hunter-gatherer economic pattern certainly persisted. Buccal microwear analysis applied to Pleistocene human teeth from different time periods and geographical areas should provide information about these dietary modifications, as well as of shifts in dietary habits due to climatic conditions and food availability" (Pérez-Pérez et al. 2003: 505). Observing the intensity in the number of striations in the Ciota Ciara samples, it can be seen that both values from molars are higher if compared to more chronologically recent Neanderthals (shown in Table 6.1) and more similar to Pre-Neanderthals populations. In fact, the Middle Pleistocene groups (Sima de los Huesos and Arago) show a peculiar microwear pattern, with the largest density of striations, followed by the Neandertals from Hortus, the Upper Paleolithic modern humans and the Middle Paleolithic Neanderthals (Table 6.2). Differences in food processing techniques and tool technologies might account for the highly abrasive diet of the Middle Pleistocene populations. The similarities in the microwear patterns of Arago and Sima de los Huesos might be indicative of similar technologies for food acquisition and processing of Middle Pleistocene populations. It has been proved that these populations did not control the fire, this phenomenon has been proposed as one of the causes contributed to the highly abrasive nature of their diets (Pérez-Pérez et al. 2003). A similar hypothesis has been proposed by looking at the dental specimens of *Homo antecessor*, in fact Lozano et al. (2017) argued that the use of a Mode 1 technology related to the absence of fire was the primary cause of the high level of dental abrasiveness recorded for this lower Pleistocene human species (Lozano et al., 2017). The Ciota Ciara assemblage, in fact, did not yield clear traces of domesticated

fire; only the presence of a small ephemeral fireplace (10x20 cm) under a wall was attested, this was also related to occasional small charcoal fragments of vegetal origin observed in the strata (Angelucci et al., 2019). Despite that, there is no presence of calcined bones, heat-treated lithics, or other evidence that allow to confirm the usual presence and use of fire in the cave. For that reason, the sporadic evidence of fire could be accidental and not of anthropogenic origin. The lithic assemblage, on the other hand, was classified as Mode 3 (Arzarello et al., 2012), and this evidence would go against what Pérez-Pérez et al. (2003) stated. Therefore, it is more likely that the lower level of food processing was due to the quality of the raw material. In fact, the study conducted by Berruti & Arzarello (2012) shows that most of the use-wear traces are found on quartz lithic artifacts (which is also the most abundant raw material of the assemblage). This finding is interesting since quartz, due to its physical properties, has a much less efficient cutting power than flint. This lower capacity in treating food items, mostly with quartz tools, could be one of the causes that led to the strong abrasiveness recorded in the Ciota Ciara's dental sample. On the other side, the DMTA analysis conducted by El Zaatari (2007) sustain that the Neanderthals from wooded environments, known from central Europe and the Levant during OIS 3 and from southern Europe during both OIS 3 and OIS 5e, did not show significant differences when compared to the Pre-Neandertals groups from similar wooded environments. Considering the occlusal evidence, the second hypothesis is that the observed pattern of dental microwear would have been influenced mostly by eco-geographical factors.

In conclusion, it is difficult to interpret which cause led one Neanderthal human group to have a more abrasive diet than others (climatic conditions, different geographic areas, different technological development to process food, or a combination of more variables). The high intragroup variation in the number of striations observed in many Neandertal specimens, including the two Ciota Ciara molars, does not sustain a hypothesis of a homogeneous and strictly carnivorous diet, with no consumption whatsoever of plant foods. Of course, this does not contradict the hypothesis that protein intake mostly came from hunting activities in the Neanderthals population. Probably dietary habits and food processing strategies of the Neandertals were highly variable and these populations were capable of adapting and shifting their dietary strategies according to environmental constraints, in a way similar to modern *Homo sapiens*. This preliminary paleodietary work shown here was an explorative analysis, the hypotheses previously listed needs to be confirmed with a larger sample and much more accurate analysis and comparisons.

TABLE 7. Summary statistics of number, length, and standard deviation of length for the fossil specimens studied[1]

	Variables															Indexes		
	NDM	XDM	STDDM	NH	XH	STDH	NMD	XMD	STDMD	NV	XV	STDV	NT	XT	STDT	NH/NV	NV/NT	NH/NT
Banyoles (ba)	35	154.58	139.10	45	154.29	97.77	16	199.85	166.83	45	195.30	134.27	145	157.70	128.72	1.000	0.310	0.310
Montmaurin (mt)	39	119.13	98.77	13	246.46	188.34	23	118.55	93.09	37	148.45	116.78	112	143.48	123.98	0.351	0.330	0.116
Broken Hill (bh)	37	123.19	105.64	51	76.29	72.66	57	97.94	86.65	58	99.13	78.92	203	97.44	86.50	0.879	0.286	0.251
La Chaise Suard (cs)	19	85.10	29.52	9	214.41	196.96	18	103.53	80.16	15	127.81	59.69	61	120.12	102.75	0.600	0.246	0.148
La Chaise Burgeois (cb)	5	83.05	21.24	21	113.28	72.01	27	109.42	162.63	29	122.66	86.31	82	113.48	113.09	0.724	0.354	0.256
Malarnaud (ml)	11	71.27	31.33	13	80.31	35.76	7	147.61	128.41	37	115.10	81.33	68	104.70	79.01	0.351	0.544	0.191
St. Cesaire (sc)	26	120.54	80.46	14	104.39	51.60	6	110.37	39.21	22	140.49	70.28	68	122.77	70.31	0.636	0.324	0.206
Marillac (mr)	27	226.61	201.42	23	127.36	122.48	17	261.42	246.70	35	245.82	186.46	102	197.67	183.72	0.657	0.343	0.225
La Quina V (q5)	9	229.71	120.64	7	263.22	227.62	26	166.41	82.93	15	203.62	111.03	57	198.08	127.23	0.467	0.263	0.123
Amud 1 (am1)	7	91.28	28.45	6	142.66	88.19	13	145.77	131.65	31	176.76	154.47	57	155.61	136.52	0.194	0.544	0.105
Tabun 1 (tb1)	3	176.24	43.17	3	127.98	95.58	11	147.21	88.97	10	248.95	141.49	27	185.98	114.20	0.300	0.370	0.111
Tabun 2 (tb2)	17	148.32	113.38	3	134.31	96.00	15	158.08	111.43	12	78.97	49.65	47	132.83	104.22	0.250	0.255	0.064
Gibraltar 2 (g2)	24	114.21	69.86	15	117.80	75.79	15	130.00	57.40	39	136.95	120.24	93	126.69	99.25	0.385	0.419	0.161
Skhül 4 (sk4)	16	122.96	74.76	14	103.07	55.60	17	129.15	84.13	44	137.65	91.85	91	128.16	83.69	0.318	0.484	0.154
Qafzeh 9 (qz9)	16	118.36	71.95	9	96.61	20.19	12	100.30	60.23	36	135.45	116.69	73	121.14	93.51	0.250	0.493	0.123
Cro-Magnon 4 (cr4)	28	155.17	84.89	32	132.66	146.68	19	147.19	82.92	44	227.91	182.78	123	174.10	148.07	0.727	0.358	0.260
La Madelaine (md)	18	158.99	122.39	35	156.90	139.76	24	99.52	44.96	23	165.39	88.09	100	145.46	111.71	1.522	0.230	0.350
Rond-du-Barry (rb)	37	117.49	66.15	17	88.74	49.64	9	78.49	30.32	33	205.55	102.73	96	139.01	91.26	0.515	0.344	0.177
Veyrier-sous-Saleve (vs)	8	171.87	219.68	12	124.04	117.10	37	156.99	107.77	53	178.77	125.30	110	164.97	129.52	0.226	0.482	0.109
Abri-Pataud (ap)	26	160.08	78.04	26	109.59	60.32	22	152.06	92.51	65	184.63	116.29	139	160.85	101.32	0.400	0.468	0.187

Table 6.1 Table showing the quantitative data and calculated indexes obtained from the human dental specimens analyzed in the work of Lalueza-Fox et al. (1996). Table taken from Lalueza-Fox et al. (1996: 380)

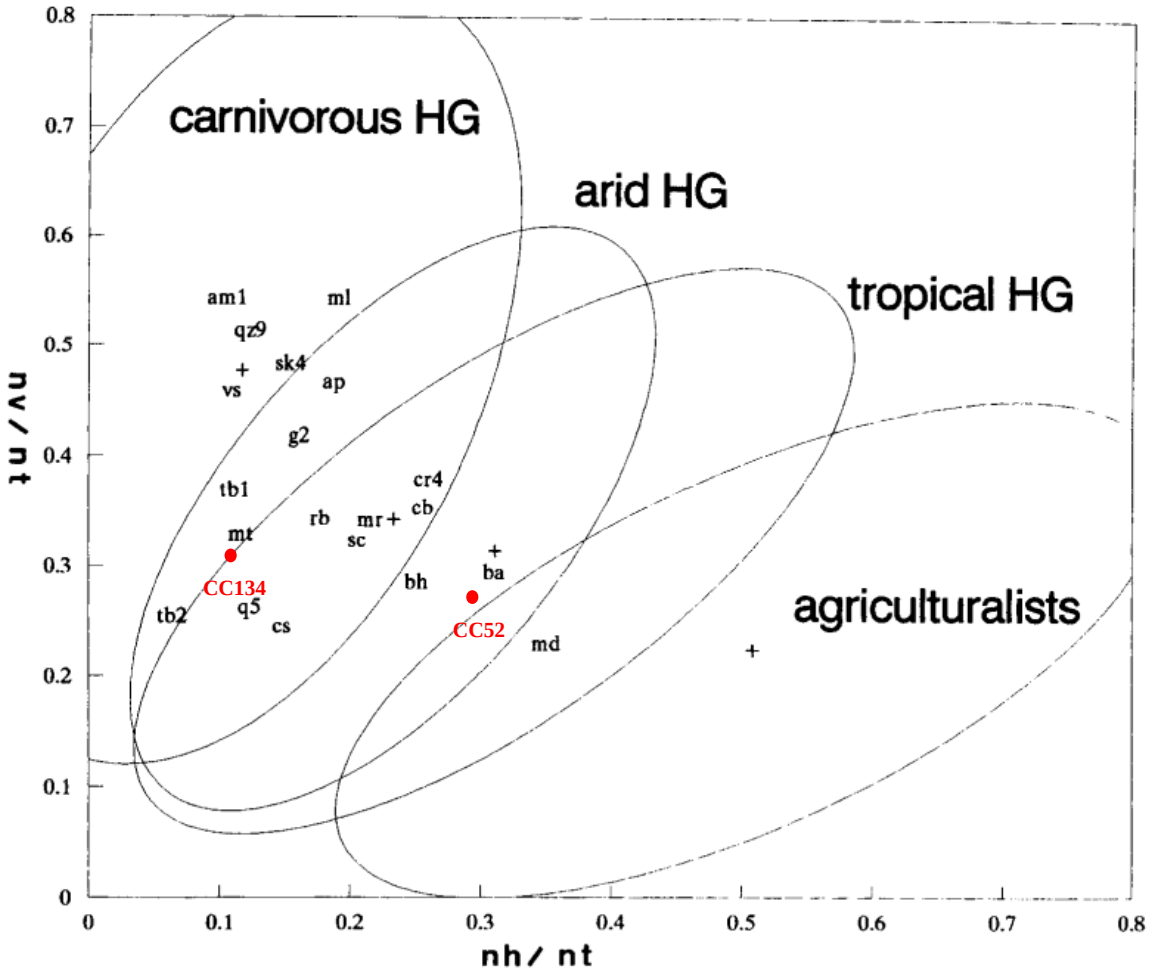

Graph 6.1 Plot of NV/NT index vs. NH/NT. Ellipses represent 95% dispersion of the modern dietary groups considered. Dental fossils specimens previously show in Table 6.1 are plotted in the graph; red points represent the Ciota Ciara specimens added to the graph. Table modified from Lalueza-Fox et al. (1996: 383)

Specimen	Tooth	OIS	Symbol	Country	Years BP	Level	NT ± σ
Summary by groups							
Arago	(n = 13)	12	R	France	423–478,000	*H. heidelbergensis*	167.6 ± 48.0
Sima de los Huesos	(n = 19)	9	T	Spain	303–339,000	*H. heidelbergensis*	179.2 ± 41.4
Middle Paleolithic	(n = 13)	3–4–5	1,2	F, S, NE	30–120,000	Neandertal	88.9 ± 37.1
Hortus	(n = 8)	4	3	France	59–71,000	Neandertal	123.5 ± 19.0
U. Pal. & Mesolithic	(n = 7)	1–2	U	France, Spain	6–30,000	modern *H. sapiens*	117.9 ± 17.9
Modern comparative collection (Lalueza et al., 1996)							
Andamanese	(n = 18)		Andaman		Tropical hunter-gatherer		74.8 ± 20.5
Veddhas	(n = 9)		Sri Lanka		Tropical hunter-gatherer		74.2 ± 28.0
Tasmanian	(n = 11)		Tasmania		Arid hunter-gatherer		73.4 ± 29.0
Bushmen	(n = 15)		Africa		Arid hunter-gatherer		67.7 ± 16.7
Australian	(n = 18)		Australia		Arid hunter-gatherer		66.2 ± 11.0
Vancouver Islanders	(n = 17)		Canada		Carnivorous hunter gatherer		41.8 ± 16.1
Inuit	(n = 20)		Greenland		Carnivorous hunter gatherer		38.4 ± 18.3
Fuegians	(n = 20)		Argentina		Carnivorous hunter gatherer		32.0 ± 13.5

Table 6.2 Table showing abrasive buccal intensity (NT) related to different human extinct and extant populations. Table taken from

CHAPTER 7: Conclusion

The main aim of this research was to perform dental microwear analysis for the first time on the newly discovered Neanderthal remains from the Middle Pleistocene site of Ciota Ciara. Therefore, the intents of this work were primarily explorative since the analysis was focused on several aspects: paleodiet reconstruction, postmortem and antemortem features identification (with a specific interest on para-masticatory activities recognition), and the application of a recent comparative methodology that included the use of multiple technical instrumentations (in addition to the traditional one). Despite the small number of samples available, the results highlighted the powerful informative potential that was obtained from these dental remains through the application of a microwear analysis protocol. Obtained results offer insights not only into the different tooth-use patterns of the Ciota Ciara's Neanderthals, but also about the status of the analyzed fossils. Specifically, the distribution of several enamel damages (e.g. postmortem chipping, fractures, and pitting) seems to reflect variant post-depositional effects that affected the dental surfaces in different ways. While, other clear antemortem features, allowed to recognize evident traces related to masticatory processes (antemortem chipping and wear) and even to possible para-masticatory activities (dental cut-marks). Comparing analyses that have been reported in previous papers, is possible to support those forceful bites of the anterior dentition, to process food, can reflect significantly greater incisor wear and dental micro-chipping, but the hypothesis of tooth-use as "third hand" needs to be tested through more accurate analysis. The buccal paleodietary reconstruction, on the other hand, suggested an abrasive diet with an important animal protein component also combined with a fibrous plant intake. These data agree with previous archaeozoological, palaeoecological and lithic use-wear analysis. The intense buccal abrasiveness seems to be more comparable with the striation patterns found on Pre-neanderthalian populations. Although there is no reliable evidence of fire domestication, the lithic technology associated to the Ciota Ciara strata is fully Mode 3; for that reason, the hypothesized limited food processing (that probably caused the abrasiveness) may be related more to the type of raw material (mostly quartz) than to the technological development level. The second hypothesis, based on other DMTA neanderthal analyses, would support that woodland areas were found to be correlated with an increasing consumption of hard items and to a much more variable level of intra-individual diet. However, the two hypotheses are not mutually exclusive and could be linked to each other. Lastly, the proposed methodological analysis yielded new data regarding the use of non-traditional instrumentations applied to human dental microwear. In fact, the results showed statistical differences mostly related to the counted number of striations between OMs and ESEM , specifically for the following variables: NT (ESEM- Hirox), NMD (ESEM – Hirox), and NV (ESEM – Zeiss). In addition, it was also possible to notice some important differences between the two types of optical microscopes, especially in the counting striations of the variable NH; for this reason, differences between the two optical microscopes also need to be tested because, apparently, they do not give similar results when compared to ESEM. However, dental microwear analysis is not sufficient to return a complete picture regarding the tooth-use reconstruction of the Ciota Ciara specimens. Thus, further analysis would be needed to confirm the hypotheses proposed in the current work. For example, chemical studies on stable isotopes or dental calculus analysis would add more information regarding the alimentary habits of the Ciota Ciara's Neanderthals. Moreover, a paleopathological assessment with careful observation of the originals, would allow further information to be extracted about their lifestyle. For future research, it would also be interesting to conduct accurate studies on

the age at death of each dental specimens to reveal the presence of more individuals. Methodologically, however, it would be appropriate to test for differences between the OMs and SEM equipment by expanding the analysis to a significantly larger sample to reduce the error. At the end, this preliminary dental microwear analysis has allowed the Neanderthal dental remains, from the Ciota Ciara site, to be well contextualized in the paleoanthropological field of study from multiple points of view, future studies will allow to add further data useful for the correct interpretation on the hominin tooth-use behavior (both dietary and non-dietary) of this archeological context.

Acknowledgements

I would like to thank Dra. Julie Arnaud and Dra. Marta Arzarello for allowing me to study the original hominin dental specimens and pursue such an ambitious and interesting project. I would especially thank my thesis co-supervisor, Dra. Julie Arnaud, for constantly assisting me during the process of this work.

I would like to thank very much my thesis supervisor Dra. Marina Lozano who wisely guided me, with kindness and helpfulness, in all the steps of this research and for teaching me, in the best way, about the application of the dental microwear technique.

I want to thank my dear friends Sarah and Daniele. Especially Sarah, to whom I dedicated this work. Thank you for being the first truly person that really believed in my capacities.

Finally, I would like to thank my supportive family plus all the dear colleagues and professors of IMQP.

Bibliography

Angelucci, D. E., Zambaldi, M., Tessari, U., Vaccaro, C., Arnaud, J., Berruti, G. L. F., Daffara, S., & Arzarello, M. (2019). New insights on the Monte Fenera Palaeolithic, Italy: Geoarchaeology of the Ciota Ciara cave. *Geoarchaeology*, *34*(4), 413–429.

Arnaud J., Arzarello M., Berruti G., & Daffara S. (2022). *Nuovi dati sull'occupazione della Ciota Ciara durante il Paleolitico Medio - Borgosesia, Monte Fenera*.

Arnaud J., Arzarello M., Berruti G., & Daffara S. (2023). Nuovi dati sull'occupazione della Ciota Ciara durante il Paleolitico medio - Borgosesia, Monte Fenera. *"In Press"*.

Arzarello, M., Daffara, S., Berruti, G., Berruto, G., Berté, D., Berto, C., Gambari, F. M., & Peretto, C. (2012). The Mousterian settlement in the Ciota Ciara cave: the oldest evidence of Homo neanderthalensis in Piedmont (Northern Italy). *Journal of Biological Research-Bollettino Della Società Italiana Di Biologia Sperimentale*, *85*(1).

Bailey, S. E., & Hublin, J.-J. (2006). Dental remains from the Grotte du Renne at Arcy-sur-Cure (Yonne). *Journal of Human Evolution*, *50*(5), 485–508.

Baker, G., Jones, L. H. P., & Wardrop, I. D. (1959). Cause of Wear in Sheeps' Teeth. *Nature 1959 184:4698*, *184*(4698), 1583–1584. https://doi.org/10.1038/1841583b0

Bax, J. S., & Ungar, P. (1999). Incisor labial surface wear striations in modern humans and their implications for handedness in Middle and Late Pleistocene hominids. *International Journal of Osteoarchaeology*. https://doi.org/10.1002/(SICI)1099-1212(199905/06)9:3

Belcastro, G., Rastelli, E., Mariotti, V., Consiglio, C., Facchini, F., & Bonfiglioli, B. (2007). Continuity or discontinuity of the life-style in central Italy during the Roman imperial age-early middle ages transition: Diet, health, and behavior. *American Journal of Physical Anthropology: The Official Publication of the American Association of Physical Anthropologists*, *132*(3), 381–394.

Belcastro, M. G., Mariotti, V., Riga, A., Bonfiglioli, B., & Frayer, D. W. (2018). Tooth fractures in the Krapina Neandertals. *Journal of Human Evolution*, *123*, 96–108.

Beniash, E., Stifler, C. A., Sun, C. Y., Jung, G. S., Qin, Z., Buehler, M. J., & Gilbert, P. U. P. A. (2019). The hidden structure of human enamel. *Nature Communications 2019 10:1*, *10*(1), 1–13. https://doi.org/10.1038/s41467-019-12185-7

Bermúdez de Castro, J., Bromage, T. G., & Jalvo, Y. F. (1988). Buccal striations on fossil human anterior teeth: evidence of handedness in the middle and early Upper Pleistocene. *Journal of Human Evolution*, *17*(4), 403–412. https://doi.org/10.1016/0047-2484(88)90029-2

Berruti, G., & Arzarello, M. (2012). L'analisi tracceologica per la ricostruzione delle attività nella preistoria: l'esempio della grotta della Ciota Ciara (Borgosesia–VC). *Annali Dell'Università Di Ferrara. Museologia Scientifica e Naturalistica*, *8*(1), 117–125.

Berruti, G. L. F., Daffara, S., Fuselli, P., & Arzarello, M. (2023). Planning a trip during Middle Palaeolithic. The mobile toolkit debate and some considerations about expedient vs curated

technologies in the light of new data from the Ciota Ciara cave (NW Italy). *Journal of Archaeological Science: Reports*, *49*, 103939.

Berto, C., Berte, D., Luzi, E., López-Garc\'\ia, J. M., Pereswiet-Soltan, A., & Arzarello, M. (2016). Small and large mammals from the Ciota Ciara cave (Borgosesia, Vercelli, Italy): an isotope stage 5 assemblage. *Comptes Rendus Palevol*, *15*(6), 669–680.

Bonfiglioli, B., Mariotti, V., Facchini, F., Belcastro, M. G., & Condemi, S. (2004). Masticatory and non-masticatory dental modifications in the epipalaeolithic necropolis of Taforalt (Morocco). *International Journal of Osteoarchaeology*, *14*(6), 448–456.

Brace, C., Ryan, A., & Smith, B. (1981). Comment on: Tooth wear in La Ferrassie Man, by P-F Puesch. *Current Anthropology*, *22*, 426–430.

Broz, M. E., Cook, R. F., & Whitney, D. L. (2006). Microhardness, toughness, and modulus of Mohs scale minerals. *American Mineralogist*, *91*(1), 135–142. https://doi.org/10.2138/AM.2006.1844

Buccheri, F., Berte, D. F., Berruti, G. L. F., Caceres, I., Volpe, L., & Arzarello, M. (2016). Taphonomic analysis on fossil remains from the Ciota Ciara Cave (Piedmont, Italy) and new evidence of cave bear and wolf exploitation with simple quartz flakes by Neanderthal. *Rivista Italiana Di Paleontologia e Stratigrafia*, *122*(3).

Butler, P. M. (1952). The milk-molars of Perissodactyla, with remarks on molar occlusion. *Proceedings of the Zoological Society of London*, *121*(4), 777–817.

Calandra, I., Pedergnana, A., Gneisinger, W., & Marreiros, J. (2019). Why should traceology learn from dental microwear, and vice-versa? *Journal of Archaeological Science*, *110*, 105012.

Calhoun, G. V, Guatelli-Steinberg, D., Lagan, E. M., & McGraw, W. S. (2022). Dental macrowear, diet, and anterior tooth use in Colobus polykomos and Piliocolobus badius. *Journal of Human Evolution*, *163*, 103123.

Constantino, P. J., & Konow, K. A. (2021). Dental chipping supports lack of hard-object feeding in Paranthropus boisei. *Journal of Human Evolution*, *156*, 103015.

Constantino, P., Lee, J. J., Chai, H., Zipfel, B., Ziscovici, C., Lawn, B. R., & Lucas, P. (2010). *Tooth chipping can reveal bite forces and diets of fossil hominins*. https://www.nist.gov/publications/tooth-chipping-can-reveal-bite-forces-and-diets-fossil-hominins

Daffara, S., Arzarello, M., Berruti, G. L. F., Berruto, G., Bertè, D., Berto, C., & Casini, A. I. (2014). The Mousterian lithic assemblage of the Ciota Ciara cave (Piedmont, Northern Italy): exploitation and conditioning of raw materials. *Journal of Lithic Studies*, *1*(2), 63–78.

Daffara, S., Berruti, G. L. F., & Arzarello, M. (2021). Expedient behaviour and predetermination at the Ciota Ciara cave (north-western Italy) during Middle Palaeolithic. *Quaternary International*, *577*, 71–92.

Daffara, S., Berruti, G. L. F., Berruto, G., Eftekhari, N., Vaccaro, C., & Arzarello, M. (2019). Raw materials procurement strategies at the Ciota Ciara cave: New insight on land mobility in

north-western Italy during Middle Palaeolithic. *Journal of Archaeological Science: Reports*, *26*, 101882.

Dahlberg, A. A., & Kinzey, W. (1962). Etude microscopique de l'abrasion et de l'attrition sur la surface des dents. *Bulletin Du Groupement International Pour La Recherche Scientifique En Stomatologie et Odontologie (Bruxelles)*, *5*, 242–251.

El Zaatari, S. (2007). *Ecogeographic variation in Neandertal dietary habits: evidence from microwear texture analysis*. State University of New York at Stony Brook.

El Zaatari, S., Grine, F. E., Ungar, P. S., & Hublin, J. J. (2011). Ecogeographic variation in Neandertal dietary habits: Evidence from occlusal molar microwear texture analysis. *Journal of Human Evolution*, *61*(4), 411–424. https://doi.org/10.1016/J.JHEVOL.2011.05.004

El-Zaatari, S. (2010). Occlusal microwear texture analysis and the diets of historical/prehistoric hunter-gatherers. *International Journal of Osteoarchaeology*, *20*(1), 67–87. https://doi.org/10.1002/oa.1027

Eshed, V., Gopher, A., & Hershkovitz, I. (2006). Tooth wear and dental pathology at the advent of agriculture: New evidence from the Levant. *American Journal of Physical Anthropology*, *130*(2), 145–159. https://doi.org/10.1002/AJPA.20362

Estalrrich, A., El Zaatari, S., & Rosas, A. (2017). Dietary reconstruction of the El Sidrón Neandertal familial group (Spain) in the context of other Neandertal and modern hunter-gatherer groups. A molar microwear texture analysis. *Journal of Human Evolution*, *104*, 13–22.

Estalrrich, A., & Rosas, A. (2015). Division of labor by sex and age in Neandertals: an approach through the study of activity-related dental wear. *Journal of Human Evolution*, *80*, 51–63.

Estebaranz, F., Galbany, J., Martinez, L. M., Turbón, D., & Pérez-Pérez, A. (2012). Buccal dental microwear analyses support greater specialization in consumption of hard foodstuffs for Australopithecus anamensis. *Journal of Anthropological Sciences = Rivista Di Antropologia : JASS*, *90*, 163–185. https://doi.org/10.4436/JASS.90006

Fiorenza, L., Benazzi, S., Estalrrich, A., & Kullmer, O. (2019). Diet and cultural diversity in Neanderthals and modern humans from dental macrowear analyses. In *Dental Wear in Evolutionary and Biocultural Contexts* (pp. 39–72). Elsevier. https://doi.org/10.1016/B978-0-12-815599-8.00003-4

Fiorenza, L., Benazzi, S., Henry, A. G., Salazar-Garc\'\ia, D. C., Blasco, R., Picin, A., Wroe, S., & Kullmer, O. (2015). To meat or not to meat? New perspectives on N eanderthal ecology. *American Journal of Physical Anthropology*, *156*, 43–71.

Fiorenza, L., Benazzi, S., & Kullmer, O. (2011). Para-masticatory wear facets and their functional significance in hunter–gatherer maxillary molars. *Journal of Archaeological Science*, *38*(9), 2182–2189. https://doi.org/10.1016/J.JAS.2011.03.012

Fiorenza, L., Benazzi, S., Tausch, J., Kullmer, O., Bromage, T. G., & Schrenk, F. (2011). Molar macrowear reveals neanderthal eco-geographic dietary variation. *PLoS ONE*, *6*(3). https://doi.org/10.1371/JOURNAL.PONE.0014769

Forestier, H. (1993). Le Clactonien: mise en application d'une nouvelle méthode de débitage s' inscrivant dans la variabilité des systèmes de production lithique du Paléolithique ancien. *Paléo, Revue d'Archéologie Préhistorique*, *5*(1), 53–82.

Fox, C. L., & Frayer, D. W. (1997). Non-dietary marks in the anterior dentition of the Krapina Neanderthals. *International Journal of Osteoarchaeology*, *7*(2), 133–149.

Fox, C. L., & Pérez-Pérez, A. (1994). Cutmarks and post-mortem striations in fossil human teeth. *Human Evolution*, *9*, 165–172.

Frayer, D. W., Fiore, I., Lalueza-Fox, C., Radovcic, J., & Bondioli, L. (2010). Right handed Neandertals: Vindija and beyond. *Journal of Anthropological Sciences*, *88*, 113–127.

Fyfe, D. M., Chandler, N. P., & Wilson, N. H. F. (1993). Alveolar bone status of some pre-seventeenth century inhabitants of Taumako, Solomon Islands. *International Journal of Osteoarchaeology*, *3*(1), 29–35. https://doi.org/10.1002/OA.1390030104

Galbany, J., Estebaranz, F., Martínez, L. M., & Pérez-Pérez, A. (2009). Buccal dental microwear variability in extant African Hominoidea: Taxonomy versus ecology. *Primates*, *50*(3), 221–230. https://doi.org/10.1007/S10329-009-0139-0/FIGURES/3

Galbany, J., Estebaranz, F., Martínez, L. M., Romero, A., De Juan, J., Turbón, D., & Pérez-Pérez, A. (2006). Comparative analysis of dental enamel polyvinylsiloxane impression and polyurethane casting methods for SEM research. *Microscopy Research and Technique*, *69*(4), 246–252.

Galbany, J., Martínez, L. M., López-Amor, H. M., Espurz, V., Hiraldo, O., Romero, A., de Juan, J., & Pérez-Pérez, A. (2005). Error rates in buccal-dental microwear quantification using scanning electron microscopy. *Scanning*, *27*(1), 23–29.

Galbany, J., Martínez, L. M., & Pérez-Pérez, A. (2004). Tooth replication techniques, SEM imaging and microwear analysis in primates: methodological obstacles. *Anthropologie (1962-)*, *42*(1), 5–12.

García-Gonz alez, R., Miguel Carretero, J., Richards, M. P., Rodríguez, L., & Quam, R. (2015). Dietary inferences through dental microwear and isotope analyses of the Lower Magdalenian individual from El Mir on Cave (Cantabria, Spain). *Journal of Archaeological Science*, *60*, 28–38. https://doi.org/10.1016/j.jas.2015.03.020

Goodall, R. H., Darras, L. P., & Purnell, M. A. (2015). Accuracy and precision of silicon based impression media for quantitative areal texture analysis. *Scientific Reports*, *5*. https://doi.org/10.1038/srep10800

Gordon, K. D. (1982). A study of microwear on chimpanzee molars: implications for dental microwear analysis. *American Journal of Physical Anthropology*, *59*(2), 195–215.

Gordon, K. D. (1984). Hominoid dental microwear: complications in the use of microwear analysis to detect diet. *Journal of Dental Research*, *63*(8), 1043–1046. https://doi.org/10.1177/00220345840630080601

Gordon, K. D. (1988). A review of methodology and quantification in dental microwear analysis. *Scanning Microscopy*, *2*(2), 1139–1147.

Grine, F. E. (1977). Analysis of early hominid deciduous molar wear by scanning electron microscopy: a preliminary report. *Proceedings of the Electron Microscopy, Society of South Africa*, *7*, 157–158.

Grine, F. E. (1986). Dental evidence for dietary differences in Australopithecus and Paranthropus: a quantitative analysis of permanent molar microwear. *Journal of Human Evolution*, *15*(8), 783–822. https://doi.org/10.1016/S0047-2484(86)80010-0

Grine, F. E., & Kay, R. F. (1988). Early hominid diets from quantitative image analysis of dental microwear. *Nature*, *333*(6175), 765–768.

Grine, F. E., Ungar, P. S., & Teaford, M. F. (2002). Error rates in dental microwear quantification using scanning electron microscopy. *Scanning: The Journal of Scanning Microscopies*, *24*(3), 144–153.

Grine, F. E., Ungar, P. S., Teaford, M. F., & El-Zaatari, S. (2006). Molar microwear in Praeanthropus afarensis: Evidence for dietary stasis through time and under diverse paleoecological conditions. *Journal of Human Evolution*, *51*(3), 297–319. https://doi.org/10.1016/J.JHEVOL.2006.04.004

Grine, F. E., Ungar, P. S., Teaford, M. F., & El-Zaatari, S. (2013). Molar Microwear, Diet and Adaptation in a Purported Hominin Species Lineage from the Pliocene of East Africa. *Vertebrate Paleobiology and Paleoanthropology*, *9789400759183*, 213–223. https://doi.org/10.1007/978-94-007-5919-0_14/COVER

Harvati, K., Darlas, A., Bailey, S. E., Rein, T. R., El Zaatari, S., Fiorenza, L., Kullmer, O., & Psathi, E. (2013). New Neanderthal remains from Mani peninsula, southern Greece: the Kalamakia middle Paleolithic cave site. *Journal of Human Evolution*, *64*(6), 486–499.

Hernando, R., Fernández-Marchena, J. L., Willman, J. C., Ollé, A., Vergès, J. M., & Lozano, M. (2020). Exploring the utility of optical microscopy versus scanning electron microscopy for the quantification of dental microwear. *Quaternary International*, *569–570*, 5–14. https://doi.org/10.1016/j.quaint.2020.05.022

Hernando, R., Willman, J. C., Souron, A., Cebrià, A., Oms, F. X., Morales, J. I., & Lozano, M. (2022). What about the buccal surfaces? Dental microwear texture analysis of buccal and occlusal surfaces refines paleodietary reconstructions. *American Journal of Biological Anthropology*, *178*(2), 347–359. https://doi.org/10.1002/ajpa.24509

Higgins, D., & Austin, J. J. (2013). Teeth as a source of DNA for forensic identification of human remains: a review. *Science & Justice*, *53*(4), 433–441.

Hillson, S. (1996). *Dental anthropology*. Cambridge University Press.

Hillson, S. (2007). Dental Pathology. *Biological Anthropology of the Human Skeleton: Second Edition*, 299–340. https://doi.org/10.1002/9780470245842.CH10

Hlusko, L. J., Carlson, J. P., Guatelli-Steinberg, D., Krueger, K. L., Mersey, B., Ungar, P. S., & Defleur, A. (2013). Neanderthal teeth from moula-guercy, Ardèche, France. *American Journal of Physical Anthropology*, *151*(3), 477–491.

Hughes, C. E., & White, C. A. (2009). Crack propagation in teeth: A comparison of perimortem and postmortem behavior of dental materials and cracks. *Journal of Forensic Sciences*, *54*(2), 263–266.

Karriger, W. M., Schmidt, C. M., & Smith, F. H. (2016). Dental microwear texture analysis of Croatian Neandertal molars. *PaleoAnthropology*, *2016*, 172–184.

Kay, R. F., & Hiiemae, K. M. (1974). Jaw movement and tooth use in recent and fossil primates. *American Journal of Physical Anthropology*, *40*(2), 227–256. https://doi.org/10.1002/AJPA.1330400210

King, T., Andrews, P., & Boz, B. (1999). Effect of taphonomic processes on dental microwear. *American Journal of Physical Anthropology: The Official Publication of the American Association of Physical Anthropologists*, *108*(3), 359–373.

Krueger, K. L., Scott, J. R., Kay, R. F., & Ungar, P. S. (2008). Dental microwear textures of "Phase I" and "Phase II" facets. *American Journal of Physical Anthropology: The Official Publication of the American Association of Physical Anthropologists*, *137*(4), 485–490.

Krueger, K. L., Ungar, P. S., Guatelli-Steinberg, D., Hublin, J. J., Pérez-Pérez, A., Trinkaus, E., & Willman, J. C. (2017). Anterior dental microwear textures show habitat-driven variability in Neandertal behavior. *Journal of Human Evolution*, *105*, 13–23. https://doi.org/10.1016/J.JHEVOL.2017.01.004

Kruzic, J. J., Nalla, R. K., Kinney, J. H., & Ritchie, R. O. (2003). Crack blunting, crack bridging and resistance-curve fracture mechanics in dentin: effect of hydration. *Biomaterials*, *24*(28), 5209–5221.

Kuhn, S. L., & Stiner, M. C. (2006). What's a Mother to Do? *Https://Doi.Org/10.1086/507197*, *47*(6), 953–980. https://doi.org/10.1086/507197

Lalueza Fox, C., Perez-Perez, A., Turbon, D., & Perez-Pbrez, A. (1996). Dietary Inferences Through Buccal Microwear Analysis of Middle and Upper Pleistocene Human Fossils. In *AMERICAN JOURNAL OF PHYSICAL ANTHROPOLOGY* (Vol. 100).

Lalueza Fox, C. (1992). Information obtained from the microscopic examination of cultural striations in human dentition. *International Journal of Osteoarchaeology*, *2*(2), 155–169. https://doi.org/10.1002/OA.1390020207

Lalueza Fox, C. L., & Pérez-Pérez, A. (1993). The diet of the Neanderthal Child Gibraltar 2 (Devil's Tower) through the study of the vestibular striation pattern. *Journal of Human Evolution*, *24*(1), 29–41.

Lozano, M., Bermúdez de Castro, J. M., Carbonell, E., & Arsuaga, J. L. (2008). Non-masticatory uses of anterior teeth of Sima de los Huesos individuals (Sierra de Atapuerca, Spain). *Journal of Human Evolution*, *55*(4), 713–728. https://doi.org/10.1016/j.jhevol.2008.04.007

Lozano, M., Estalrrich, A., Bondioli, L., Fiore, I., de Castro, J.-M., Arsuaga, J. L., Carbonell, E., Rosas, A., & Frayer, D. W. (2017). Right-handed fossil humans. *Evolutionary Anthropology: Issues, News, and Reviews*, *26*(6), 313–324.

Lozano, M., Subirà, M. E., Aparicio, J., Lorenzo, C., & Gómez-Merino, G. (2013). Toothpicking and periodontal disease in a Neanderthal specimen from Cova Foradà site (Valencia, Spain). *PloS One*, *8*(10), e76852.

Lozano Ruiz, M., Romero-Rameta, A., de Castro, J. M., Carbonell, E., Arsuaga, J. L., & Pérez-Pérez, A. (2017). *The diet of Homo antecessor*.

Lozano Ruiz, M., Bermúdez de Castro, J. M., Martinón-Torres, M., & Sarmiento, S. (2004). Cutmarks on fossil human anterior teeth of the Sima de los Huesos Site (Atapuerca, Spain). *Journal of Archaeological Science*, *31*(8), 1127–1135. https://doi.org/10.1016/J.JAS.2004.02.005

Lucas, P. W. (2004). Dental Functional Morphology: How Teeth Work. *Dental Functional Morphology*. https://doi.org/10.1017/CBO9780511735011

Lukacs, J. R., & Pastor, R. F. (1988). Activity-induced patterns of dental abrasion in prehistoric Pakistan: evidence from Mehrgarh and Harappa. *American Journal of Physical Anthropology*, *76*(3), 377–398. https://doi.org/10.1002/AJPA.1330760310

Lumley-Woodyear, M. A. de. (1973). *Anténéandertaliens et néandertaliens du bassin méditerranéen occidental européen : Cova Negra, Le Lazaret, Bañolas, Grotte du Prince, Carigüela, Hortus, Agut, Macassargues, La Masque, Rigabe, La Crouzade, Les Peyrards, Bau de l'Aubesier*.

Mahoney, P. (2006). Dental microwear from Natufian hunter-gatherers and early neolithic farmers: Comparisons within and between samples. *American Journal of Physical Anthropology*, *130*(3), 308–319. https://doi.org/10.1002/AJPA.20311

Maier, W., & Schneck, G. (1981). Konstruktionsmorphologische Untersuchungen am Gebiß der hominoiden Primaten. *Zeitschrift Für Morphologie Und Anthropologie*, *72*(2), 127–169. https://doi.org/10.1127/ZMA/72/1981/127

Martínez, L. M., & Pérez-Pérez, A. (2004). Post-mortem wear as indicator of taphonomic processes affecting enamel surfaces of hominin teeth from Laetoli and Olduvai (Tanzania) implications to dietary interpretations. *Anthropologie (1962-)*, *42*(1), 37–42.

Martín-Viveros, J. I., & Ollé, A. (2020). Use-wear and residue mapping on experimental chert tools. A multi-scalar approach combining digital 3D, optical, and scanning electron microscopy. *Journal of Archaeological Science: Reports*, *30*. https://doi.org/10.1016/j.jasrep.2020.102236

Micó, C., Blasco, R., Muñoz Del Pozo, A., Jiménez-Garc\'\ia, B., Rosell, J., & Rivals, F. (2023). Differentiating taphonomic features from trampling and dietary microwear, an experimental approach. *Historical Biology*, 1–23.

Mihlbachler, M. C., Foy, M., & Beatty, B. L. (2019). Surface replication, fidelity and data loss in traditional dental microwear and dental microwear texture analysis. *Scientific Reports*, *9*(1), 1595.

Mills, J. R. E. (1955). Ideal dental occlusion in the primates. *Dent Practit*, *6*, 47–61.

Minozzi, S., Manzi, G., Ricci, F., Di Lernia, S., & Borgognini Tarli, S. M. (2003). Nonalimentary tooth use in prehistory: an example from early Holocene in Central Sahara (Uan Muhuggiag, Tadrart Acacus, Libya). *American Journal of Physical Anthropology*, *120*(3), 225–232. https://doi.org/10.1002/AJPA.10161

Molnar, S., Barrett, M. J., Brian, L., Brace, C. L., Brose, D. S., Dewey, J. R., Frisch, J. E., Ganguly, P., Gejvall, N.-G., Greene, D. L., & others. (1972). Tooth wear and culture: a survey of tooth functions among some prehistoric populations [and comments and reply]. *Current Anthropology*, *13*(5), 511–526.

Mottura, A. (1980). Un frammento di osso temporale di tipo neandertaliano dalla grotta della Ciota Ciara. *Antropologia Contemporanea*, *3*, 373–379.

Palombo, M. R., Filippi, M. L., Iacumin, P., Longinelli, A., Barbieri, M., & Maras, A. (2005). Coupling tooth microwear and stable isotope analyses for palaeodiet reconstruction: the case study of Late Middle Pleistocene Elephas (Palaeoloxodon) antiquus teeth from Central Italy (Rome area). *Quaternary International*, *126–128*(1 SPEC.ISS.), 153–170. https://doi.org/10.1016/J.QUAINT.2004.04.020

Pastor, R. F. (1993). *Dental microwear among prehistoric inhabitants of the Indian subcontinent: a quantitative and comparative analysis*. University of Oregon.

Pearsall, D. M. (2016). Paleoethnobotany, Third Edition: A Handbook of Procedures. *Paleoethnobotany, Third Edition: A Handbook of Procedures*, 1–513. https://doi.org/10.4324/9781315423098/PALEOETHNOBOTANY-DEBORAH-PEARSALL

Pérez-Pérez, A., de Castro, J. M., & Arsuaga, J. L. (1999). Nonocclusal dental microwear analysis of 300,000-year-old Homo heilderbergensis Teeth from Sima de los Huesos (Sierra de Atapuerca, Spain). *American Journal of Physical Anthropology: The Official Publication of the American Association of Physical Anthropologists*, *108*(4), 433–457.

Pérez-Pérez, A., Espurz, V., de Castro, J. M. B., de Lumley, M. A., & Turbón, D. (2003). Non-occlusal dental microwear variability in a sample of Middle and Late Pleistocene human populations from Europe and the Near East. *Journal of Human Evolution*, *44*(4), 497–513.

Pérez-Pérez, A., Lalueza, C., & Turbón, D. (1994). Intraindividual and intragroup variability of buccal tooth striation pattern. *American Journal of Physical Anthropology*, *94*(2), 175–187. https://doi.org/10.1002/AJPA.1330940203

Pérez-Pérez, A., Lozano, M., Romero, A., Martínez, L. M., Galbany, J., Pinilla, B., Estebaranz-Sánchez, F., De Castro, J. M. B., Carbonell, E., & Arsuaga, J. L. (2017). The diet of the first Europeans from Atapuerca. *Scientific Reports*, *7*. https://doi.org/10.1038/SREP43319

Piperno, D. R. (2014). *Phytolyth Analysis: An Archaeological and Geological Perspective*. 280. https://books.google.com/books/about/Phytolyth_Analysis.html?hl=it&id=9oWLBQAAQBAJ

Power, R. C., Salazar-Garcia, D. C., Rubini, M., Darlas, A., Harvati, K., Walker, M., Hublin, J.-J., & Henry, A. G. (2018). Dental calculus indicates widespread plant use within the stable Neanderthal dietary niche. *Journal of Human Evolution*, *119*, 27–41.

Puech P. F. (1976). *Recherche sur le mode d'alimentation des hommes du Paléolithique par l'étude microscopique des couronnes dentaires*.

Puech, P.-F. (1979). The Diet of Early Man: Evidence From Abrasion of Teeth and Tools. *Https://Doi.Org/10.1086/202335*, *20*(3), 590–592. https://doi.org/10.1086/202335

Puech, P.-F. (1981). Tooth wear in La Ferrassie man. *Current Anthropology*, *22*(4), 424–430.

Puech, P.-F., Prone, A., Roth, H., & Cianfarani, F. (1985). Reproduction expérimentale de processus d'usure des surfaces dentaires des Hominidés fossiles: conséquences morphoscopique et exoscopiques avec application à l'Hominidé I de Garusi. *Comptes Rendus de l'Académie Des Sciences. Série 2, Mécanique, Physique, Chimie, Sciences de l'univers, Sciences de La Terre*, *301*(1), 59–64.

Purnell, M. A., Hart, P. J. B., Baines, D. C., & Bell, M. A. (2006). Quantitative analysis of dental microwear in threespine stickleback: A new approach to analysis of trophic ecology in aquatic vertebrates. *Journal of Animal Ecology*, *75*(4), 967–977. https://doi.org/10.1111/j.1365-2656.2006.01116.x

Rasmussen, S. T., Patchin, R. E., Scott, D. B., & Heuer, A. H. (1976). Fracture properties of human enamel and dentin. *Journal of Dental Research*, *55*(1), 154–164.

Ready, E. (2010). Neandertal man the hunter: a history of Neandertal subsistence. *Vis-à-Vis: Explorations in Anthropology*, *10*(1).

Rensberger, J. M. (1978). Scanning electron microscopy of wear and occlusal events in some small herbivores. *Development, Function and Evolution of Teeth*, 415–438.

Rensberger, J. M. (1987). Cracks in fossil enamels resulting from premortem vs. postmortem events. *Scanning Microscopy*, *1*(2), 19.

Richards, M. P., & Trinkaus, E. (2009). Isotopic evidence for the diets of European Neanderthals and early modern humans. *Proceedings of the National Academy of Sciences*, *106*(38), 16034–16039.

Rivals, F., & Deniaux, B. (2003). Dental microwear analysis for investigating the diet of an argali population (Ovis ammon antiqua) of mid-Pleistocene age, Caune de l'Arago cave, eastern Pyrenees, France. *Palaeogeography, Palaeoclimatology, Palaeoecology*, *193*(3–4), 443–455. https://doi.org/10.1016/S0031-0182(03)00260-8

Romero, A., Galbany, J., De Juan, J., & Pérez-Pérez, A. (2012). Brief communication: Short- and long-term in vivo human buccal–dental microwear turnover. *American Journal of Physical Anthropology*, *148*(3), 467–472. https://doi.org/10.1002/AJPA.22054

Romero, A., Ramírez-Rozzi, F. V., De Juan, J., & Pérez-Pérez, A. (2013). Diet-related buccal dental microwear patterns in central african pygmy foragers and bantu-speaking farmer and pastoralist populations. *PLoS ONE*, *8*(12). https://doi.org/10.1371/journal.pone.0084804

Ryan, A. S. (1979). Wear striation direction on primate teeth: a scanning electron microscope examination. *American Journal of Physical Anthropology*, *50*(2), 155–167.

Ryder, J. A. (1878). *On the Mechanical Genesis of Tooth-Forms*. *30*, 45–80.

Sawaura, R., Kimura, Y., & Kubo, M. O. (2022). Accuracy of dental microwear impressions by physical properties of silicone materials. *Frontiers in Ecology and Evolution*, *10*, 975283.

Schmidt, C. W., Beach, J. J., McKinley, J. I., & Eng, J. T. (2015). Distinguishing dietary indicators of pastoralists and agriculturists via dental microwear texture analysis. *Surface Topography: Metrology and Properties*, *4*(1), 014008. https://doi.org/10.1088/2051-672X/4/1/014008

Schmidt, C. W., El Zaatari, S., & Van Sessen, R. (2019). Dental microwear texture analysis in bioarchaeology. In *Dental Wear in Evolutionary and Biocultural Contexts* (pp. 143–168). Elsevier. https://doi.org/10.1016/B978-0-12-815599-8.00007-1

Schubert, B. W., Schubert, P. S. U., Ungar, B. W., & Edu], S. (2005). Wear facets and enamel spalling in tyrannosaurid dinosaurs. *Acta Palaeontologica Polonica*, *50*(1). http://app.pan.pl/acta50/app50

Scott, G. R., & Winn, J. R. (2011). Dental chipping: contrasting patterns of microtrauma in Inuit and European populations. *International Journal of Osteoarchaeology*, *21*(6), 723–731.

Scott, R. S., Ungar, P. S., Bergstrom, T. S., Brown, C. A., Grine, F. E., Teaford, M. F., & Walker, A. (2005). Dental microwear texture analysis shows within-species diet variability in fossil hominins. *Nature 2005 436:7051*, *436*(7051), 693–695. https://doi.org/10.1038/nature03822

Semprebon, G., Janis, C., & Solounias, N. (2010). The diets of the Dromomerycidae (Mammalia: Artiodactyla) and their response to Miocene vegetational change. *Http://Dx.Doi.Org/10.1671/2431*, *24*(2), 427–444. https://doi.org/10.1671/2431

Silvester, C. M., Kullmer, O., & Hillson, S. (2021). A dental revolution: The association between occlusion and chewing behaviour. *PLoS ONE*, *16*(12 December). https://doi.org/10.1371/journal.pone.0261404

Simpson, G. G. (1933). *Paleobiology of Jurassic mammals*. na.

Solounias, N., & Semprebon, G. (2002). Advances in the reconstruction of ungulate ecomorphology with application to early fossil equids. *American Museum Novitates*, *2002*(3366), 1–49.

Staines, M., Robinson, W. H., & Hood, J. A. A. (1981). Spherical indentation of tooth enamel. *Journal of Materials Science*, *16*(9), 2551–2556. https://doi.org/10.1007/BF01113595/METRICS

Teaford, M. F. (1988). A review of dental microwear and diet in modern mammals. *Scanning Microscopy*, *2*(2), 1149–1166. https://pure.johnshopkins.edu/en/publications/a-review-of-dental-microwear-and-diet-in-modern-mammals-5

Teaford, M. F. (1994). Dental microwear and dental function. *Evolutionary Anthropology: Issues, News, and Reviews*, *3*(1), 17–30.

Teaford, M. F., & Lytle, J. D. (1996). Brief communication: Diet-induced changes in rates of human tooth microwear: A case study involving stone-ground maize. *American Journal of Physical Anthropology*, *100*(1), 143–147. https://doi.org/10.1002/(SICI)1096-8644(199605)100:1

Teaford, M. F., & Runestad, J. A. (1992). Dental microwear and diet in Venezuelan primates. *American Journal of Physical Anthropology*, *88*(3), 347–364. https://doi.org/10.1002/AJPA.1330880308

Teaford, M. F., & Walker, A. (1984). Quantitative differences in dental microwear between primate species with different diets and a comment on the presumed diet of Sivapithecus. *American Journal of Physical Anthropology*, *64*(2), 191–200. https://doi.org/10.1002/AJPA.1330640213

Toussaint, M., Olejniczak, A. J., El Zaatari, S., Cattelain, P., Flas, D., Letourneux, C., & Pirson, S. (2010). The Neandertal lower right deciduous second molar from Trou de l'Ab\^\ime at Couvin, Belgium. *Journal of Human Evolution*, *58*(1), 56–67.

Towle, I., Irish, J. D., & De Groote, I. (2017). Behavioral inferences from the high levels of dental chipping in Homo naledi. *American Journal of Physical Anthropology*, *164*(1), 184–192.

Towle, I., Irish, J. D., & Loch, C. (2021). Paranthropus robustus tooth chipping patterns do not support regular hard food mastication. *Journal of Human Evolution*, *158*, 103044.

Trinkaus, Erik. (1983). *The Shanidar Neandertals*. 502.

Ungar, P. S. (1995). A semiautomated image analysis procedure for the quantification of dental microwear II. *Scanning*, *17*(1), 57–59.

Ungar, P. S. (2015). Mammalian dental function and wear: A review. *Biosurface and Biotribology*, *1*(1), 25–41. https://doi.org/10.1016/J.BSBT.2014.12.001

Ungar, P. S. (2018). Dental microwear. In *The International Encyclopedia of Biological Anthropology* (pp. 1–4). John Wiley & Sons, Inc. https://doi.org/10.1002/9781118584538.ieba0127

Ungar, P. S. (2019). Inference of Diets of Early Hominins from Primate Molar Form and Microwear. *Https://Doi.Org/10.1177/0022034518822981*, *98*(4), 398–405. https://doi.org/10.1177/0022034518822981

Ungar, P. S., Brown, C. A., Bergstrom, T. S., & Walker, A. (2003). Quantification of dental microwear by tandem scanning confocal microscopy and scale-sensitive fractal analyses. *Scanning: The Journal of Scanning Microscopies*, *25*(4), 185–193.

Ungar, P. S., & Grine, F. E. (1991). Incisor size and wear in Australopithecus africanus and Paranthropus robustus. *Journal of Human Evolution*, *20*(4), 313–340.

Ungar, P. S., Grine, F. E., Teaford, M. F., & El Zaatari, S. (2006). Dental microwear and diets of African early Homo. *Journal of Human Evolution*, *50*(1), 78–95.

Ungar, P. S., Scott, P. S., Scott, J. R., & Teaford, M. (2009). Dental microwear analysis: historical perspectives and new approaches. In *Technique and Application in Dental Anthropology* (pp. 389–425). Cambridge University Press. https://doi.org/10.1017/cbo9780511542442.017

Ungar, P. S., & Spencer, M. A. (1999). Incisor microwear, diet, and tooth use in three Amerindian populations. *American Journal of Physical Anthropology: The Official Publication of the American Association of Physical Anthropologists*, *109*(3), 387–396.

Ungar, P. S., & Sponheimer, M. (2011a). The diets of early hominins. *Science*, *334*(6053), 190–193. https://doi.org/10.1126/SCIENCE.1207701/SUPPL_FILE/UNGAR.SOM.PDF

Ungar, P. S., & Sponheimer, M. (2011b). The diets of early hominins. In *Science* (Vol. 334, Issue 6053, pp. 190–193). American Association for the Advancement of Science. https://doi.org/10.1126/science.1207701

Uzunidis, A., Pineda, A., Jimenez-Manchon, S., Xafis, A., Ollivier, V., & Rivals, F. (2021). The impact of sediment abrasion on tooth microwear analysis: an experimental study. *Archaeological and Anthropological Sciences*, *13*, 1–17.

Vietti, A. (2016). Combined Electron Spin Resonance and U-series dating (ESR/U-series) of fossil tooth enamel: application to dental remains from different Palaeolithic Italian sites. *Universtià Degli Studi Di Torino*.

Villa, G., Giacobini, G., & others. (1996). Neandertal teeth from alpine caves of Monte Fenera (Northern Italy). Description of the remains and microwear analysis. *Anthropologie*, *34*, 225–238.

Walker, A. (1981). Diet and teeth: Dietary hypotheses and human evolution. *Philosophical Transactions of the Royal Society of London. B, Biological Sciences*, *292*(1057), 57–64. https://doi.org/10.1098/RSTB.1981.0013

Walker, A., Hoeck, H. N., & Perez, L. (1978). Microwear of Mammalian Teeth as an Indicator of Diet. *Science*, *201*(4359), 908–910. https://doi.org/10.1126/SCIENCE.684415

Walker, P. L. (1976). Wear striations on the incisors of ceropithecid monkeys as an index of diet and habitat preference. *American Journal of Physical Anthropology*, *45*(2), 299–307. https://doi.org/10.1002/AJPA.1330450215

Watson, J. T., & Schmidt, C. W. (2019). An introduction to dental wear in evolutionary and biocultural contexts. In *Dental Wear in Evolutionary and Biocultural Contexts* (pp. 1–10). Elsevier. https://doi.org/10.1016/B978-0-12-815599-8.00001-0

Weber, K., Winkler, D. E., Schulz-Kornas, E., Kaiser, T. M., & Tütken, T. (2022). Post-mortem enamel surface texture alteration during taphonomic processes—do experimental approaches reflect natural phenomena? *PeerJ*, *10*, e12635.

Weinstein, K. J. (2008). Thoracic morphology in Near Eastern Neandertals and early modern humans compared with recent modern humans from high and low altitudes. *Journal of Human Evolution*, *54*(3), 287–295.

Welborn, V. V. (2020). Enamel synthesis explained. *Proceedings of the National Academy of Sciences of the United States of America*, *117*(36), 21847–21848. https://doi.org/10.1073/PNAS.2014394117/ASSET/11F17E3A-1EB9-4CE7-8383-CF4A0C35D590/ASSETS/IMAGES/LARGE/PNAS.2014394117FIG01.JPG

Willerslev, E., & Cooper, A. (2005). Ancient DNA. In *Proceedings of the Royal Society B: Biological Sciences* (Vol. 272, Issue 1558, pp. 3–16). Royal Society. https://doi.org/10.1098/rspb.2004.2813

Williams, E., Schmidt, C. W., Henry, A. G., Discamps, E., Droke, J. L., Becam, G., & de Lumley, M.-A. (2022). *The Ice Age diet of the La Quina 5 Neandertal of southwest France Le re´gime alimentaire du Ne´andertalien La Quina 5 durant ladernière pe´riode glaciaire dans le sud-ouest de la France ScienceDirect*. https://doi.org/10.1016/j.anthro.2022.103056

Williams, F. L., Droke, J. L., Schmidt, C. W., Willman, J. C., Becam, G., & de Lumley, M.-A. (2018). Dental microwear texture analysis of Neandertals from Hortus cave, France. *Comptes Rendus Palevol*, *17*(8), 545–556.

Williams, V. S., Barrett, P. M., & Purnell, M. A. (2009). *Quantitative analysis of dental microwear in hadrosaurid dinosaurs, and the implications for hypotheses of jaw mechanics and feeding*. *106*.

Williams, V. S., & Doyle, A. M. (2010). Cleaning fossil tooth surfaces for microwear analysis: use of solvent gels to remove resistant consolidant. *Palaeontologia Electronica*, *13*, 2T.

Wood, B., Schroer, K., Wood, B., & Schroer, : K. (2012). Reconstructing the Diet of an Extinct Hominin Taxon: The Role of Extant Primate Models. *International Journal of Primatology 2012 33:3*, *33*(3), 716–742. https://doi.org/10.1007/S10764-012-9602-7